AFIT/GE/EE/78-14

(1)

AD A064679

DDC FILE COPY

(6) EFFECTS OF ANTENNA ARRAYS ON BROADBAND SIGNALS.

(9) Master's THESIS,

(14) AFIT/GE/EE/78-14

(10) Edward Kaska, Jr.
Capt. USAF

DDC
FEB 1 1979
A

(11) Sep 78

Approved for public release; distribution unlimited

(12) 142p.

012 225

79 01 30 128

AFIT/GE/EE/78-14

EFFECTS OF ANTENNA ARRAYS ON BROADBAND SIGNALS

THESIS

Presented to the Faculty of the School of Engineering
of the Air Force Institute of Technology
Air Training Command
in Partial Fulfillment of the
Requirements for the Degree of
Master of Science

by

Edward Raska, Jr., B.S.

Capt USAF

Graduate Electrical Engineering

September 1978

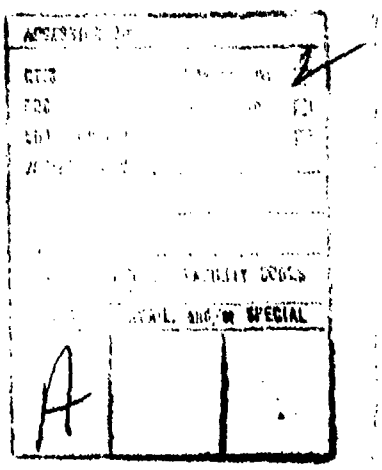

Preface

In January 1978 I knew nothing about antenna arrays or spread spectrum signals other than the fact that I had heard the terms before. Capt. Stanley R. Robinson steered me onto a thesis topic suggested by Maj. Jurgen O. Gobien. The basic study involved the study of adaptive antenna arrays in order to determine if their adaptive nature would have any adverse effects on the performance of spread spectrum communications systems. By February, I made the commitment to take on this research effort as my Master's level thesis work.

Capt. Robinson and I spent many hours together in the months that followed studying this problem. He provided most of the guidance by suggesting many possible avenues of research effort. I provided the legwork required to travel down each of these paths. After having performed many calculations, made many mistakes, and many false starts, we eventually organized the many efforts into the document that follows.

There were many times that I thought the research was going to be fruitless. Once we did make our major breakthrough it became a question of my ability to write faster than the clock could move. The clock eventually won the race and the effort for this document had to be stopped. As with most research efforts, the material included here is mostly incomplete and just hints at other areas for

continuing research. Also, like so many other research projects, the questions answered are not exactly the questions we started out to answer.

I wish to thank Capt. Robinson, my advisor, for the many hours he devoted to my education during this period. I also want to thank my sponsor, Maj. Gobien, for the time he devoted to get me started on this study. Thanks go, also, to Maj. Carl and Maj. Carpinella for taking the time to read my draft and advise me on the format and contents. To these people I give my thanks and my friendship.

A special thanks goes to my wife, Elsie, and my three daughters, Lois, Karen, and Christine, who stayed with me through the trying times and long nights I spent working on the details and the writing. To these four ladies I give my thanks and my love.

Edward Raska, Jr.

Contents

Abstract

This paper develops a complex, baseband model for an adaptive array. The array is assumed to have N isotropic elements. Only two aspects of arrays are modeled: spatial propagation delays and the weighting coefficients. The array model is used to determine the effects of arrays on wideband signals. The most important finding is that the output of the array consists of the input signal and its time derivatives. Each of these signal components is multiplied by a complex number that is a function of the array and signal parameters. Properties of these complex numbers are investigated. A four element linear array is used as a specific example to illustrate these properties. Two models of the weighting coefficients are analyzed to develope information about "adaptive" effects. These models are used to show how the array output is degraded by changing coefficients.

EFFECTS OF ANTENNA ARRAYS ON BROADBAND SIGNALS

I Introduction

Spread spectrum is an information transmission technique whereby a signal is modulated in such a way that the transmitted signal has a spectrum that can be orders of magnitude wider than the information spectrum. At the receiver, incoming signals are again modulated by the same spreading signal. This results in two effects: (1) all noise source signals are modulated by the spreading signal and their bandwidths are spread out by the same ratio that the signal was spread at the modulator, (2) the modulation of the information signal a second time results in compressing the information back down to its original bandwidth. Thus, when the received signals are passed through the appropriate filter, only the desired signal is passed without loss. Dixon (Ref 4) is a very good introduction into all aspects of current spread spectrum technology.

Antenna arrays are simply a group of antennas that are tied together electrically to yield a resultant antenna that has certain desired reception properties. One of the most important uses of arrays is to form a highly directional antenna beam that will receive signals from basically one direction. Arrays can be pointed in a given direction via two methods: mechanical positioning or electronic steering. The mechanical positioning technique has been used quite

extensively in radar applications. There are several drawbacks to this technique: (1) the antenna radiation pattern is fixed in shape and can only be pointed; (2) the physical positioning of the antenna places limitations on its size; (3) the rate at which the antenna can change directions is limited by the mechanical system; (4) it is very difficult to place a moving antenna on the exterior surfaces of an aircraft.

Electronically steered antenna arrays can reduce or eliminate all of the above limitations. However, they still have drawbacks of their own. The electronics required to shape and point the array pattern are very complex and expensive. These drawbacks have limited their use to applications where the advantages heavily outweigh the cost, such as in satellite systems (Ref 17).

Today efforts are underway to design and build equipment that combines these two techniques into a single communications system. Most of the analysis performed on antenna arrays has assumed that incoming signals are monochromatic or quasi-monochromatic. Little analytic work has been done to determine the effects of an adaptive array on a wideband signal. It is the purpose of this thesis to study these effects. Since the purpose is to study the effect of arrays on signals, most of the analysis is done without interference or noise being considered as a parameter.

Chapter II begins the analysis by introducing the various models and assumptions that are the basis for the

ensuing work. Certain spread spectrum concepts are discussed and a complex model for a spread spectrum signal is developed. Next, the basic properties of an adaptive array are introduced. From this, a general input/output equation for an N element adaptive array is developed. Finally, two receiver models are developed for use in later analysis. They are a coherent receiver and an envelope or phase incoherent receiver.

Chapter III is devoted to the analysis of static arrays. Thus, the first thing it does is modify the models so that the array is fixed. Two characteristics of the spread spectrum signal are picked out and studied separately: its wideband nature and its autocorrelation function. In the initial analysis the signal is simply assumed to be a nonzero bandwidth signal. Certain properties of the output of the array are then developed and discussed. Next, the properties of the output correlation function are discussed and demonstrated. Through this development, the effect of the pulse (or code) rate becomes evident. This chapter looks at three specific examples: a linear, equally spaced array of four elements and two four element sparse arrays.

Chapter IV then moves on to a study of adaptive effects. Two models of adaptive arrays are studied. There are a variety of algorithms which control the weighting coefficients (Ref 16). It was not the purpose of this thesis to study these algorithms or even study a particular algorithm. However, it was desirable to determine if time varying weighting

coefficients have any additional effect on the incoming signal. As a result, the adaptive nature is viewed as a perturbation of a desired static condition. The first model of the perturbations assumes they are sinusoidal. The effects of both the amplitude and the frequency are then investigated. The second model assumes that the perturbations are Gaussian processes with known statistics and a statistical analysis of the effects is presented.

Chapter V is devoted to summarizing the conclusions drawn throughout the thesis. It then proceeds to make several recommendations for further study based on these conclusions.

II System Models

This chapter introduces a complex baseband model for the spread spectrum signal. It then develops a model for the adaptive array. Using the spread spectrum signal as the input, an equation for the output of the array is then developed. This equation will be used in the later chapters as the basis for all the analysis. Next, the models for the two receivers used are presented. Finally, the chapter ends with a discussion of the performance criteria to be used in the analysis.

A. Signal and Array Equation

It is the purpose of this section to introduce those ideas from the theories of antenna arrays and spread spectrum techniques that are used as a basis for the main thrust of this thesis. It is assumed that the reader has a background in antenna theory and is familiar with spread spectrum techniques. Thus, this section will prove to be a short review and will also introduce the various simplifying assumptions used to keep the array analysis tractable.

Figure 1 illustrates the basic coordinate system that is used. It is a spherical coordinate axis with parameters (θ, φ, r) to designate position. The location of the i'th element of an antenna array is designated by $(\theta_i, \varphi_i, r_i)$. The source of the signal is located in the far field or Fraunhofer region at angles (θ, φ). This region is usually defined to begin at a distance of $2L^2/\lambda$ from the antenna

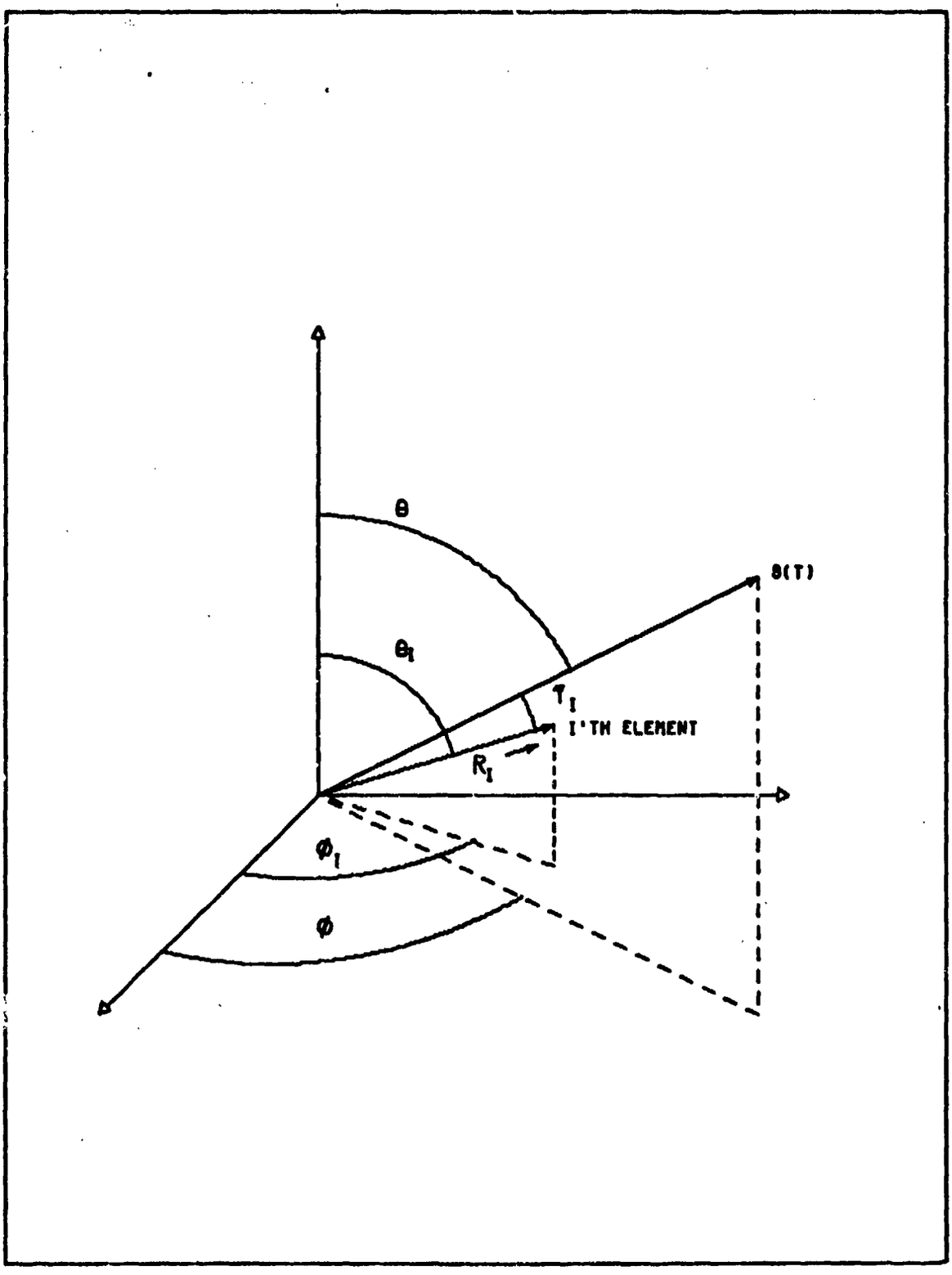

Figure 1. Reference Coordinate System.

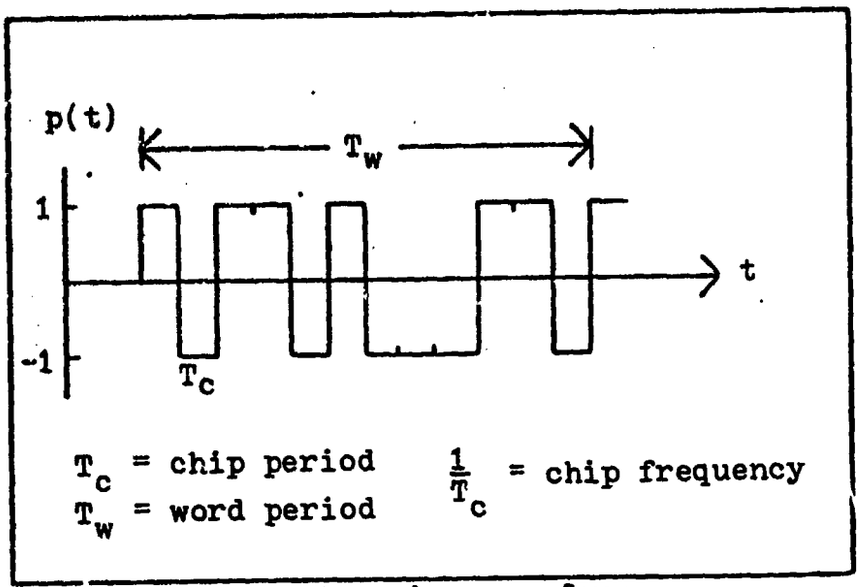

Figure 2. Pseudo-noise waveform.

where L is the largest antenna dimension and λ is the wavelength of the carrier frequency (Refs 8:6 and 19:32-60).

The spread spectrum signal used in this thesis is composed of two parts: the information signal and the pseudo-noise signal (PN code). The information signal is considered to be a voice signal or a digitally sampled voice signal, $v(t)$. Thus, the information signal can be considered a low frequency signal with a bandwidth in the range of 10 KHz or less.

The pseudo-noise signal can be thought of as a train of ± 1's that switches states randomly at a relatively high rate, such as 5 MHz. This pulse train, p(t), becomes periodic after some fixed number of pulses has passed. Each bit of the code is usually referred to as a chip; the entire periodic sequence is called a code word (Figure 2). Pulse trains can easily be implemented by properly connecting a recirculating

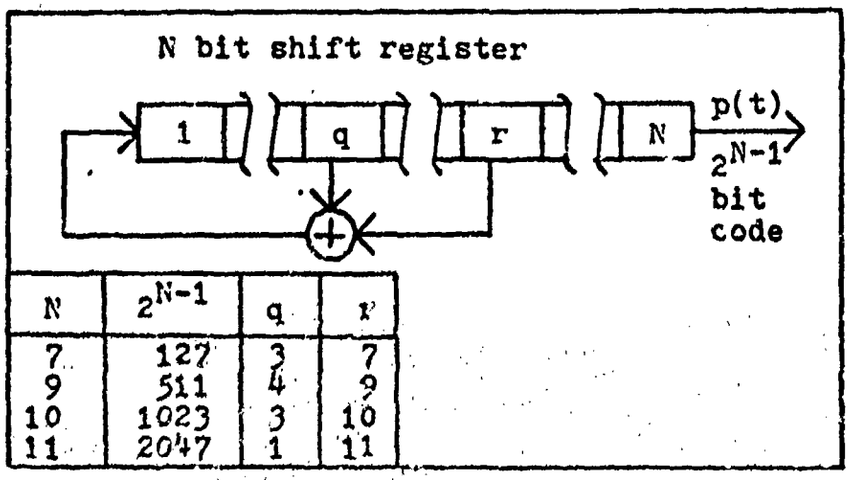

N	2^{N-1}	q	r
7	127	3	7
9	511	4	9
10	1023	3	10
11	2047	1	11

Figure 3. Maximal length code generator.

register of N bits in length to create a $2^N - 1$ bit pulse train (Ref 4:80) (Figure 3). This type of code sequence is called a maximal length code. One of the desirable properties of the code word is that it has low autocorrelation if the time shift is a full chip width or greater. It has been shown (Ref 9:148) that the codes generated by the recirculating register of Figure 3 have this property.

As Dixon (Ref 4:14-23) has illustrated the power spectrum of a PN code always has a $(\sin x/x)^2$ character where the first null of the spectrum is at the clock rate of the code; i.e., the first null of a 5 MHz code is located at $f = 5$ MHz . He also shows that about 90% of the code power is located within the first null. Thus, the code bandwidth can usually be considered to be the bandwidth of the main lobe of the power spectrum. Modulation of the information signal by the pseudo-noise signal creates the spread spectrum signal. Since the purpose of the code is to spread the

signal spectrum, its spectrum is usually much wider than the signal's spectrum. Thus, the bandwidth of the spread spectrum signal is very nearly the bandwidth of the code. This modulation can be modeled in one of two ways. The pulse train can be thought of as a direct amplitude modulation of the signal or it can be looked at as a phase modulation, $\phi_p(t)$, of the carrier frequency, where $\phi_p(t) = 0$ or π.

The spread spectrum signal is then translated to the carrier frequency, f_o, for transmission. During any numerical calculations performed later, f_o will be considered in the UHF range; about 350 MHz. Bringing these elements together using the phase shift model for p(t), the spread spectrum signal becomes

$$s(t) = v(t)\cos[2\pi f_o t + \phi_p(t)] \tag{1}$$

This can be written as

$$s(t) = \mathrm{Re}\{v(t)e^{j[2\pi f_o t + \phi_p(t)]}\}$$

$$= \mathrm{Re}\{v(t)e^{j\phi_p(t)}e^{j2\pi f_o t}\} \tag{2}$$

where $\mathrm{Re}\{\cdot\}$ stands for the real part of the complex expression. The complex envelope of s(t) is

$$\tilde{s}(t) = v(t)e^{j\phi_p(t)} \tag{3}$$

Thus,

$$s(t) = Re\{\tilde{s}(t)\, e^{j2\pi f_o t}\} \qquad (4)$$

$\tilde{s}(t)$ is considered the complex baseband representation of the spread spectrum signal.

The array is also modeled using a complex baseband representation. Since our primary interest is to model the propagation and weighting effects of the adaptive array, a variety of simplifying assumptions are made. First, all antenna elements are assumed to be isotropic in nature. Second, since we are concerned primarily with small arrays (few elements), mutual coupling effects are ignored.

With these assumptions, there are only two effects to model: the spatial effects and the adaptive effects. The spatial effects modeled are simply the relative propagation time differences between the elements of the array and the origin. Typically, one element of the array is chosen as the origin and the propagation delays (or advances) are measured with respect to this element. The propagation delay, τ_i, is the time that elapses from the moment the signal wavefront reaches the origin. Figure 4 shows a typical relationship between the signal and two elements, one of which is considered the origin. The propagation delay from the i'th element to the origin is precisely (X - Y)/c where c is the velocity of light. However, it is well known that if the angle, a, is small then Y is approximately the

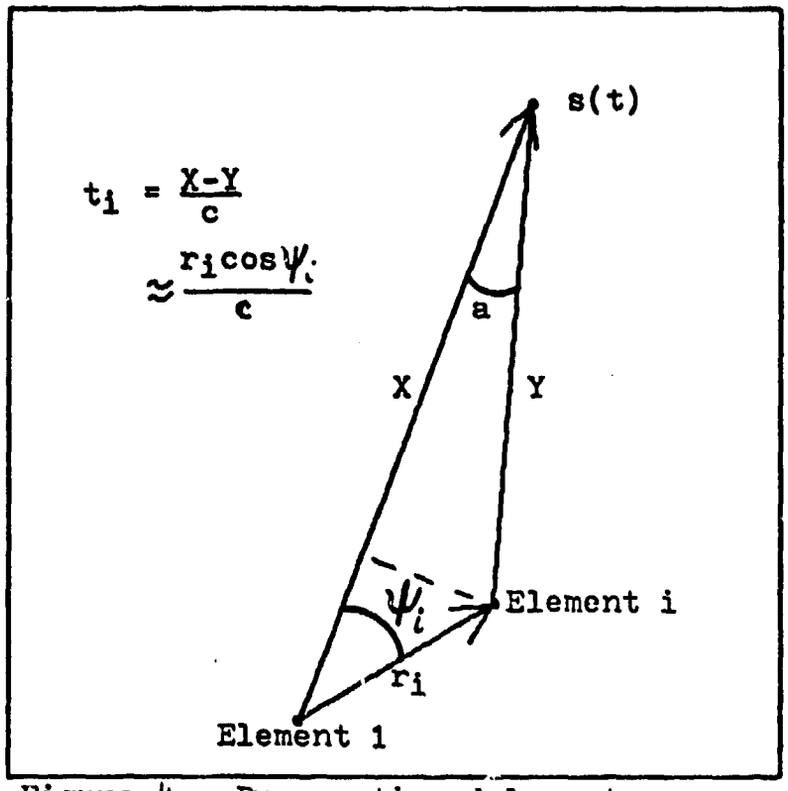

Figure 4. Propagation delay, t_i.

same as its projection onto X. Thus, the distance X - Y can be closely approximated by the distance $r_i \cos \psi_i$. This is basically the same assumption used to identify the far field region, i.e., X and Y are approximately parallel. This approximation is correct to within 1% error if the angle a is less than 8° . The worst case for this approximation is when X = Y , because r_i then subtends the largest angle a. In this case, the ratio Y/r_i must be greater than 7.2 to keep angle a less than 8°.

Using the above approximation for the propagation delay, we obtain

$$t_i = \frac{r_i}{c} \cos \psi_i \qquad (5)$$

where the angle ψ_i can be calculated as follows (see Fig. 1):

$$\cos\psi_i = \cos\theta\cos\theta_i + \sin\theta\sin\theta_i\cos(\varphi - \varphi_i) \tag{6}$$

The propagation delay, t_i, has the effect of delaying (or advancing) the signal by the amount, t_i. Thus, the signal at the i'th element can be represented by

$$\begin{aligned} s_i(t) &= s(t + t_i) \\ &= \mathrm{Re}\left\{ v(t+t_i)\, e^{j\phi_p(t+t_i)}\, e^{j2\pi f_0(t+t_i)} \right\} \end{aligned} \tag{7}$$

Thus, the complex envelope of the delayed signal becomes

$$\tilde{s}_i(t) = v(t+t_i)\, e^{j\left[\phi_p(t+t_i) + 2\pi f_0 t_i\right]} \tag{8}$$

As stated earlier, the array is to be modeled using a complex baseband representation. Therefore, the adaptive effects can be modeled simply by a complex weighting term, $A_i(t)e^{j\alpha_i(t)}$, used as a multiplier on the signal at the i'th antenna element. Multiplying the signal by the weighting coefficient results in the complex output of the i'th element.

$$\begin{aligned} \tilde{o}_i(\theta, \varphi, t) &= \tilde{s}_i(t)\, A_i(t) \exp\left[j\alpha_i(t)\right] \\ &= A_i(t)\, v(t+t_i) \exp\left[j\left\{\phi_p(t+t_i) + 2\pi f_0 t_i + \alpha_i(t)\right\}\right] \end{aligned} \tag{9}$$

Now, since mutual coupling effects are being ignored in this analysis, the output of the array is simply the summed outputs of the individual elements. Thus, the resultant output of the array is represented by

$$v(\theta,\phi,t) = \sum_{i=1}^{N} v(t+t_i)\, e^{j[\phi_p(t+t_i)+2\pi f_0 t_i]} A_i(t) e^{j\alpha_i(t)}$$

$$= \sum_{i=1}^{N} A_i(t)\, v(t+t_i)\, e^{j[\phi_p(t+t_i)+2\pi f_0 t_i+\alpha_i(t)]} \qquad (10)$$

This, then, is the complex baseband model of the array for a spread spectrum signal. $A_i(t)$, t_i and $\alpha_i(t)$ are all parameters of the array. They each have an effect on the output signal of the array. Chapters III and IV of this thesis analyze the effect of these parameters on the ability of the array to pass the information undistorted.

B. Receivers

Eq (10) is the output of the array. This becomes the input to the receiver. One of the objectives of this thesis is to determine what effects Eq (10) will have on receivers. The operation of two receivers is analyzed in Chapters III and IV. This section presents the models for those two receivers.

One receiver used is the correlation detector shown in Figure 5. With this receiver we assume a priori knowledge of both the transmission frequency and the pseudo-noise code. However, it is assumed that there is a start time uncertainty, τ, in the code generator resulting in mismatch

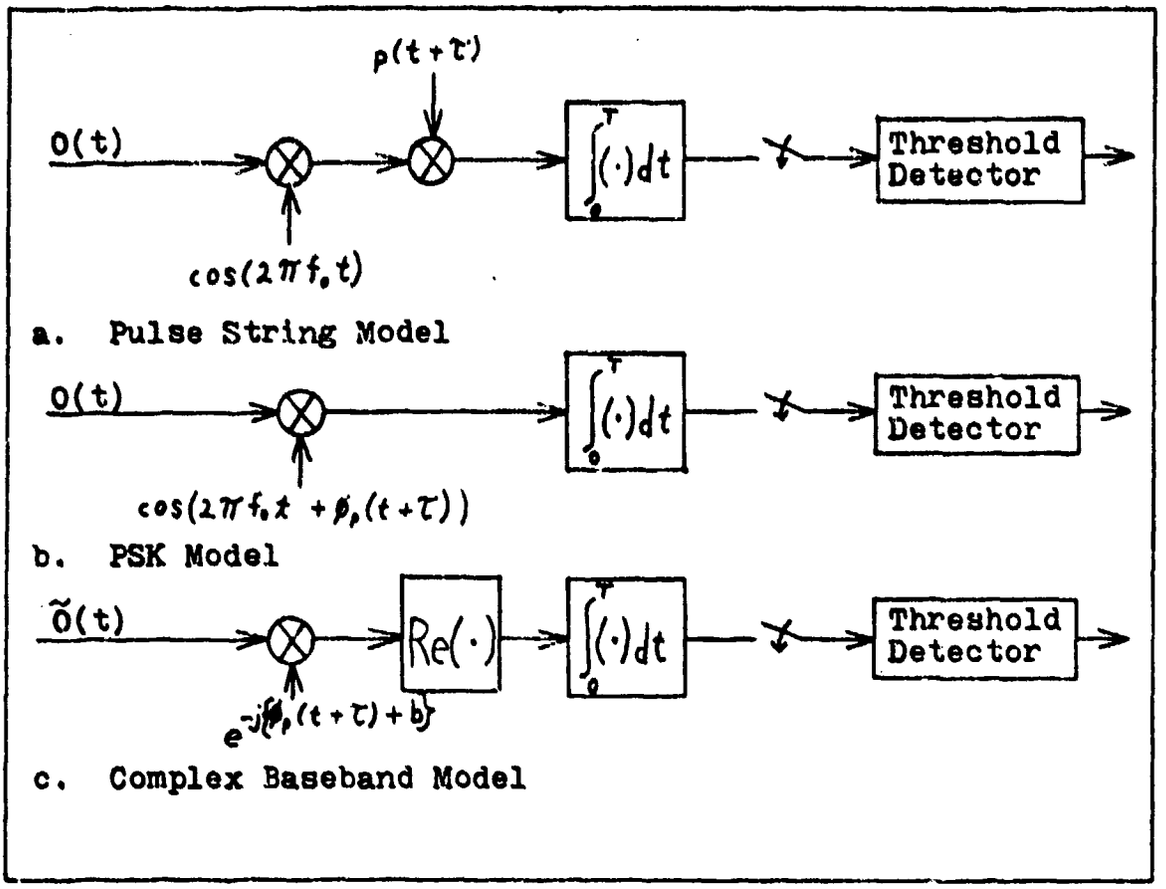

Figure 5. Correlation Detector.

between the transmitter and the receiver. Both are used to modulate the output of the adaptive array and the result is passed through an integrator. This system would be used if the information, v(t), is also transmitted digitally. The integrator period, T, is the period of the information code. Recalling that the array was modeled using a complex, baseband representation, it is desirable to use the same type model for the receivers. By employing the PSK form for the PN code, the model for the correlation receiver becomes a

multiplication by the complex exponential, $e^{\{-j[\phi_p(t+\tau)+b]\}}$, followed by the detection circuitry (Fig.5c). The phase shift, b, is used to shift the signal phase so that any desired component of the complex signal can be observed at the output of the detector.

The other receiver examined in this thesis is the envelope detector illustrated in Figure 6. It is used in an analysis to judge the effect of not knowing or even estimating the phase of the carrier on the output. The baseband model of this system (Fig. 6c) is simply a correlation operation followed by an absolute value operation.

Both models have used the offset τ to represent timing mismatch between the transmitter and receiver codes. If τ is kept as a parameter, then the receiver output is a function of τ. As τ is allowed to vary the output becomes the correlation function of the array output and the code. The properties of the correlation function are emphasized in the examples of Chapter III.

C. Performance

The designers of adaptive arrays consider performance in terms of parameters like the antenna directivity, the main lobe beamwidth, the number of degrees of freedom, etc. (Ref 10). They also investigate how fast the array adapts from one steady state to another, how well the array nulls point sources of interference, how many noise sources can be nulled or how many degrees of freedom are used up to null a

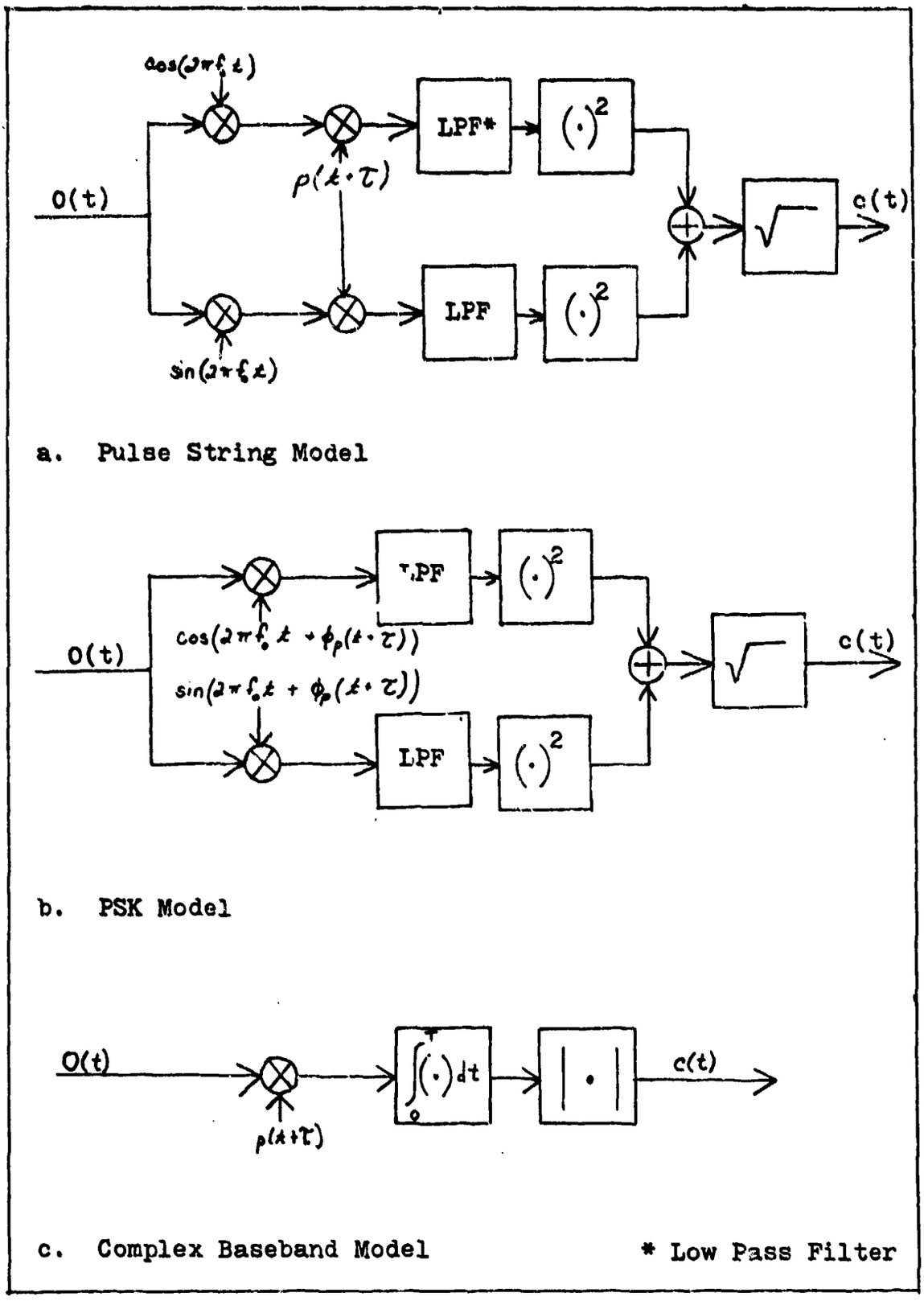

Figure 6. Envelope Detector.

specific noise source or group of noise sources (Refs 11 and 12). All of these performance characteristics are important and need to be known for any given system. But these are incomplete for total description of the communication system of which the array is one part.

There is another series of performance criteria that should be studied. The effect of the array on a signal can be analyzed from the viewpoint of the array as a filter. As such, the array's performance can be discussed in terms of signal distortion. The array affects incoming signals in several ways, each of which causes distortion. First, the arrays have frequency dependent radiation patterns (as do all antennas). These patterns cause attenuations and phase shifts of the various frequency components of incoming signals. Since the effect is different at different frequencies, this will result in a distortion of wideband signals such as spread spectrum signals. If the distortion is great enough, the characteristics of the pseudo-noise code will be lost and the receiver's internally generated code will not be able to synchronize with the signal's code. Without code lock, the system cannot recompress the spread spectrum signal back down to its original bandwidth and the information will be lost. The receivers perform a correlation of the received signal with the code. Therefore, instead of looking at the signal directly, we will investigate the effects of the array on the properties of the correlation function of the code.

Second, the weighting coefficients are time varying in an adaptive system. They are used as multipliers to the incoming signal and thus they become a direct modulation of the incoming signal. In Chapter IV, two models for the weighting coefficients are investigated to determine conditions under which the time varying properties of the weighting coefficients cause additional signal distortion.

III Performance of Static Arrays

This chapter analyzes the performance of arrays when the weighting coefficients are fixed. A variety of static cases are studied. The cases analyzed are not in themselves supposed to represent actual systems. The effects on the output of the system geometry and the location of the signal in the antenna pattern are studied.

A. Fixed Array Equation

The analysis begins by modifying the array equation for static conditions. Thus, assume

$$A_i(t)e^{j\alpha_i(t)} = A_i e^{j\alpha_i} \tag{11}$$

where A_i and α_i are real constants. Then Eq (10) becomes

$$\tilde{o}(\theta,\phi,t) = \sum_{i=1}^{N} A_i\, v(t+t_i)e^{j[\phi_p(t+t_i)+2\pi f_o t_i+\alpha_i]} \tag{12}$$

or as written in the frequency domain

$$\tilde{o}(\theta,\phi,f) = \mathcal{F}\{v(t)e^{j\phi_p(t)}\}\sum_{i=1}^{N} A_i e^{j[2\pi(f_o+f)t_i+\alpha_i]} \tag{13}$$

where $\mathcal{F}\{\cdot\}$ represents the Fourier transform.

At this point, it becomes interesting to study the array properties separately. As such, the specific signal form is uninteresting. Thus, for simplicity, let m(t)

represent $v(t)e^{j\phi_p(t)}$ and M(f) represent $\mathcal{F}\{v(t)e^{j\phi_p(t)}\}$ Eq (13) becomes

$$\tilde{o}(\theta, \phi, f) = M(f)\sum_{i=1}^{N} A_i e^{j[2\pi(f+f_o)\tau_i + \alpha_i]} \qquad (14)$$

This is a function of the variable f. $\tilde{o}(\theta, \phi, f)$ is the system output and M(f) is the system input. From linear system theory, the ratio of the output to the input is considered the system transfer function, H(f). In this case, the summation term becomes the transfer function

$$H(f) = \sum_{i=1}^{N} A_i e^{j[2\pi(f+f_o)\tau_i + \alpha_i]} \qquad (15)$$

However, the transfer function in this case is no simply a function of frequency. It is also a function of the weighting coefficients (α_i and A_i), the signal's location (θ and ϕ), and the array's geometry (θ_i, ϕ_i, r_i). All these other parameters, except the signal location parameters, become fixed for the case of the static array. Thus, the array's transfer function can be considered as a function of θ , ϕ , and f . The dependence of the transfer function on θ and ϕ is in the dependence of the τ_i's on θ and ϕ (see Eq (5) for details).

At this point it becomes necessary to introduce the concept of the phase center (Ref 19:72). In essence, the phase center is the geometric center of the array. If the origin is located at the phase center, then the sum of the

time delays becomes zero.

$$\sum_{i=1}^{N} t_i = 0 \tag{16}$$

In an arbitrarily located coordinate system, the phase center will be located at a time delay point t_c . It then becomes true that

$$\sum_{i=1}^{N} (t_i - t_c) = 0 \tag{17}$$

Thus,

$$\sum_{i=1}^{N} t_i = \sum_{i=1}^{N} t_c = N t_c \tag{18}$$

Therefore,

$$t_c = \frac{1}{N} \sum_{i=1}^{N} t_i \tag{19}$$

With this concept in mind return to Eq (15) and factor out the phase center term. The result is

$$H(\theta, \phi, f) = e^{j2\pi(f+f_o)t_c} \sum_{i=1}^{N} A_i e^{j[2\pi(f+f_o)(t_i - t_c) + \alpha_i]}$$

$$= e^{j2\pi f_o t_c} e^{j2\pi f t_c} \sum_{i=1}^{N} A_i e^{j[2\pi(f+f_o)(t_i - t_c) + \alpha_i]} \tag{20}$$

Now the summation term can be expanded into a Taylor series. The result is

$$\sum_{i=1}^{N} A_i e^{j[2\pi(f+f_0)(x_i - x_0) + \alpha_i]}$$

$$= \sum_{i=1}^{N} A_i e^{j[2\pi f_0 (x_i - x_c) + \alpha_i]} + j2\pi f \sum_{i=1}^{N} A_i (x_i - x_c) e^{j[2\pi f_0 (x_i - x_c) + \alpha_i]}$$

$$+ \cdots + \frac{(j2\pi f)^m}{(m-1)!} \sum_{i=1}^{N} A_i (x_i - x_c)^m e^{j[2\pi f_0 (x_i - x_c) + \alpha_i]} + \cdots$$

$$= A + j2\pi f B + \cdots \tag{21}$$

where

$$A = \sum_{i=1}^{N} A_i e^{j[2\pi f_0 (x_i - x_0) + \alpha_i]} \tag{22}$$

and

$$B = \sum_{i=1}^{N} A_i (x_i - x_c) e^{j[2\pi f_0 (x_i - x_c) + \alpha_i]} \tag{23}$$

It should be noted that A and B are functions of all the physical array parameters, the carrier frequency, and (through the x_i) the angular relation between the signal location and the array orientation. Because of the functional dependence on a wide variety of system parameters, the author has decided to make the functional dependence

implicit in the terms themselves. Later, however, functional relationship with the signal's location will be made explicit by referring to these terms as $A(\theta)$ and $B(\theta)$, where θ will represent the signal's location. However, the reader should recall that the dependence on all the other system parameters still exists.

Combining the results of Eqs (20) and (21) into Eq (14) we obtain the system output

$$\tilde{o}(\theta, \phi, f) = M(f)\, e^{j2\pi f_o t_c}\, e^{j2\pi f t_c} \times \left\{ A + j2\pi f B + \cdots \right\} \tag{24}$$

The first exponential is recognized as a phase shift that is functionally dependent on the relationship between the location of the signal, the location of the phase center, and the location of the origin of our coordinate system. The second exponential is a linear phase term that is also a function of the same points. Eq (24) can easily be transformed into the time domain by recalling that a linear phase shift transforms into a time delay and that $(j2\pi x)^m$ transforms into the n'th derivative. Thus Eq (24) becomes

$$\tilde{o}(\theta, \phi, t) = e^{j2\pi f_o t_c} \left\{ m(t + t_c) A + \frac{dm(t+t_c)}{dt} B + \cdots \right.$$

$$\left. + \frac{d^m m(t+t_c)}{dt^m} \frac{1}{(m-1)!} \sum_{i=1}^{N} A_i (t_i - t_c)^m\, e^{j[2\pi f_o (t_i - t_c) + \alpha_i]} + \cdots \right. \tag{25}$$

It should be explained at this point that Eq (25) is a baseband representation of the system. Thus, signals used in this equation must be written in their complex baseband form. For example, a monochromatic signal, $\cos 2\pi f_o t$, at the array's center frequency, f_o, has a baseband representation of $m(t) = 1.0$ (i.e., a d.c. component) in this equation. Thus, the monochromatic signal has no derivative terms and the output of the array is just the first term of the series.

At this point one might ask why the phase center terms were factored out of Eq (15) before performing the Taylor series expansion. The purpose is to separate the array geometry effects from effects due to selection of the origin. The terms factored out of the array's transfer function were dependent on the selection of the origin. The remaining terms are simply a function of the array and signal geometry. As Eq (25) shows, the origin dependent terms result in a phase shift and a time delay.

Now Eq (25) provides several very important insights into the operation of antenna arrays. Foremost is that, in general, the output of an array is the sum of the signal and all of its time derivatives. The signal and its derivatives are each weighted by complex numbers before they are added. These complex weightings are derived from the signal and array geometry. They account for most of the typically observed properties of arrays. Eq (25) was obtained through a power series expansion. A similar operation can be performed on any system transfer function providing the

expansion is carried out using inverse powers of f, also. As will be seen later, the utility of this expansion is in the fact that the first two terms are sufficient to represent the system output of arrays.

The first term, $m(t+t_c)e^{j2\pi f_o t}\sum_{i=1}^{N} A_i e^{j2\pi f_o(t_i-t_c)+\alpha_i}$, has usually been considered the sole output of the array. The summation term is commonly called the array factor and is used to determine the properties of arrays (Ref 10:Chapter 1). Such things as the radiation pattern of the array, the main lobe location and beamwidth, null locations, and sidelobe properties are derived from this term. In fact, all the usual properties of arrays have been studied using only this first term of the series expansion. From the viewpoint of this Taylor series expansion the first term is the sole output of the array if and only if $f = 0$; i.e., the input is monochromatic at the array's center frequency, f_o. Nearly all antenna work makes this assumption or assumes the signal is close enough to a monochromatic signal in nature that the assumption yields valid results.

The derivation of Eq (25) shows that the time derivatives are present at the output of the array. The question should arise, then, why haven't the higher order terms of Eq (25) been observed? There are a variety of reasons of which the two most basic ones will be described: (1) the complex weighting factors and (2) typical operating techniques.

Under most circumstances the higher order terms are

extremely small compared to the first term and are not observable as a result. The basic reason for this has to do with the $(t_i - t_c)^n$ factors found in the other terms of the series. The t_i and t_c of most systems are on the order of 10^{-6} seconds or less. By attenuating the output of the first derivative term by this amount it is virtually undetectable in comparison to the first term of the series expansion under most operating conditions. However, in the neighborhood of nulls the first term of the series expansion becomes almost zero. Thus, in the neighborhood of nulls, the derivative term should be of comparable magnitude with the signal term and its existence and effects should be observable.

The second reason for not seeing the higher order terms is related strongly to the first reason. No present day system operates with the signal located at a null of the system. In fact, most systems attempt to steer the array at the signal. Recall that $t_i = \frac{r_i \cos \psi_i}{c}$. When $\psi_i = 90°$ the t_i are identically zero and there are no propagation delays (the same holds true for t_c). This location is the natural main beam axis of the array. Replacing the t_i and t_c in Eq (25) by zero results in the loss of all terms of the series except the first term, the term containing the signal m(t). This means that none of the signal's derivatives are passed through the array. The output is simply an amplified and phase shifted version of the input signal. Thus, there is no distortion. This is why the main beam is

an ideal location for the signal as has been known from all previous work in this field. Thus, most operating systems have not observed derivative terms at the output.

There is another observation that can be made about Eq (25) at this time. In general, the signal and all its derivatives will each be multiplied by different complex numbers. Each of these complex numbers will change the gain and phase of the signal and its derivatives. Thus, all the terms will have different phase angles. This means that if a phase tracking system could lock onto the phase of the signal then only the projection of the time derivatives onto this phase axis would be observed at the output. In fact, if the signal and its derivatives are shifted with respect to each other by a full 90^{o} there would be no time derivatives observed at the output. This property will be illustrated in the example in the next section.

There is one final concept about Eq (25) to be studied here. It was shown above that the derivative term is multiplied by a complex number that is usually many orders of magnitude smaller than the complex number that is combined with the signal. Thus, at most locations the signal term is dominant. However, this implies that the signal and its derivative are comparable in magnitude. The true determination of the output is the product of the signal and its gain and the product of the derivative and its gain. If the derivative term is many orders of magnitude larger than the signal term, this could offset the effect of the complex

constants to the extent that both the signal term and its derivative term would be observable in areas other than at the nulls of the array. In fact, if the derivative is large enough it could, in itself, become the dominant output everywhere except at the main beam axis.

Papoulis (Ref 15:178-182) develops a bound on signal derivatives based on the signal's energy and bandwidth. The energy of the bandlimited signal, x(t), is defined as

$$E = \int_{-\infty}^{\infty} |x(t)|^2 \, dt = \int_{-f_c}^{f_c} |X(f)|^2 \, df \qquad (26)$$

where X(f) is the Fourier transform of the signal x(t) and f_c is the frequency limit on the transform; i.e., $X(f) = 0$ for $|f| \geq f_c$. Using this, linear system theory, and the Schwarz inequality, Papoulis shows that

$$\left| \frac{d(x(t))}{dt} \right|^2 \leq \frac{8}{3} E \pi^2 f_c^3 \qquad (27)$$

The equality holds at time $t = t_o$ only if $X(f) = -jkfe^{jft_o}$, where k is a constant.

This bound is very useful in that it shows two methods by which the derivative term can be kept below certain desired levels. The first is to keep the signal energy low and the second is to keep the bandwidth of the signal low. However, both of these conditions counteract other desirable features such as the desire to have E large for high signal to noise ratios and to have wideband (f_o large) signal

transmission (spread spectrum, for instance) for anti-jamming purposes.

Eq (27) is not an equality; it is simply a bound on the derivative. It leaves the impression that the derivative increases with increases in the energy or the bandwidth, but it doesn't prove this. What Eq (25) has shown is that the derivative term is passed by the array. Papoulis has defined two parameters that can be controlled to keep the derivative bounded and thus keep the derivative's effects under some arbitrary level. However, research in this area could determine signal sets that have much smaller derivatives than this bound indicates. This research will become necessary if the trend toward using both antenna arrays and wideband signals continues.

The analysis to this point has shown the effect the array has on the incoming signal. As Eq (25) shows, the output of the array is, in general, somewhat different than the signal that entered. The question arises, then, what effect does this output have on the system's receiver. Eq (25) is too general to give specific results, but certain characteristics can be discussed.

First, we look at the coherent receiver of Figure 5. To operate properly, this receiver must measure the phase of the incoming signal and set the local oscillator phase to match this phase. Then the receiver will be "locked" onto the signal. Eq (25) reveals a potential problem with this scheme. There are a variety of signals coming through;

the signal and all its derivatives. They are all at different phases. The overall effective phase is a weighted sum of all these phases. A phase tracking system will probably lock onto the overall phase and thus will not be precisely aligned with the desired signal. When the derivative terms are small compared to the signal term, the composite phase will be almost identical to the signal phase and the coherent receiver should function normally. However, near the null points, the signal term is highly attenuated and the phase will become more controlled by the derivative term. If the phase shifts away from the signal, the loss of coherence will obviously degrade the performance of the coherent receivers. The example of Section III. C. will explore the output phase in detail and show, for a specific array and signal, just how drastically the phase can change near the nulls.

Although it is difficult to determine how Eq (25) will affect the operation of coherent receivers, it is very easy to see how it will affect the envelope detector of Figure 6. The envelope detector will just be the magnitude of the overall signal. Thus, if any of the terms is significantly larger than the other terms, the output of the envelope detector will basically be that term. Thus, qualitatively we realize that in most areas, the output will be the desired signal. Close to the nulls the first derivative term will become dominant and the output will appear to be the first derivative. At some angular distance from the null, the

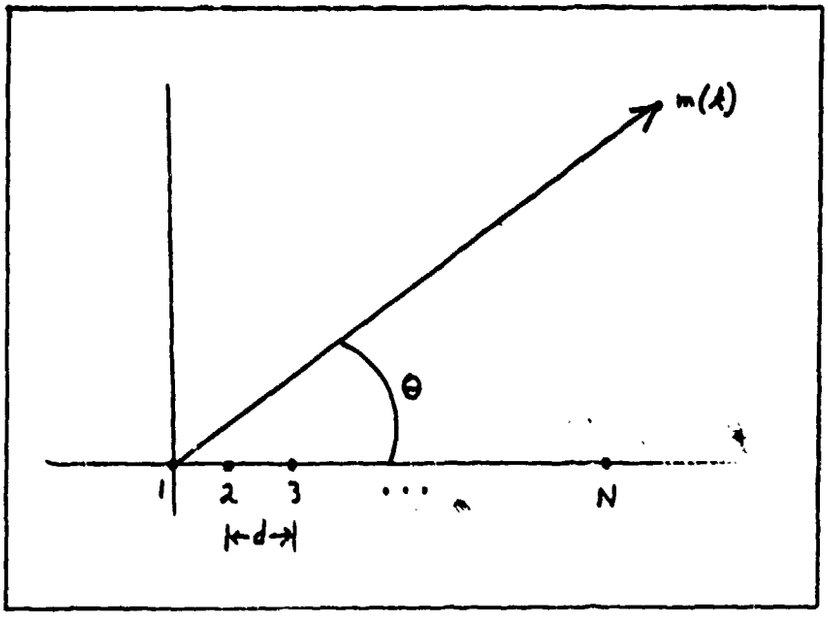

Figure 7. Linear, Equally Spaced Array.

signal term and the first derivative term will be approximately the same and the output will become their vector sum. The example of Section III. C. will also examine this situation in more detail.

Although Eq (25) contains the necessary information needed to draw all the above conclusions it is still useful to examine several specific cases that make the results more quantitative. The specific examples will illustrate more clearly just how far off the nulls that the derivative term is still significant. The examples will also discuss more quantitatively the effect of the relationship between the signal and its first derivative.

B. Linear, Equally Spaced Elements

Consider the case of a linear array with N elements all spaced equally as shown in Figure 7. Also, assume there are

no element weights; i.e.; $A_i = 1$, $\alpha_i = 0$. With the spacing and geometry shown the time delays t_i become $t_i = (i-1)\frac{d}{c}\cos\theta$. It should be noted that this geometry has removed dependence on the spatial parameter, ρ . Thus, ρ will be dropped from the equations hereafter. After substitution Eq (14) becomes

$$\tilde{s}(\theta, f) = M(f)\sum_{i=1}^{N} e^{j2\pi(f+f_0)(i-1)\frac{d}{c}\cos\theta} \tag{28}$$

Following the example of the general case, we would expand Eq (28) in a Taylor series at this point. This would result in an infinite series of summations of N elements each. However, the summation in Eq (28) can be performed directly resulting in

$$\tilde{s}(\theta, f) = M(f)\exp\left[\frac{j(N-1)\pi(f+f_0)d\cos\theta}{c}\right] \frac{\sin\frac{N\pi(f+f_0)d\cos\theta}{c}}{\sin\frac{\pi(f+f_0)d\cos\theta}{c}}$$

$$= M(f)\exp\left[\frac{j(N-1)\pi d f\cos\theta}{c}\right]$$

$$\times \exp\left[\frac{j(N-1)\pi d f_0\cos\theta}{c}\right] \frac{\sin\left[\frac{N\pi}{c}(f+f_0)d\cos\theta\right]}{\sin\left[\frac{\pi}{c}(f+f_0)d\cos\theta\right]} \tag{29}$$

We now observe that M(f) is multiplied by two exponentials and a trigonometric ratio. The exponentials are the phase-center terms obtained in Eq (20) where

$$t_c = \frac{N-1}{2}\frac{d\cos\theta}{c} \tag{30}$$

The first exponential is independent of f and is simply a complex constant when the array parameters are defined. As such it just creates a constant phase shift of the array output that can be measured and compensated for by a phase tracking system. The second exponential is a linear function of the frequency f. As such it causes a simple time delay of the signal output.

Now the trigonometric term in Eq (29) can be analyzed using a Taylor series expansion. The result is

$$\frac{\sin\left[\frac{N\pi}{c}(f+f_o)\,d\cos\theta\right]}{\sin\left[\frac{\pi}{c}(f+f_o)\,d\cos\theta\right]} = A + j2\pi f B + (j2\pi f)^2 C + \cdots \tag{31}$$

$$= \frac{\sin(N\gamma)}{\sin(\gamma)} + \frac{\frac{N\pi d\cos\theta}{c}\sin(\gamma)\cos(N\gamma) - \frac{\pi d\cos\theta}{c}\sin(N\gamma)\cos(\gamma)}{\sin^2(\gamma)} f + \cdots \tag{33}$$

where

$$\gamma = \frac{\pi f_o d\cos\theta}{c} \tag{33}$$

where the expansion has only been carried out for the first two terms. Thus,

$$A = \frac{\sin(N\gamma)}{\sin(\gamma)} \tag{34}$$

and

$$B = \frac{-j\left\{\frac{Nd\cos\theta}{2c}\sin(\gamma)\cos(N\gamma) - \frac{d\cos\theta}{2c}\sin(N\gamma)\cos(\gamma)\right\}}{\sin^2(\gamma)} \tag{35}$$

Obviously, both A and B are functions dependent on the array parameters and the signal location, θ. However, they are shown as simple constants in this frequency domain analysis.

A is the familiar radiation pattern for linear, equally spaced arrays and is used to obtain all the monochromatic and "quasi-monochromatic" results that have been published. Inserting these expressions into Eq (29) and inverse transforming yields

$$\gamma(\theta, t) = m(t + t_c) \exp\left[j 2\pi f_o t_c \right] A$$

$$+ \frac{d[m(t+t_c)]}{dt} \exp\left[j 2\pi f_o t_c \right] B + \cdots \qquad (36)$$

The value of this expression is in the following observations. First, $m(t + t_c)$ and its first derivative are multiplied by the same complex constant. Thus, this term shifts both terms by the same phase. Second, the factor A is purely real, while the factor B, although complicated, is purely imaginary. Thus, these two terms will force the signal $m(t + t_c)$, and its first derivative to be separated in phase by 90°.

This is a very interesting result because it reveals a possible technique for improving the array operation. If a phase tracking loop can lock onto the phase of the signal term, then the phase can be shifted so that only the signal will be along the imaginary axis and will not be observed at

the output of the correlator.

The linear array results obtained from Eq (36) are useful, but quantitative results still haven't been investigated to determine the extent of these effects. Thus, the next section derives results for a specific case of Eq (29).

C. Four Element, Linear Array

The specific example to be studied here will have the following parameters:

$$N = 4$$
$$d = \lambda_o/2$$
$$f_o = 350 \text{ MHz}$$

Substituting the first two parameters into Eq (29) yields

$$\tilde{o}(\theta, f) = M(f) \exp\left[j \frac{3\pi}{2} \cos\theta\right] \exp\left[j \frac{3\pi f}{2 f_o} \cos\theta\right] \frac{\sin\left[2\pi \left(1 + \frac{f}{f_o}\right) \cos\theta\right]}{\sin\left[\frac{\pi}{2}\left(1 + \frac{f}{f_o}\right) \cos\theta\right]} \qquad (37)$$

This equation can be analyzed in exactly the same way the linear array equation was analyzed in the last section. First, it is easy to recognize the first exponential as a constant phase shift that is a function of the signal's location, θ. Second, the other exponential is the time delay term that is also a function of θ. It should be noted that both these terms reduce to 1 for $\theta = 90°$. This is the location of the main beam axis for this array. Thus, for signals located on the main beam axis there is no phase shift or time delay caused by the array. Finally, it should be realized that these terms do not distort the signal; they only shift it in time and phase. However, the system

designer must compensate for these terms in his design (this may not be trivial for multiple signals and multiple locations). Thus, for this example, only the ratio of the sine functions is left to cause any signal distortion.

In the last section, this term was expanded around $f = 0$ and only two terms in the expansion were analyzed. No analysis was made to indicate when the third and higher order terms can be ignored. The usual criteria for ignoring the higher order terms is that the function that has been expanded is almost linear in the region of interest around the expansion point. In this case, the region of interest is the bandwidth of the signal.

The (sin Nx/sin x) term of this example can be expanded exactly like the similar term of the last section. This will, in fact, be done shortly. First, however, a slightly different approach will yield more insight into when the higher order terms can be ignored.

Figure 8 is a plot of the sinusoidal ratio for several values of θ. This figure shows the effect on frequency components as far as 100% away from the carrier frequency, f_o. For moderately wideband signals in the UHF range, the bandwidth-to-carrier ratio would be less than 10% and in most cases more like 1% or 2%. Thus, the region of interest is confined close to the vertical axis in Figure 8. When f/f_o is small, Figure 8 shows that the curve is very nearly linear.

Assume for a moment that in the bandwidth of interest

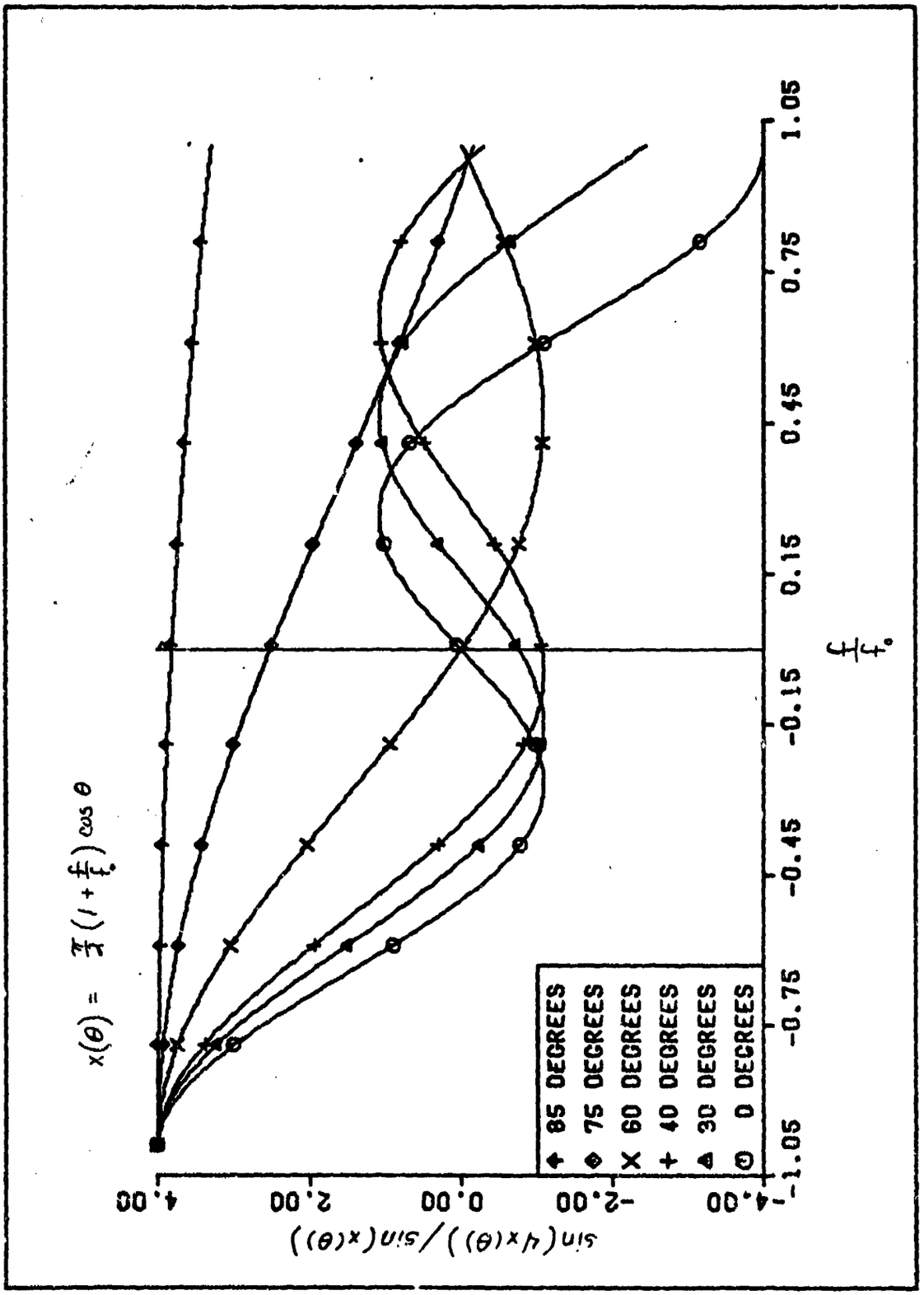

Figure 8. sin (4x(θ))/sin (x(θ)) for selected θ.

the curve is precisely linear. Then the last term in Eq (37) could be replaced by a term of the form $A + j2\pi Bf$, where A and B are real constants that are evaluated for each value of θ. Letting $t_o = \frac{\lambda \cos\theta}{4f_o}$, Eq (37) then becomes

$$\tilde{o}(\theta, f) = M(f) e^{j\frac{3\pi}{2}\cos\theta} e^{j2\pi f t_o} (A + j2\pi Bf)$$

$$= A e^{j\frac{3\pi}{2}\cos\theta} M(f) e^{j2\pi f t_o} + (j2\pi f) B e^{j\frac{3\pi}{2}\cos\theta} M(f) e^{j2\pi f t_o} \qquad (38)$$

Now the above can be transformed back into the time domain.

$$\tilde{o}(\theta, t) = e^{j\frac{3\pi}{2}\cos\theta} A m(t + t_o) + B e^{j(\frac{3\pi}{2}\cos\theta)} \frac{d}{dt}\left[m(t + t_o)\right] \qquad (39)$$

The first term is simply the signal shifted in time and moved in quadrature by the exponential term. The second term is the time derivative of the time shifted signal. It is also shifted in phase by a constant amount. Note that this phase shift is 90° less than the other phase shift.

If a receiver could track one of these components, it would not see the other component. If a coherent receiver locks onto the phase of the first term, the output will be the desired signal. If it locks onto the phase of the second term, the output will be the derivative term. If it locks onto the composite phase of the output, then the output will be determined by the relative magnitude of the various terms. As will be shown shortly, the signal term is

dominant in most regions. Thus, the phase will be close to the signal phase. Near nulls, however, the dominant term is the derivative and the phase will shift toward the derivative's phase axis.

An envelope detector (as shown in Fig. 6) would pass the magnitude to the receiver. Thus, the output of the envelope detector would be

$$c(t) = \left[\left\{ A m(t+t_0) \right\}^2 + \left\{ B \frac{d[m(t+t_0)]}{dt} \right\}^2 \right]^{\frac{1}{2}} \qquad (40)$$

after the quadrature detection. The first term is the desired signal. The other term can be considered a noise term. As long as this term is small compared to the signal, the receiver will be able to operate. This can occur in several ways: B can be very small compared to A or the derivative can be small compared to the signal.

The results of Eqs (39) and (40) were obtained based on the assumption that the trigonometric term in Eq (37) can validly be modeled as a linear function of frequency. As stated earlier, the curves of Figure 8 indicate that this model is valid for $f/f_0 < .1$.

We can now evaluate the constants of the linear model through the use of the Taylor series expansion. Substituting the array parameter into Eq (32) yields

$$\frac{\sin\left[2\pi\left(1+\frac{f}{f_0}\right)\cos\theta\right]}{\sin\left[\frac{\pi}{2}\left(1+\frac{f}{f_0}\right)\cos\theta\right]} = \frac{\sin(2\pi\cos\theta)}{\sin\left(\frac{\pi}{2}\cos\theta\right)}$$

$$+ \frac{\pi\cos\theta}{f_0}\left[\frac{2\sin\left(\frac{\pi}{2}\cos\theta\right)\cos(2\pi\cos\theta) - \frac{1}{2}\cos\left(\frac{\pi}{2}\cos\theta\right)\sin(2\pi\cos\theta)}{\sin^2\left(\frac{\pi}{2}\cos\theta\right)}\right] f + \cdots \qquad (41)$$

Thus,

$$A = \frac{\sin(2\pi\cos\theta)}{\sin(\frac{\pi}{2}\cos\theta)} \tag{42}$$

and

$$B = -j\frac{\cos\theta}{4f_o}\left[\frac{4\sin(\frac{\pi}{2}\cos\theta)\cos(2\pi\cos\theta) - \cos(\frac{\pi}{2}\cos\theta)\sin(2\pi\cos\theta)}{\sin^2(\frac{\pi}{2}\cos\theta)}\right] \tag{43}$$

The term A is the usual array factor term used for antenna analysis. By plotting $|A|$ in a polar plot, we obtain the antenna radiation pattern (Fig. 9). The main lobe, side lobes, and nulls are defined according to this term. As can be seen, this array has nulls at 0° and 60°. By plotting $|B|$ in a similar way we have what can be called the "time derivative radiation pattern" (Fig. 10).

By observing these two plots, a very interesting phenomenon is observed. The location of the main lobe and sidelobe peaks in the antenna radiation pattern is the location of the nulls in the time derivative radiation pattern. Furthermore, it is seen that the opposite occurs. The peaks in the time derivative radiation pattern are the same as the nulls for the antenna radiation pattern. Later examples (Section III. D.) seems to indicate that the reciprocal relationship between these two parameters holds in general. No effort has been expended to determine under which conditions this phenomenon exists or whether it has any practical uses. It is just pointed out that the phenomenon exists in

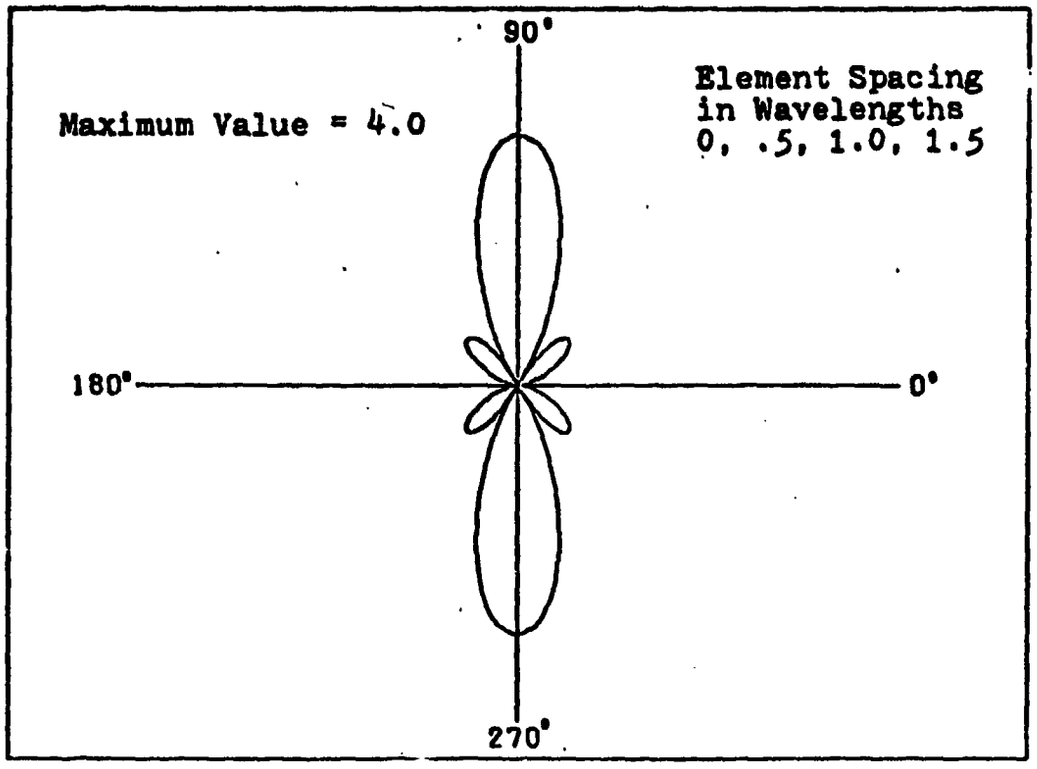

Figure 9. Four Element Equally Spaced Array, Plot of $|A(\theta)|$.

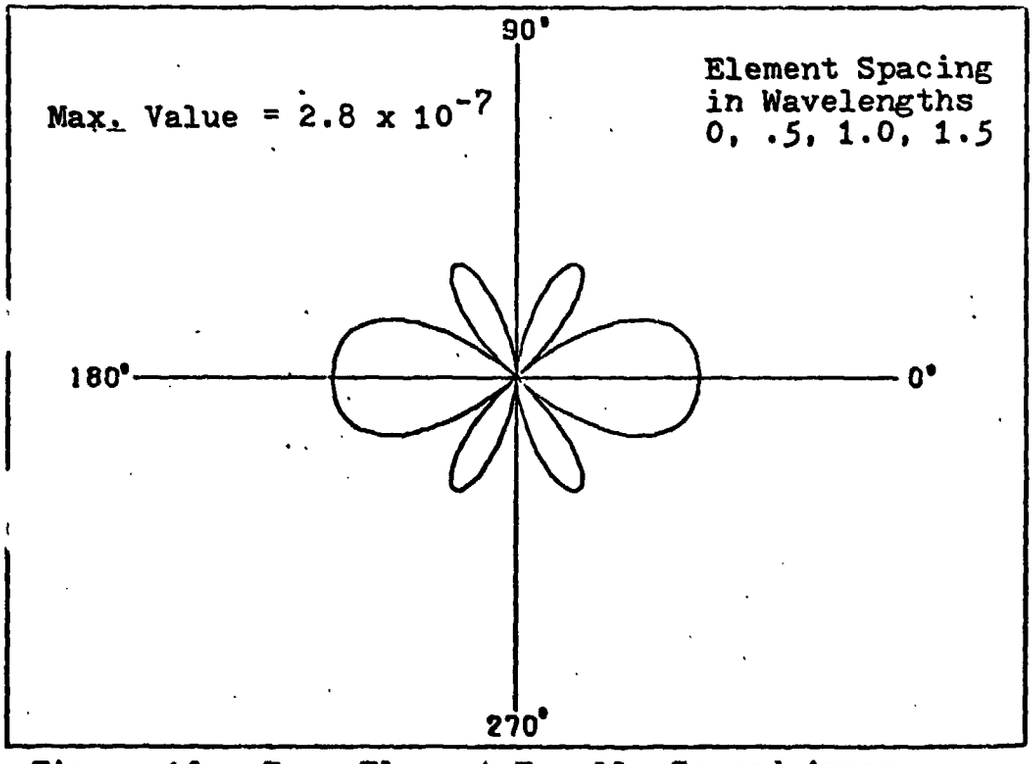

Figure 10. Four Element Equally Spaced Array, Plot of $|B(\theta)|$.

the examples used in this thesis and the author suggests that it be given a closer examination.

It is easy to show that $|A|$ and $|B|$ are symmetrical about both $\theta = 0^\circ$ and $\theta = 90^\circ$. Thus, data about these numbers in the first quadrant are sufficient to describe their values everywhere. Table I tabulates these two numbers in the first quadrant. As can be observed, B is very small compared to A except in the neighborhood of the two null points at 0° and 60°. Tables II and III tabulate these numbers in more detail around the null points. These latter tables show that A decreases and becomes comparable to B near the two nulls.

The values in the tables were calculated using a computer to evaluate Eqs (42) and (43). Thus, roundoff errors are a concern when the numbers become small. This effect is evident at the two null points 0° and 60°. By simple substitution into Eq (42), it is readily seen that A is zero at these locations. Also, B should be zero at $\theta = 90^\circ$. The tables do not show zero results at these points. The calculations were run a second time using double precision numbers. The results at these three points became closer to the correct values indicating that the errors are due to roundoff errors that accumulate during the calculations. What is important, however, is that none of the other entries changed when the double precision calculations were carried out. This indicates that there is no roundoff error (to seven significant figures) in any of the other entries.

TABLE I. TABULATION OF A AND B FROM EQUATIONS (42) AND (43).

ANGLE (DEGREES)	A	B	ANGLE	A	B	ANGLE	A	B
1.00	-.956[illegible]E-03	.2650797E-08	31.00	-.8018325E+00	.1576545E-08	61.00	.1331077E+00	-.2049420E-08
2.00	-.3[illegible]E-02	.235[illegible]335E-08	32.00	-.8339746E+00	.1554710E-08	62.00	.2635250E+00	-.2062945E-08
3.00	-.3510[illegible]E-02	.265311[illegible]E-08	33.00	-.8757770E+00	.1449335E-08	63.00	.4357624E+00	-.2067035E-08
4.00	-.1779[illegible]E-01	.2843912E-08	34.00	-.9116897E+00	.1319104E-08	64.00	.5942563E+00	-.2051193E-08
5.00	-.2399[illegible]E-01	.2845010E-08	35.00	-.9449553E+00	.1187778E-08	65.00	.7533734E+00	-.2025251E-08
6.00	-.3[illegible]E-01	.2840124E-08	36.00	-.9756081E+00	.1051172E-08	66.00	.9774073E+00	-.1965397E-08
7.00	-.4592[illegible]E-01	.2833319E-08	37.00	-.1003450E+01	.9096703E-09	67.00	.1109583E+01	-.1935164E-08
8.00	-.5111[illegible]E-01	.2828[illegible]E-08	38.00	-.1026030E+01	.7627209E-09	68.00	.1277082E+01	-.1877226E-08
9.00	-.7[illegible]E-01	.2811134E-08	39.00	-.1045115E+01	.6139401E-09	69.00	.1459994E+01	-.1798791E-08
10.00	-.9[illegible]E-01	.2803320E-08	40.00	-.1055107E+01	.4605946E-09	70.00	.1630745E+01	-.1714624E-08
11.00	-.11[illegible]E+00	.2789475E-08	41.00	-.1075647E+01	.3046755E-09	71.00	.1617265E+01	-.1621977E-08
12.00	-.13[illegible]E+00	.2773372E-08	42.00	-.1055296E+01	.1467455E-09	72.00	.1937643E+01	-.1521640E-08
13.00	-.15[illegible]E+00	.2754622E-08	43.00	-.1056641E+01	-.1241465E-10	73.00	.2173426E+01	-.1414636E-08
14.00	-.18[illegible]E+00	.2733109E-08	44.00	-.1035275E+01	-.1719829E-09	74.00	.2352544E+01	-.1293122E-08
15.00	-.212[illegible]E+00	.2709512E-08	45.00	-.1017576E+01	-.3213921E-09	75.00	.2524917E+01	-.1167753E-08
16.00	-.241[illegible]E+00	.268[illegible]1E-08	46.00	-.1059725E+01	-.4565302E-09	76.00	.2637456E+01	-.1073246E-08
17.00	-.271[illegible]E+00	.2649[illegible]E-08	47.00	-.1035741E+01	-.6442511E-09	77.00	.2654681E+01	-.3522443E-09
18.00	-.3[illegible]E+00	.2613[illegible]7E-08	48.00	-.1005571E+01	-.7967521E-09	78.00	.3003723E+01	-.4351626E-09
19.00	-.3[illegible]E+00	.2573307E-08	49.00	-.9557017E+00	-.9442313E-09	79.00	.3133363E+01	-.7206255E-09
20.00	-.371[illegible]E+00	.2528316E-08	50.00	-.9231011E+00	-.1060504E-08	80.00	.3229098E+01	-.6100872E-09
21.00	-.4[illegible]E+00	.2480236E-08	51.00	-.8692777E+00	-.1223102E-08	81.00	.3420545E+01	-.5030307E-09
22.00	-.44[illegible]E+00	.2421102E-08	52.00	-.8070974E+00	-.1352143E-08	82.00	.3537473E+01	-.4068511E-09
23.00	-.48[illegible]E+00	.2366[illegible]E-08	53.00	-.7352764E+00	-.1472988E-08	83.00	.3647616E+01	-.3163596E-09
24.00	-.5[illegible]E+00	.2301591E-08	54.00	-.6570101E+00	-.1584703E-08	84.00	.3773334E+01	-.2362575E-09
25.00	-.551[illegible]E+00	.2230977E-08	55.00	-.5539315E+00	-.1656444E-08	85.00	.3814560E+01	-.1651266E-09
26.00	-.591[illegible]E+00	.215[illegible]E-08	56.00	-.4721355E+00	-.1777795E-08	86.00	.3833915E+01	-.1074095E-09
27.00	-.6[illegible]E+00	.2073535E-08	57.00	-.3656627E+00	-.1156545E-08	87.00	.3937725E+01	-.6069819E-10
28.00	-.6[illegible]E+00	.1992[illegible]E-08	58.00	-.2526997E+00	-.1924151E-08	88.00	.3973009E+01	-.2721915E-10
29.00	-.72[illegible]E+00	.1835515E-08	59.00	-.1303629E+00	-.1970760E-08	89.00	.3992468E+01	-.6027667E-11
30.00	-.7[illegible]E+00	.1760237E-08	60.00	.5226692E-14	-.2020325E-08	90.00	.4000009E+01	-.1442574E-36

TABLE II. TABULATION OF A AND B FROM EQUATIONS (42) AND (43).

ANGLE (DEGREES)	A	B	ANGLE	A	B	ANGLE	A	B
0.00	[illegible]E-14	.2657143E-08	1.50	-.2153089E-02	.2656158E-08	3.00	-.8610581E-02	.2653141E-08
.05	[illegible]E-05	.2657142E-08	1.55	-.2239012E-02	.2656091E-08	3.05	-.8900145E-02	.2653004E-08
.10	[illegible]E-05	.2657139E-08	1.60	-.2449717E-02	.2656022E-08	3.10	-.9194266E-02	.2652864E-08
.15	-.217[illegible]E-04	.2657133E-08	1.65	-.2605206E-02	.2655950E-08	3.15	-.9493165E-02	.2652722E-08
.20	[illegible]E-04	.2657125E-08	1.70	-.2765471E-02	.2655876E-08	3.20	-.9796840E-02	.2652577E-08
.25	[illegible]E-04	.2657116E-08	1.75	-.2930532E-02	.2655800E-08	3.25	-.1010523E-01	.2652429E-08
.30	[illegible]E-04	.2657104E-08	1.80	-.3100369E-02	.2655722E-08	3.30	-.1041852E-01	.2652279E-08
.35	-.117[illegible]E-03	.2657090E-08	1.85	-.3274986E-02	.2655641E-08	3.35	-.1073652E-01	.2652127E-08
.40	-.15[illegible]E-03	.2657073E-08	1.90	-.3454390E-02	.2655558E-08	3.40	-.1105930E-01	.2651972E-08
.45	[illegible]E-03	.2657055E-08	1.95	-.3638573E-02	.2655473E-08	3.45	-.1138685E-01	.2651815E-08
.50	[illegible]E-03	.2657034E-08	2.00	-.3827579E-02	.2655385E-08	3.50	-.1171919E-01	.2651655E-08
.55	[illegible]E-03	.2657011E-08	2.05	-.4021287E-02	.2655295E-08	3.55	-.1205623E-01	.2651492E-08
.60	[illegible]E-03	.2656985E-08	2.10	-.4219815E-02	.2655203E-08	3.60	-.1239817E-01	.2651327E-08
.65	[illegible]E-03	[illegible]E-08	2.15	-.4423127E-02	.2655109E-08	3.65	-.1274487E-01	.2651159E-08
.70	[illegible]E-03	.2656927E-08	2.20	-.4631219E-02	.2655012E-08	3.70	-.1309625E-01	.2650989E-08
.75	[illegible]E-03	.2656898E-08	2.25	-.4844097E-02	.2654913E-08	3.75	-.1345245E-01	.2650816E-08
.80	-.612[illegible]E-03	[illegible]E-08	2.30	-.5061747E-02	.2654811E-08	3.80	-.1381343E-01	.2650640E-08
.85	[illegible]E-03	[illegible]E-08	2.35	-.5284142E-02	.2654708E-08	3.85	-.1417917E-01	.2650462E-08
.90	[illegible]E-03	[illegible]E-08	2.40	-.5511396E-02	.2654601E-08	3.90	-.1454969E-01	.2650281E-08
.95	[illegible]E-03	.2656749E-08	2.45	-.5743305E-02	.2654493E-08	3.95	-.1492198E-01	.2650098E-08
1.00	[illegible]E-03	.2656707E-08	2.50	-.5980171E-02	.2654382E-08	4.00	-.1530504E-01	.2649912E-08
1.05	[illegible]E-02	[illegible]E-08	2.55	-.6221770E-02	.2654215E-08	4.05	-.1569387E-01	.2649723E-08
1.10	-.115[illegible]E-02	.26566[illegible]E-08	2.60	-.6468054E-02	.2654153E-08	4.10	-.1608347E-01	.2649531E-08
1.15	-.12[illegible]E-02	[illegible]E-08	2.65	-.6719180E-02	.2654035E-08	4.15	-.1647884E-01	.2649337E-08
1.20	-.137[illegible]E-02	.2656514E-08	2.70	-.6975075E-02	.2653915E-08	4.20	-.1687299E-01	.2649140E-08
1.25	[illegible]E-02	.26564[illegible]E-08	2.75	-.7235780E-02	.2653792E-08	4.25	-.1727690E-01	.2648941E-08
1.30	-.151[illegible]E-02	.26564[illegible]E-08	2.80	-.7501203E-02	.2653667E-08	4.30	-.1768558E-01	.2648738E-08
1.35	-.174[illegible]E-02	[illegible]E-08	2.85	-.7771435E-02	.2653539E-08	4.35	-.1809903E-01	.2648533E-08
1.40	-.18[illegible]E-02	.2656265E-08	2.90	-.8046446E-02	.2653409E-08	4.40	-.1851724E-01	.2648325E-08
1.45	-.2011[illegible]E-02	.2656223E-08	2.95	-.8326234E-02	.2653275E-08	4.45	-.1894023E-01	.2648115E-08

TABLE III. TABULATION OF A AND B FROM EQUATIONS (42) AND (43).

ANGLE (DEGREES)	A	B	ANGLE	A'	B	ANGLE	A	B
59.12	-.11[illegible]E+00	-.1964462E-08	59.72	-.3730190E-01	-.2010013E-08	60.32	.4337279E-01	-.2030772E-08
59.14	-.112[illegible]E+00	-.196[illegible]331E-08	59.74	-.3465377E-01	-.2010763E-08	60.34	.4610915E-01	-.2031390E-08
59.16	-.11[illegible]E+00	-.198[illegible]314E-08	59.76	-.3201046E-01	-.2011553E-08	60.36	.4834957E-01	-.2031993E-08
59.18	-.1[illegible]E+00	-.195[illegible]232E-08	59.78	-.2936006E-01	-.2012311E-08	60.38	.5159[illegible]E-01	-.2032[illegible]E-08
59.20	-.10[illegible]E+00	-.196[illegible]1[illegible]E-08	59.80	-.2670651E-01	-.2013006E-08	60.40	.5437769E-01	-.2033[illegible]E-08
59.22	-.1[illegible]E+00	-.19[illegible]E-08	59.82	-.2404995E-01	-.2013[illegible]E-08	60.42	.5731[illegible]E-01	-.2033[illegible]E-08
59.24	-.9[illegible]1[illegible]E-01	-.19[illegible]E-08	59.84	-.2139012E-01	-.2014[illegible]E-08	60.44	.59[illegible]E-01	-.20[illegible]E-08
59.26	-.[illegible]E-01	-.19[illegible]E-08	59.86	-.1[illegible]7772[illegible]E-01	-.2015[illegible]E-08	60.46	.62[illegible]E-01	-.2034[illegible]E-08
59.28	-.[illegible]E-01	-.199174[illegible]E-08	59.88	-.1[illegible]035172E-01	-.2016025E-08	60.48	.65[illegible]E-01	-.2035[illegible]E-08
59.30	-.[illegible]E-01	-.19[illegible]30[illegible]E-08	59.90	-.1333211E-01	-.2016752E-08	60.50	.69112[illegible]E-01	-.2035[illegible]E-08
59.32	-.[illegible]E-01	-.199[illegible]11E-08	59.92	-.1071035E-01	-.2017473E-08	60.52	.70876[illegible]E-01	-.2036613E-08
59.34	-.[illegible]E-01	-.1[illegible]337E-08	59.94	-.8[illegible]4[illegible]E-02	-.2018189E-08	60.54	.735[illegible]E-01	-.2037167E-08
59.36	-.[illegible]E-01	-.19[illegible]2[illegible]7E-08	59.96	-.5356143E-02	-.2018[illegible]E-08	60.56	.7E[illegible]E-01	-.2037716E-08
59.38	-.[illegible]E-01	-.1[illegible]177E-08	59.98	-.2[illegible]4[illegible]E-02	-.2019[illegible]E-08	60.58	.791[illegible]3E-01	-.2038[illegible]E-08
59.40	-.7[illegible]E-01	-.1[illegible]2E-08	60.00	-.2[illegible]120[illegible]E-13	-.2020[illegible]E-08	60.60	.8[illegible]2565E-01	-.2038796E-08
59.42	-.[illegible]E-01	-.1[illegible]37E-08	60.02	.2[illegible]7717E-02	-.202[illegible]E-08	60.62	.8[illegible]E-01	-.2039[illegible]E-08
59.44	-.[illegible]E-01	-.1[illegible]E-08	60.04	.5375[illegible]E-02	-.2021[illegible]E-08	60.64	.8[illegible]E-01	-.2039[illegible]E-08
59.46	-.7[illegible]E-01	-.19[illegible]E-08	60.06	.3077[illegible]E-02	-.2022373E-08	60.66	.9[illegible]E-01	-.2040[illegible]E-08
59.48	-.[illegible]E-01	-.2000359E-08	60.08	.1075977E-01	-.2023051E-08	60.68	.93[illegible]E-01	-.2040[illegible]E-08
59.50	-.[illegible]E-01	-.200[illegible]E-08	60.10	.13[illegible]E-01	-.2023724E-08	60.70	.9[illegible]E-01	-.2041407E-08
59.52	-.[illegible]E-01	-.2002031E-08	60.12	.1[illegible]E-01	-.202[illegible]E-08	60.72	.9[illegible]151E-01	-.2041912E-08
59.54	-.[illegible]E-01	-.2002[illegible]E-08	60.14	.1337875E-01	-.2025054E-08	60.74	.1014784E+00	-.2042412E-08
59.56	-.[illegible]E-01	-.20[illegible]E-08	60.16	.2[illegible]E-01	-.2025711E-08	60.76	.10[illegible]E+00	-.2042907E-08
59.58	-.[illegible]E-01	-.200[illegible]3E-08	60.18	.2[illegible]E-01	-.202[illegible]E-08	60.78	.107[illegible]E+00	-.204[illegible]E-08
59.60	-.[illegible]E-01	-.200[illegible]E-08	60.20	.27[illegible]E-01	-.2027[illegible]E-08	60.80	.10[illegible]E+00	-.2043[illegible]E-08
59.62	-.[illegible]E-01	-.200[illegible]E-08	60.22	.2[illegible]E-01	-.2027[illegible]E-08	60.82	.112[illegible]E+00	-.2044[illegible]E-08
59.64	-.[illegible]E-01	-.200[illegible]E-08	60.24	.3[illegible]577E-01	-.202[illegible]E-08	60.84	.11[illegible]E+00	-.204[illegible]E-08
59.66	-.[illegible]E-01	-.200[illegible]E-08	60.26	.3[illegible]E-01	-.2028915E-08	60.86	.1187223E+00	-.204[illegible]E-08
59.68	-.4[illegible]E-01	-.20[illegible]E-08	60.28	.3730[illegible]E-01	-.202[illegible]E-08	60.88	.121140[illegible]E+00	-.2045761E-08
59.70	-.3[illegible]E-01	-.2003[illegible]E-08	60.30	.4053[illegible]E-01	-.2030156E-08	60.90	.1235506E+00	-.204621[illegible]E-08

THIS PAGE IS BEST QUALITY PRACTICABLE FROM COPY FURNISHED TO DDC

These tables illustrate, for this example, the statement in Section III. A. that the multiplier of the derivative term is usually orders of magnitude smaller than the multiplier of the signal term. This table also indicates another valid reason why the derivative term is not normally observed. As can be seen from the tables, B is on the order of 10^{-8}. Thus, the derivative term is attenuated by a voltage ratio of 80 dB or more at all signal locations. This amount of attenuation will normally push the derivative term down into the system's noise region.

At this point, then, it appears ludicrous to study such an insignificant signal further. However, there are two things that will counter this attenuation effect. The first reason is the concept of spread spectrum itself. By using a PN coded signal, spread spectrum techniques typically give the system an extra 20 - 30 dB of SNR capabilities with a practical upper limit of about 70 dB (Ref 4:7 and 24). Thus, spread spectrum systems have the capability to detect low level signals if they know what they're looking for. The analysis of this thesis indicates what the form of that low level signal happens to be.

The second reason comes from the increasing demand for higher data transmission rates. For certain signal sets, the higher the data rate the higher the time derivatives for constant amplitude signals. Thus, for high data or code rates the derivative could itself be orders of magnitude higher than the signal. This would offset the 80 dB loss

considerably. These two reasons can combine to make the derivative term a signal that can be observed and can have an effect on the system output.

The fact that signals and their derivatives can be orders of magnitude different leads to the problem of determining at which locations around the array that the derivative term has a noticeable effect on the array output. Tables I, II, and III are not really in a format that quickly show this.

Typically a designer would indicate that the effect of the derivative term is ignorable if the signal output-to-derivative output ratio is greater than some value, η .

$$\frac{Am(t)}{B\frac{dm(t)}{dt}} \geq \eta \tag{44}$$

Rearranging and taking logarithms yields

$$\log \frac{A}{B} \geq \log\left(\frac{m'(t)}{m(t)}\right) + \log \eta \tag{45}$$

Now, the designer can use this as a criterion to determine those regions where the array will operate satisfactorily. The ratio, log A/B, for the array example of this section has been plotted in Figure 11.

To see how to use this figure, a signal and its derivative are required. One of the purposes of this thesis was to determine the effects of arrays on spread spectrum signals. This can be partially accomplished by determining

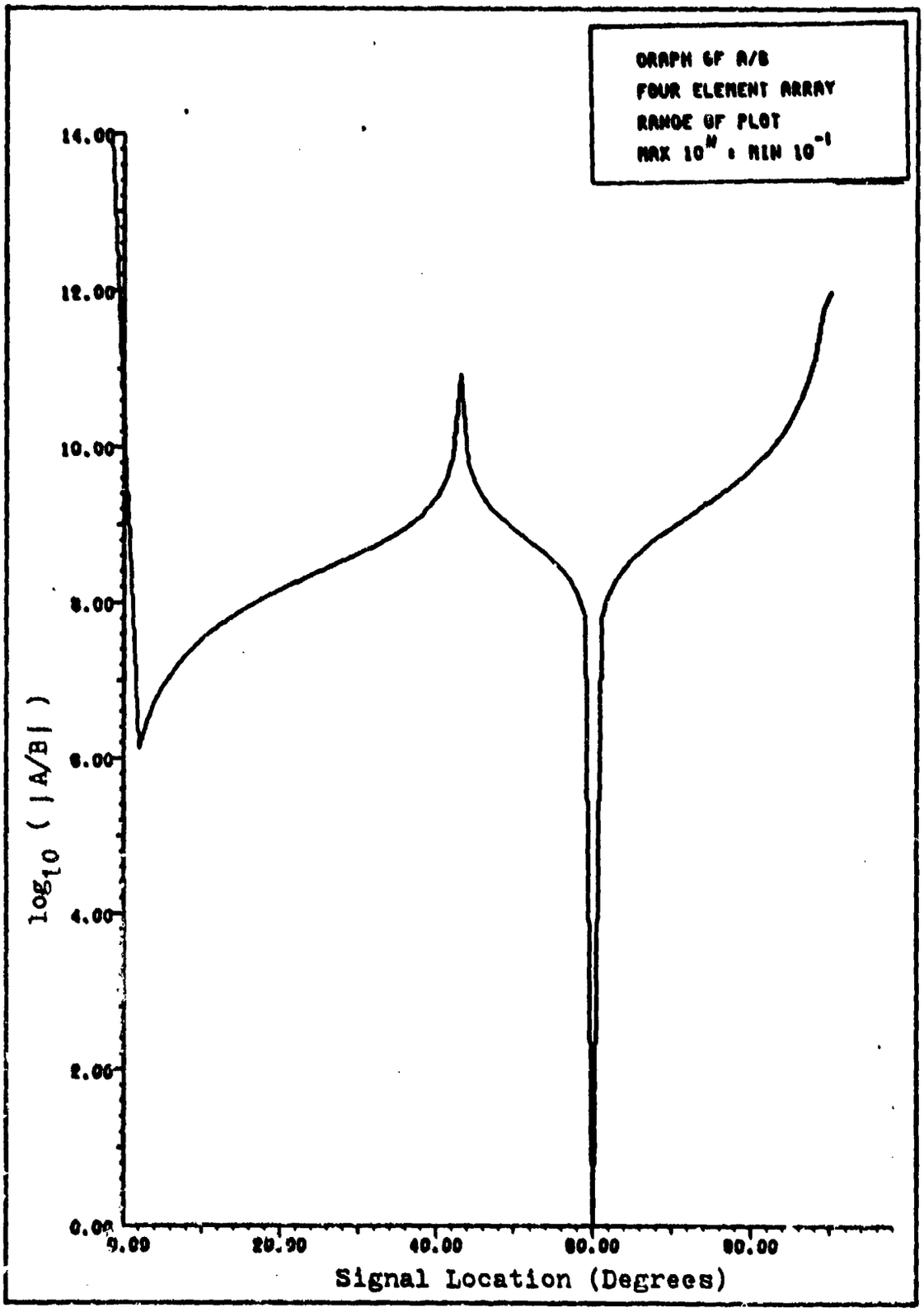

Figure 11. Plot of the Ratio, |A/B| .

the array effects on just the PN code. We recall that the incoming signal is correlated with the code in order to despread the signal. Thus, if the code is the sole input, we are ultimately interested in the array effects on the code's correlation function. It is true that the correlation of a PN code word with itself is a triangular waveform of height NT and width 2T, where T is the chip period and N is the code length (Ref 4:64-67). Therefore, for the remainder of this example the signal will be considered to be the triangular waveform of Figure 12.

Using the specific values in Figure 12, the ratio has the value 5×10^5 near $\ell = 0$. Also, assume that an acceptable value for η is 10. Eq (45) becomes

$$\begin{aligned} \log \frac{A}{B} &\geq \log 5 \times 10^5 + \log 10 \\ &= 5.7 + 1.0 \\ &= 6.7 \end{aligned} \tag{46}$$

Figure 11 shows that A/B exceeds this threshold everywhere except very close to the two null points. If either η or the ratio is increased, the area of acceptable operation will decrease. This example illustrates the procedure that can be followed by the engineer in evaluating his system's operation.

In the course of studying the properties of this array, a computer program was written to implement Eq (14). The

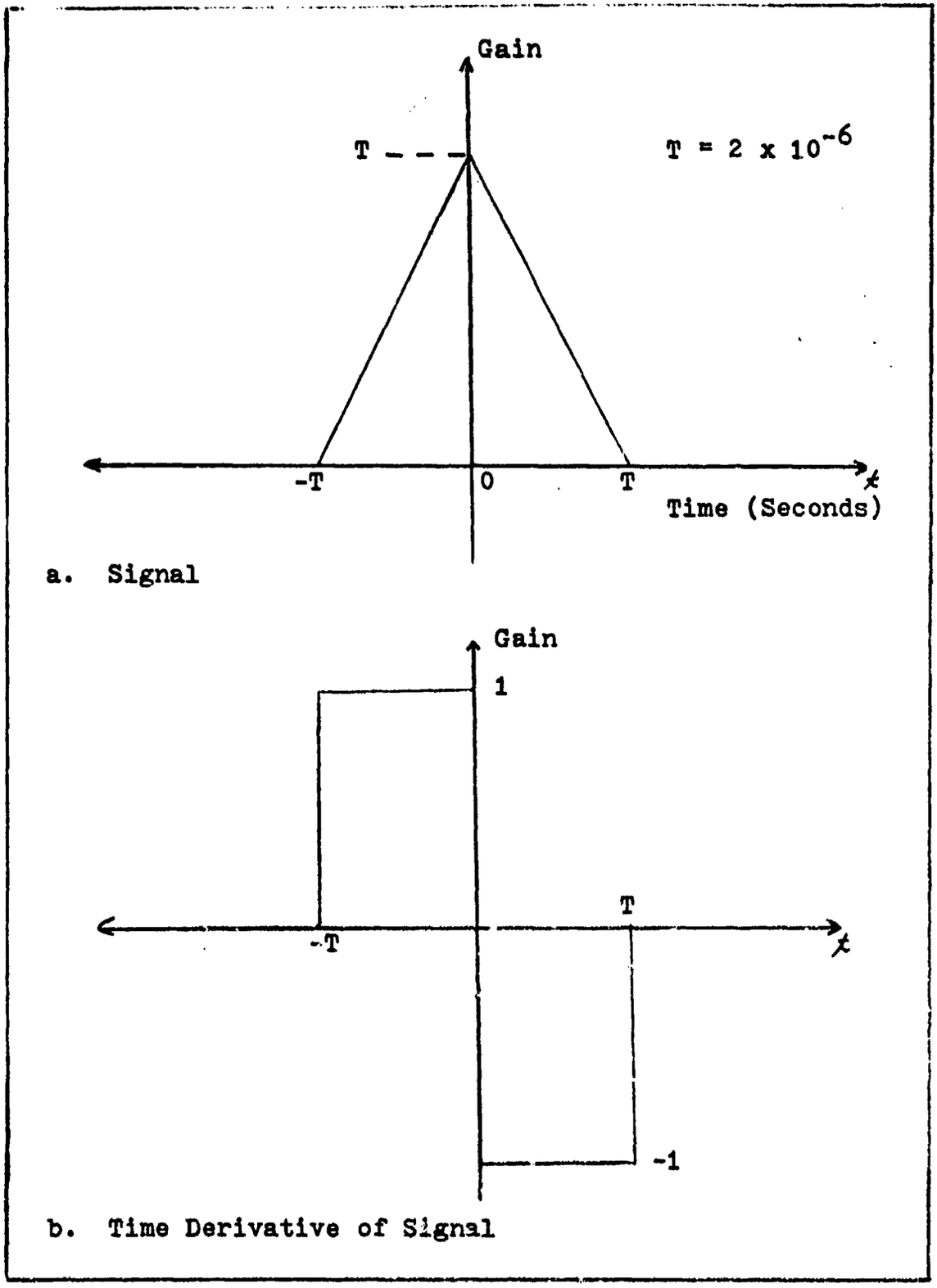

Figure 12. Sample Signal.

appendix discusses the details of this program. The only important details needed here are that the parameters of this example were included in the program, plots for various signal locations were requested, and the signal used was the triangular signal of Figure 12.

As is easily shown, the first derivative of a triangular signal is a square wave. The basic form of the signal and its derivative were illustrated in Figure 12. This signal was originally selected because it represents the correlation function of a PN code. Notice that the time derivative has an amplitude that is 5×10^5 times larger than the signal. This will cause the time derivative term to have more effect on the overall output than predicted by the constants A and B alone. This should lead the reader to the realization that signals with triangular correlation functions are not good signals to use with arrays if the effect of derivatives is undesirable.

As will be shown momentarily, the plots from this computer program illustrate quite nicely the results discussed to this point. By substituting the parameters of this example into the program we are in essence programming the time domain version of Eq (37) which is basically Eq (39).

The computer program was run for seven different signal locations: 0°, 1°, 10°, 40°, 60°, 70.53°, and 90°. These locations include the two null positions, 0° and 60°, and the main beam axis, 90°. The output waveform is complex. It can be manipulated in several different ways to obtain

the equivalent output of real systems.

The first operation performed is to plot the real part of the complex waveform. This is equivalent to looking at a coherent detector that is locked onto zero relative phase. As can be seen from the phase shift terms of Eq (39), the phase of the signal varies from 270° to 0° (passing through 180°) as the signal location moves from 0° to 90° while the phase of the derivative term moves from 180° to -90° in the same interval. Thus, at 0° and at $\cos^{-1}(1/3)$ (approximately 70.53°) it is seen that the time derivative's phase places it on the real axis and the signal's phase places it on the imaginary axis. Thus, this coherent receiver will not see the signal at these locations. At other signal locations, the receiver will see components of both signals on the real axis. The size of the signal will be large compared to the derivative in most cases and the derivative won't be observable. Near 60°, though, the signal's magnitude drops and the derivative component becomes observable. Figures 13 through 19 illustrate what the real part of the output looks like. As can be seen, the output is mostly the derivative near the two nulls, 0° and 60°, and it is mostly the derivative at 70.53°. At 10° we observe the effect of both signals on the output. If we had selected a signal closer to the null at 0°, the derivative term would be more evident in the output.

The reader should note that the figures that contain the square wave signal have low amplitude oscillations near

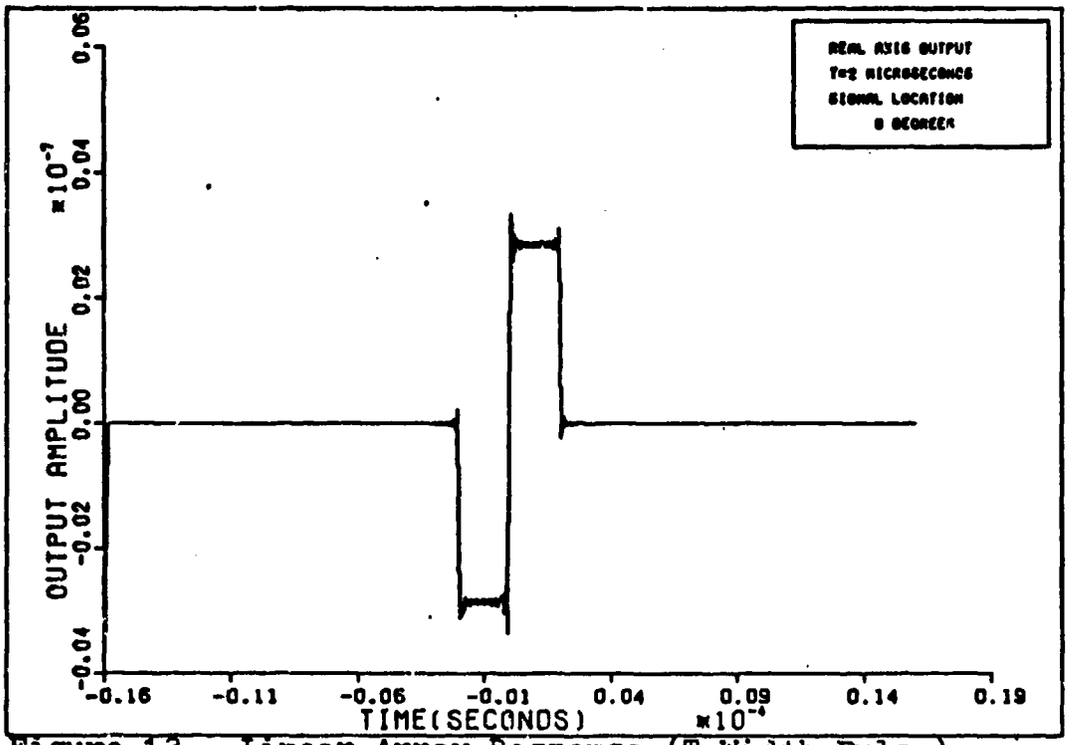

Figure 13. Linear Array Response (T Width Pulse).

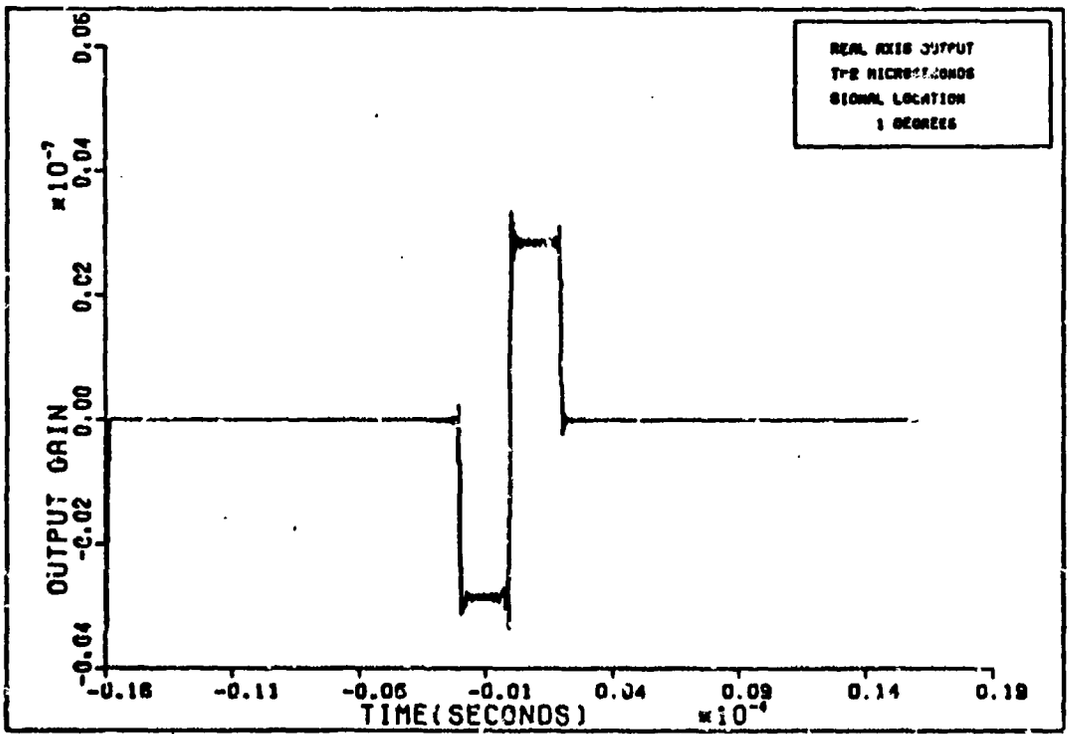

Figure 14. Linear Array Response (T Width Pulse).

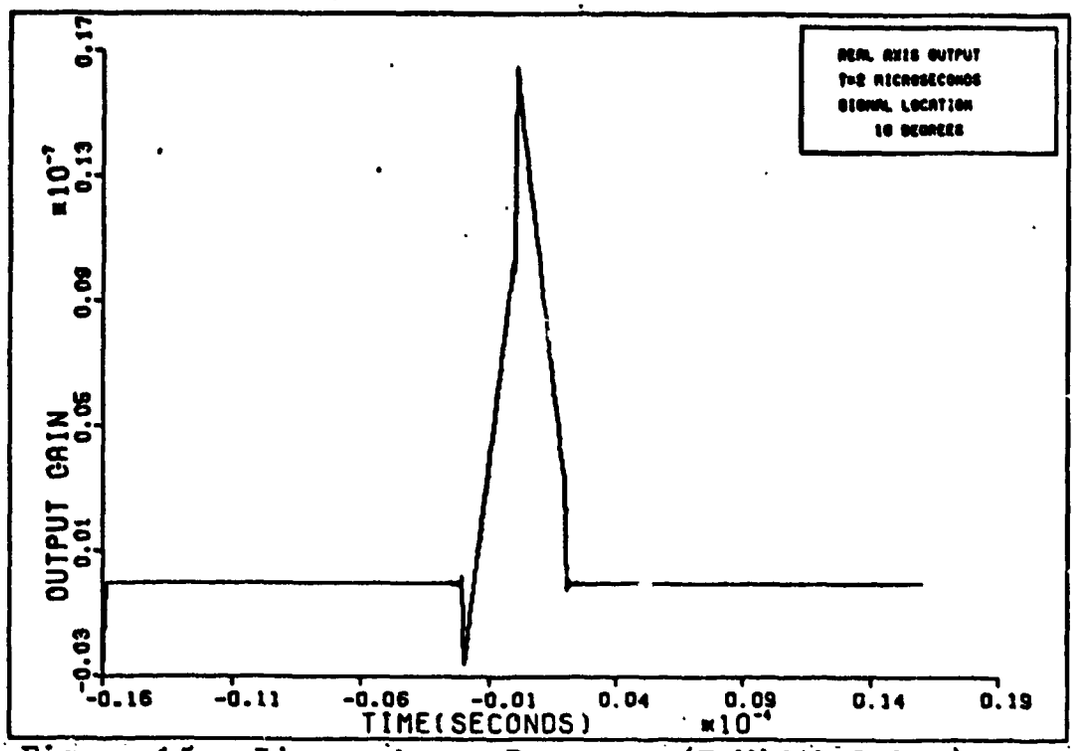

Figure 15. Linear Array Response (T Width Pulse).

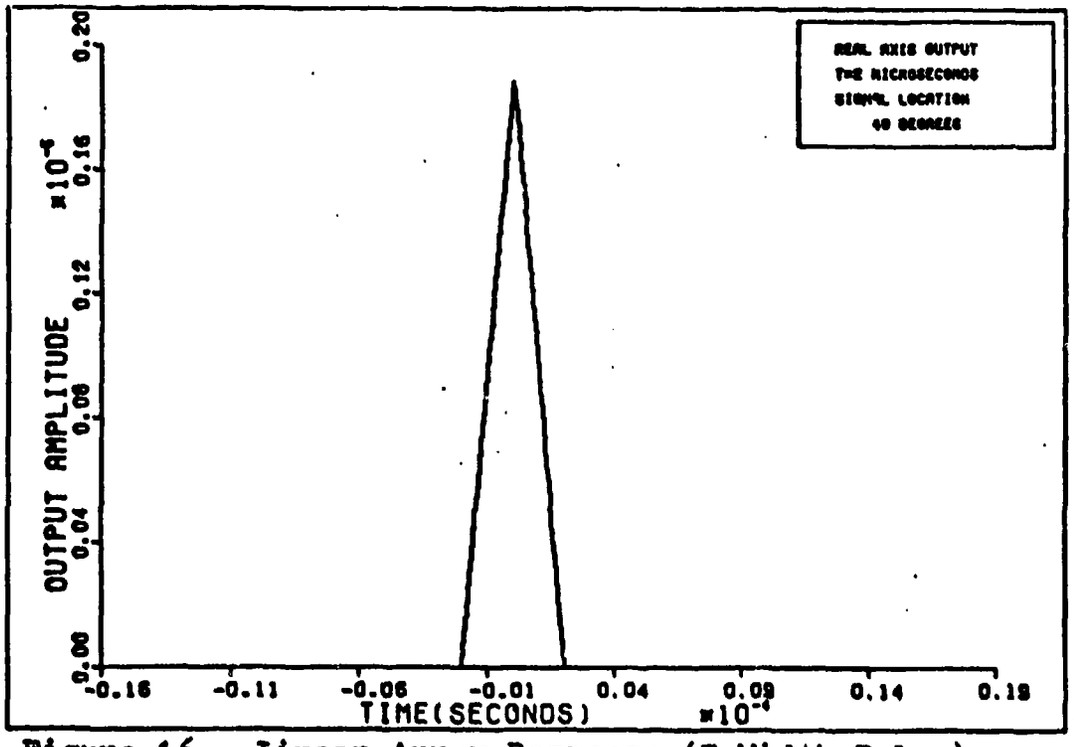

Figure 16. Linear Array Response (T Width Pulse).

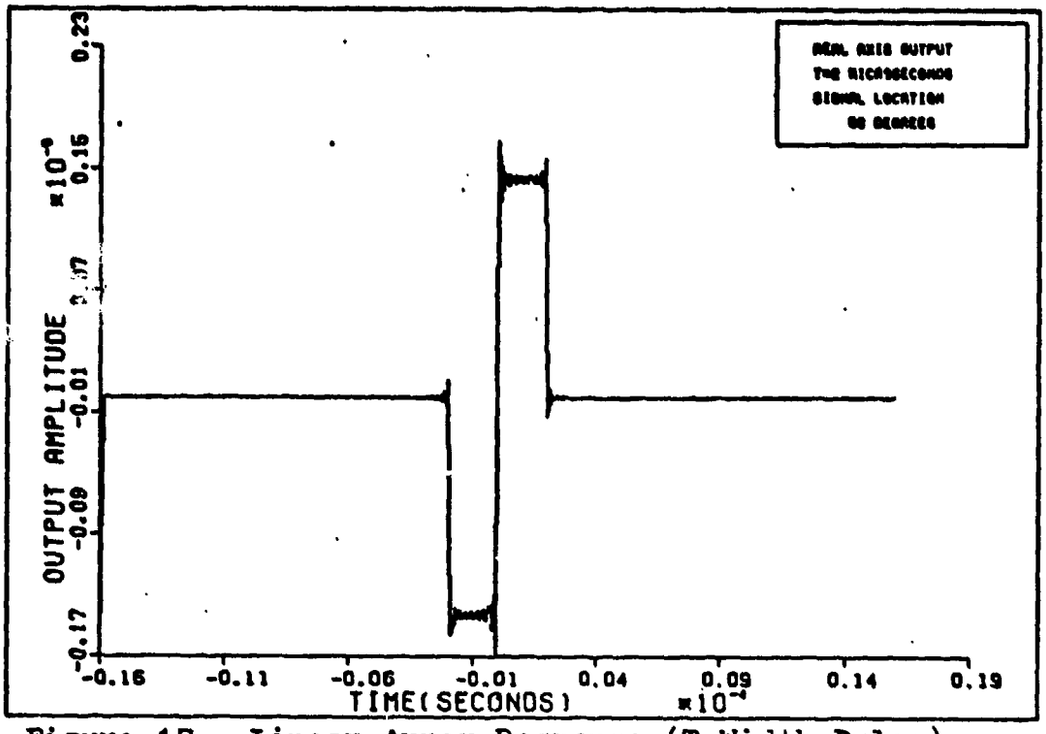

Figure 17. Linear Array Response (T Width Pulse).

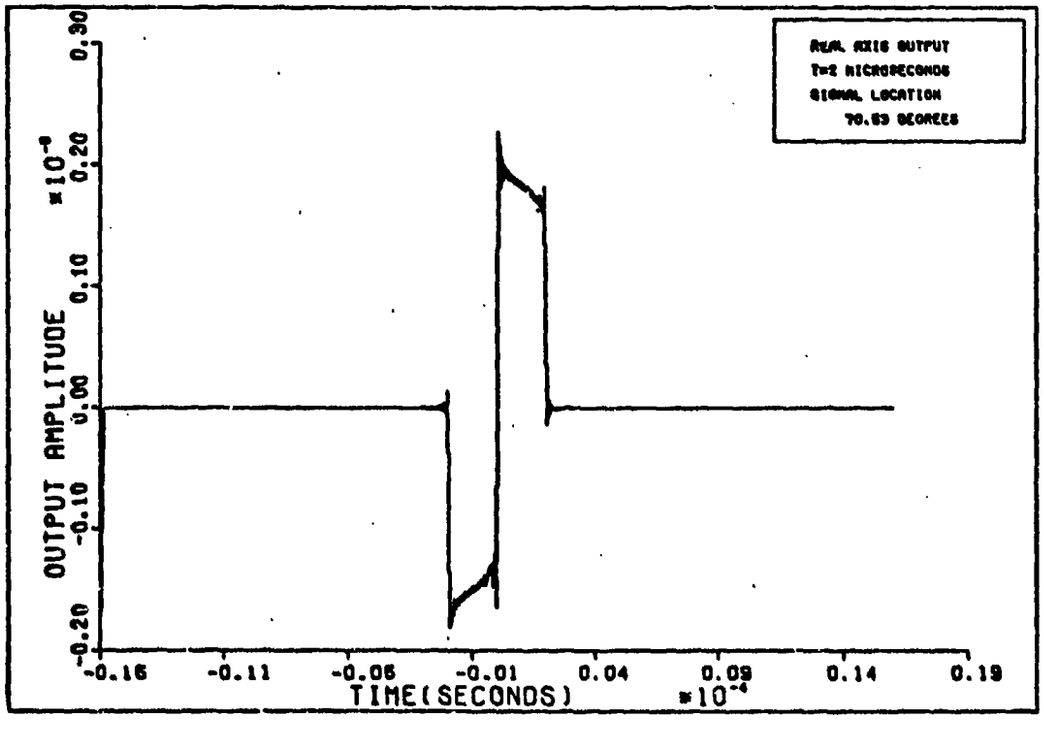

Figure 18. Linear Array Response (T Width Pulse).

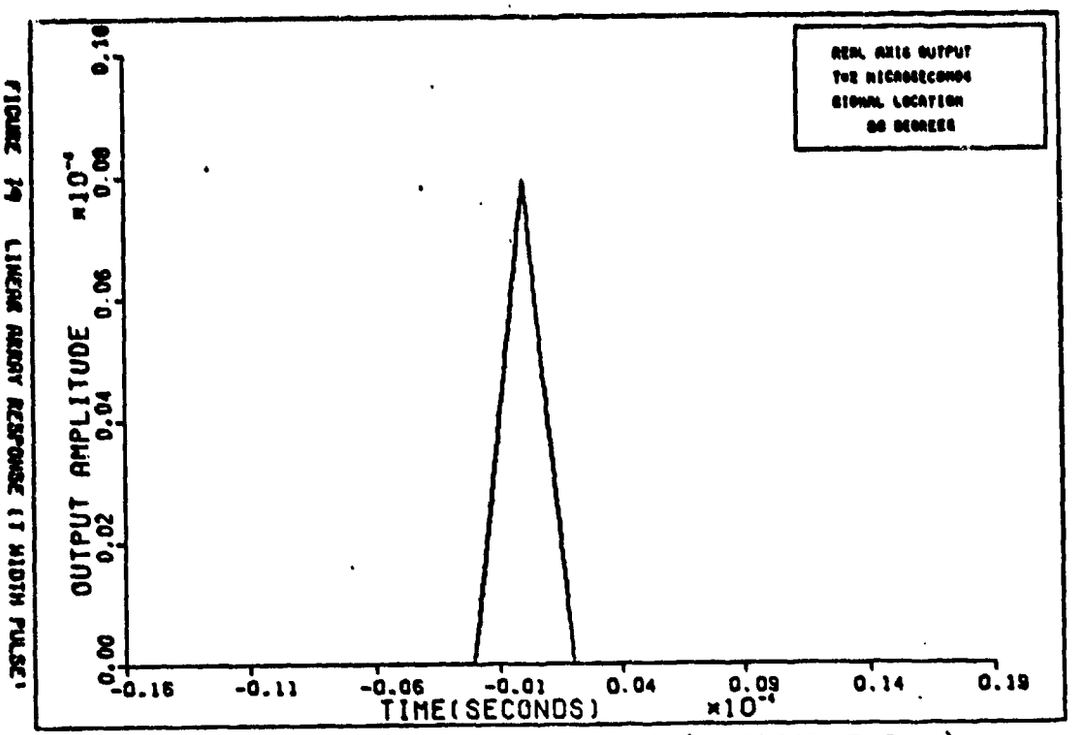

Figure 19. Linear Array Response (T Width Pulse).

the corners of the square wave. These oscillations are caused by the Gibbs phenomenon (Ref 2:105-107). In essence, these oscillations are created any time a signal with discontinuities is represented by a finite length Fourier series.

The next operation performed by the program is to plot the magnitude of the complex waveform. This is equivalent to looking at the output of an envelope detector. The results are shown in Figures 20 through 26. Comparing these plots with Figures 13 through 19 shows that the envelope detector yields the desired signal as an output more often than the coherent receiver used; e.g., compare Figure 18 with Figure 25. Figure 21 is the most interesting of this group. It illustrates the appearance of the output when

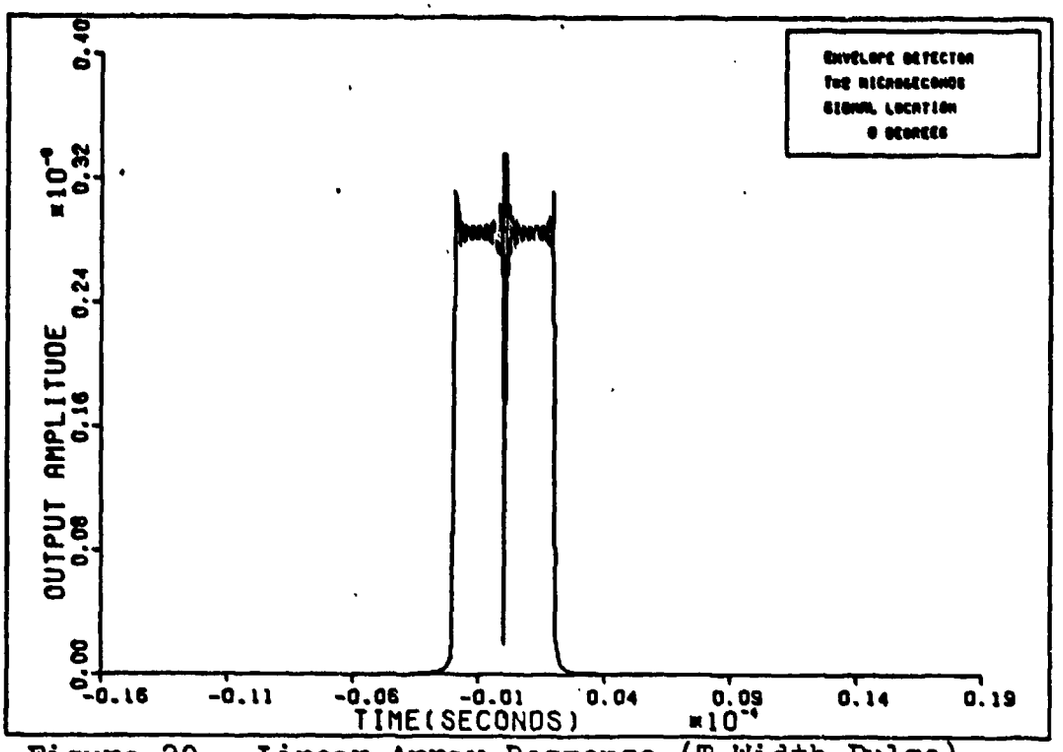

Figure 20. Linear Array Response (T Width Pulse).

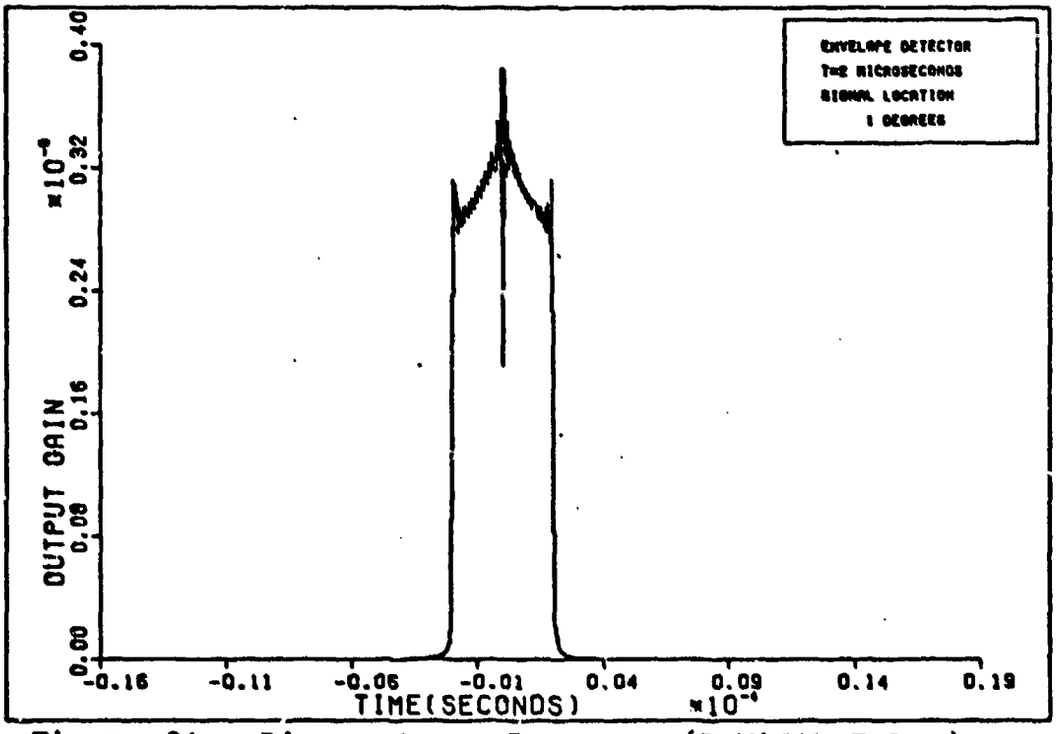

Figure 21. Linear Array Response (T Width Pulse).

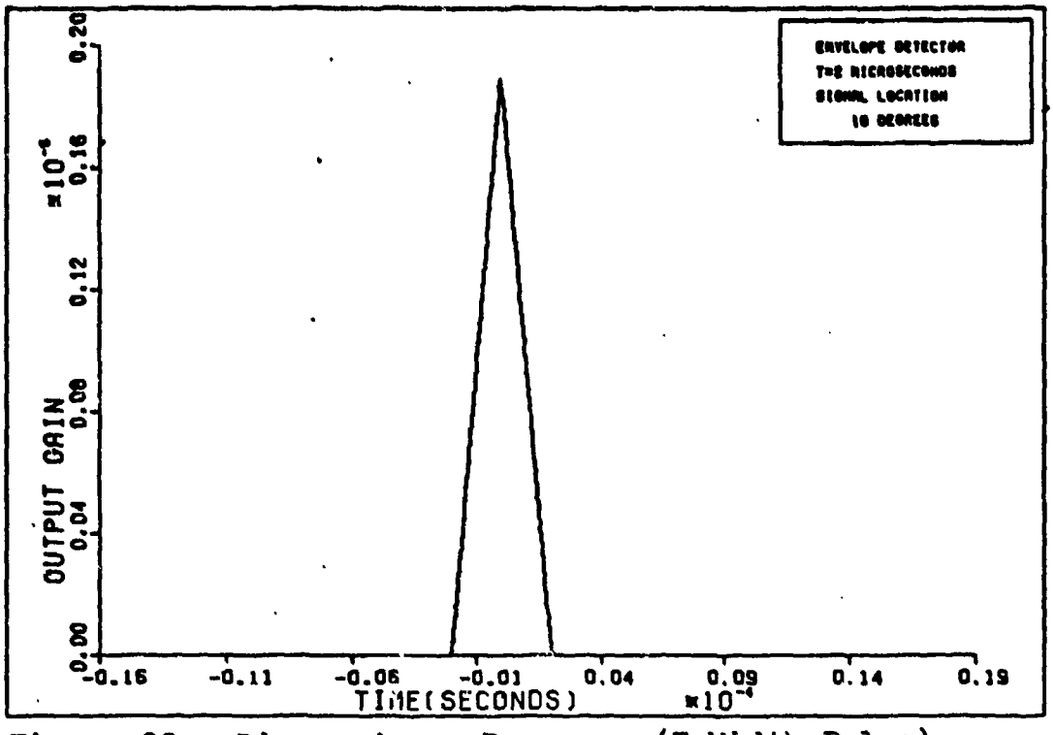

Figure 22. Linear Array Response (T Width Pulse).

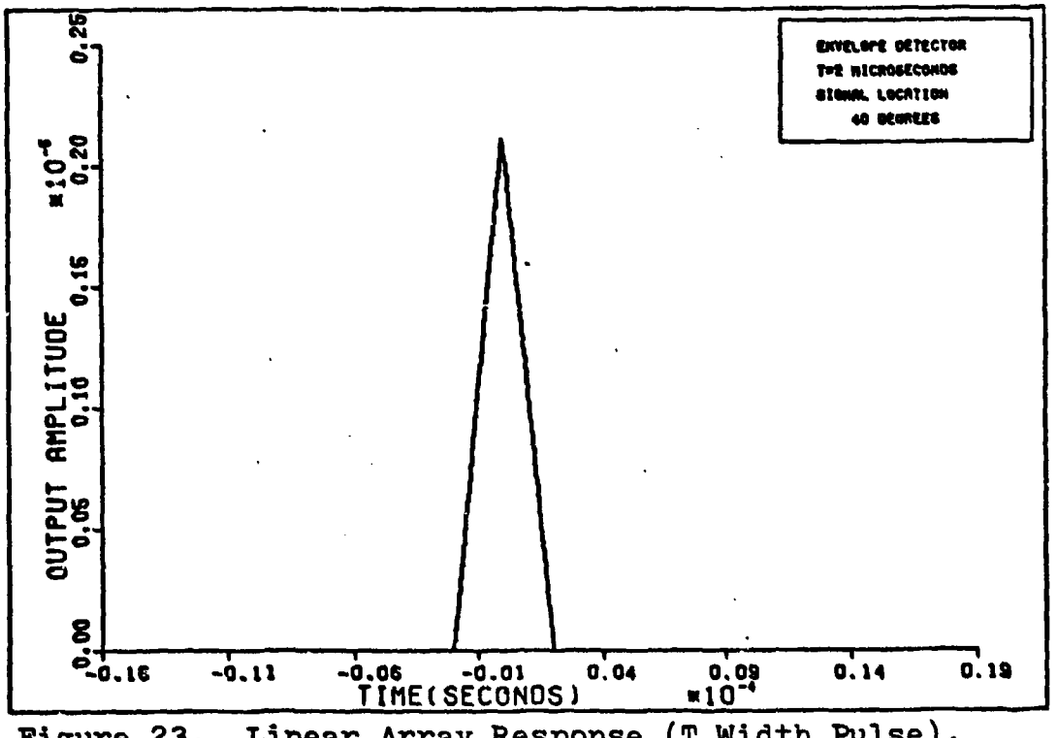

Figure 23. Linear Array Response (T Width Pulse).

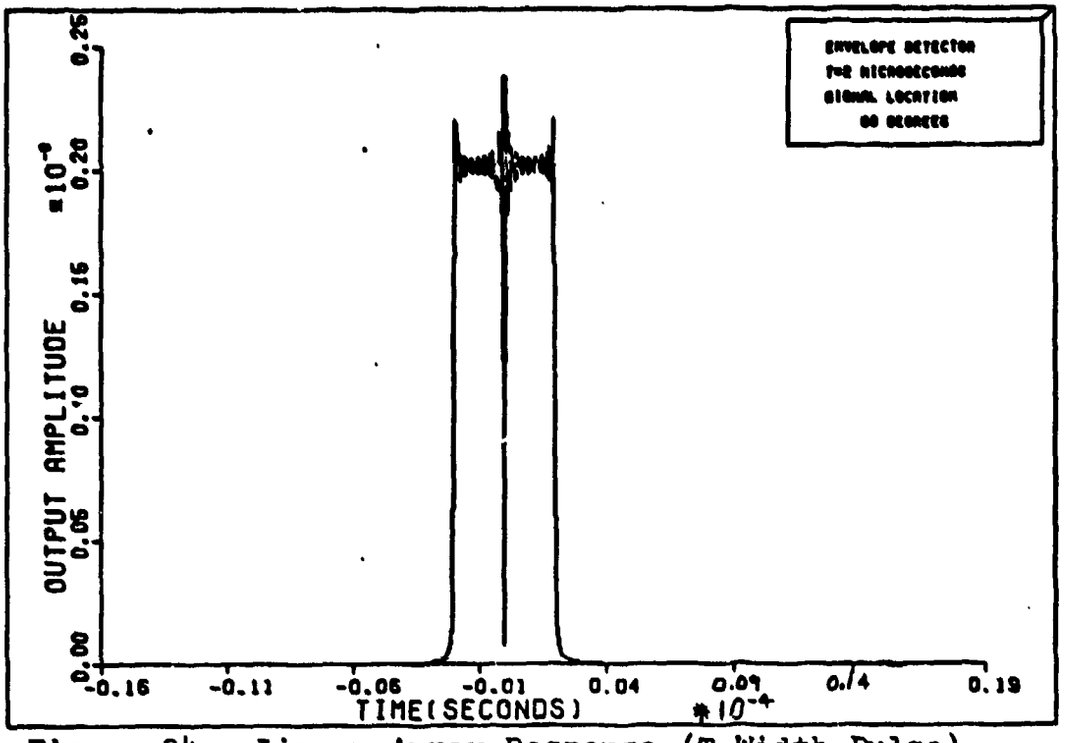

Figure 24. Linear Array Response (T Width Pulse).

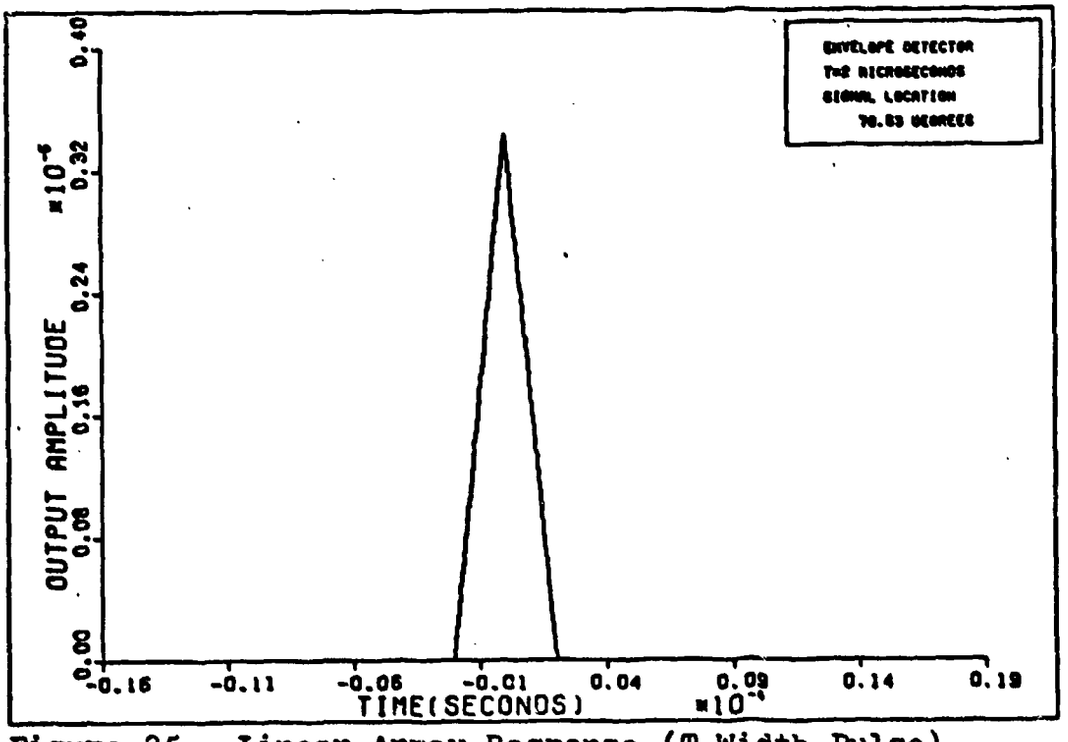

Figure 25. Linear Array Response (T Width Pulse).

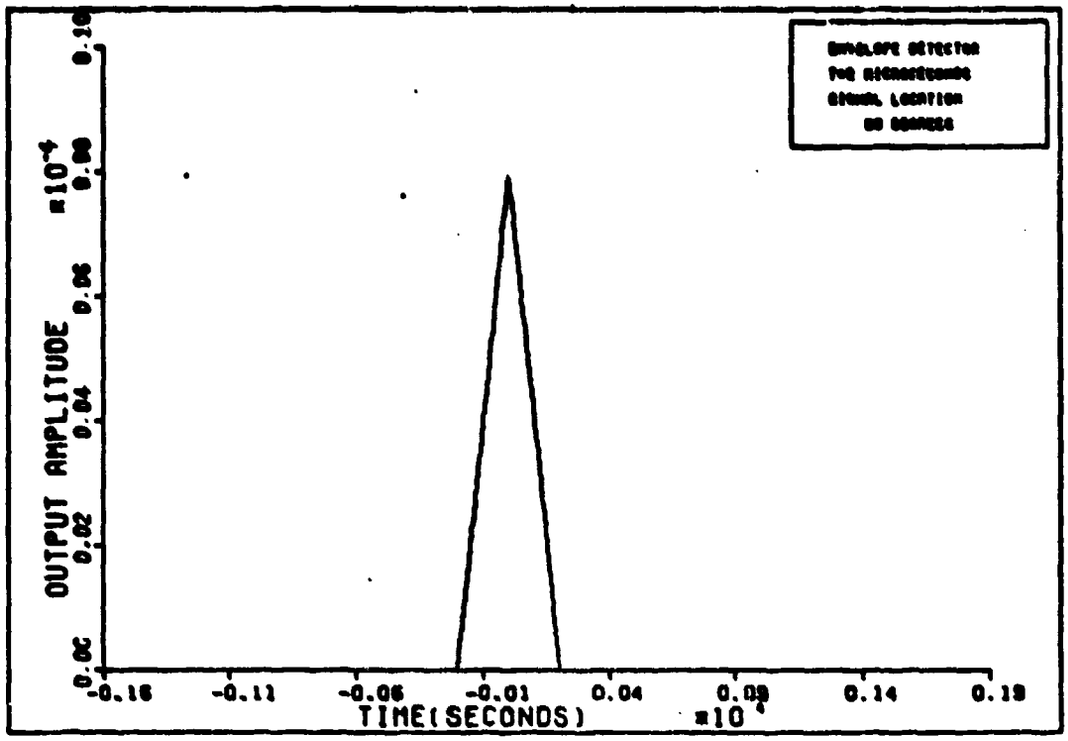

Figure 26. Linear Array Response (T Width Pulse).

the signal term and the derivative term are both about the same magnitude.

The third operation performed by the program is to separate the signal and its derivative into separate quadratures. This is possible because the signal and the derivative are separated by 90° of phase shift. Recall that this is not necessarily true for all arrays. It holds for all linear, equally spaced arrays and this example is a member of that set, but it does not hold for all array geometries. Thus, we can separate the signal and its derivative here, but they cannot be separated into separate quadratures in any system. The technique used in the program is to multiply the complex output by the complex conjugate of the phase of the signal

term in Eq (39). This multiplier is $e^{-j\frac{2\pi}{\lambda}\cos\theta}$. The result of this operation is to leave the signal as the real part of the complex waveform and the derivative term as the imaginary part. The program then plots these two waveforms separately. The results are shown in Figures 27 through 40.

Figures 27 and 35 show that the signal term vanishes at the two nulls and Figure 40 shows that the derivative term vanishes at 90°, the main beam axis. These figures quite nicely illustrate the effect of the constants A and B from Table I on the magnitude of the output terms. For example, the signal triangle peaks at 2×10^{-6} (Fig. 12a). The parameter A has the value of -9.5×10^{-4} at 1° (Table I). Thus, the output of the signal quadrature should be

$$2 \times 10^{-6} \times -9.5 \times 10^{-4} = -1.9 \times 10^{-9} \qquad (47)$$

As can be seen, this is the peak value of the triangular waveform in Figure 29. This result can be confirmed in all the other figures shown here.

The inverted waveform of Figure 29 brings up an interesting point about threshold detector systems. If this array was used with a system that transmitted positive going pulses to represent a +1 and negative going pulses to represent 0, then the detector would have interpreted the pulse at 1° incorrectly. Figure 37 shows that the same pulse would have been interpreted correctly if the signal were at 70°. With a little thought the reader should realize that

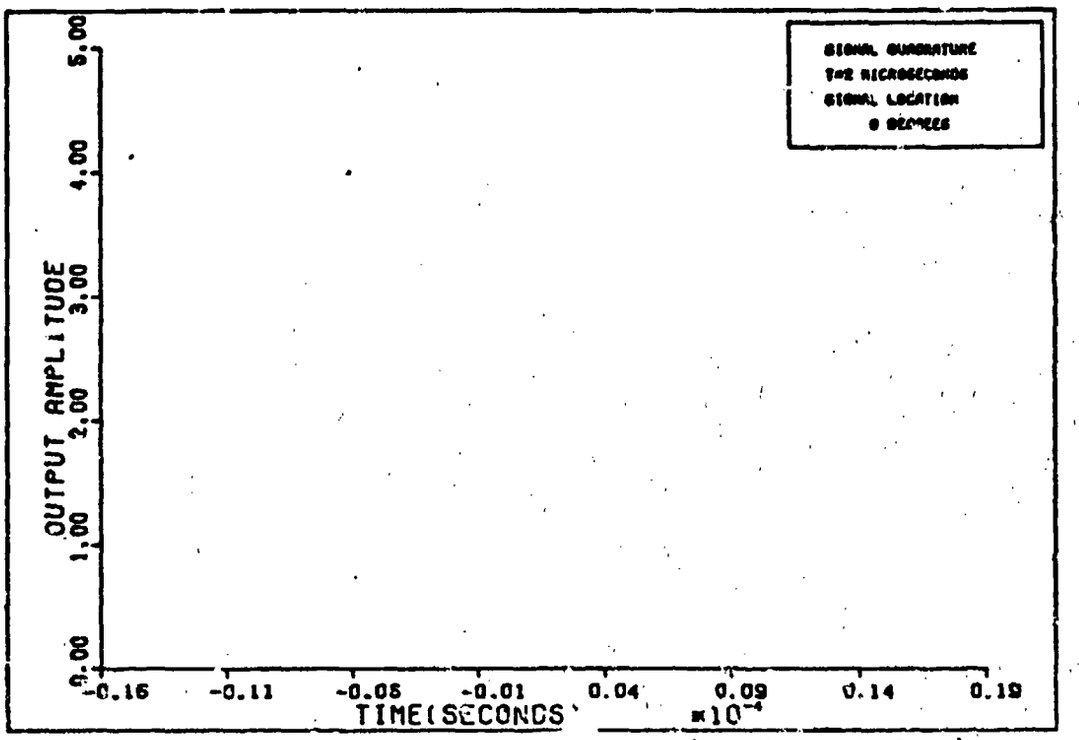

Figure 27. Linear Array Response (T Width Pulse).

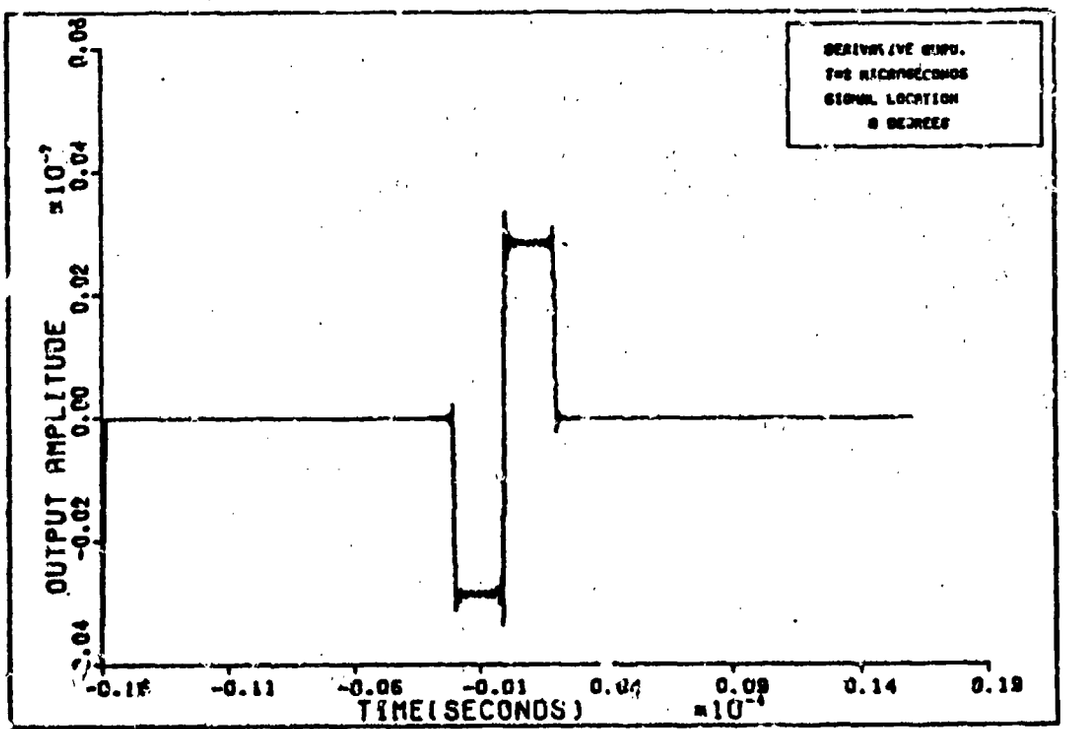

Figure 28. Linear Array Response (T Width Pulse).

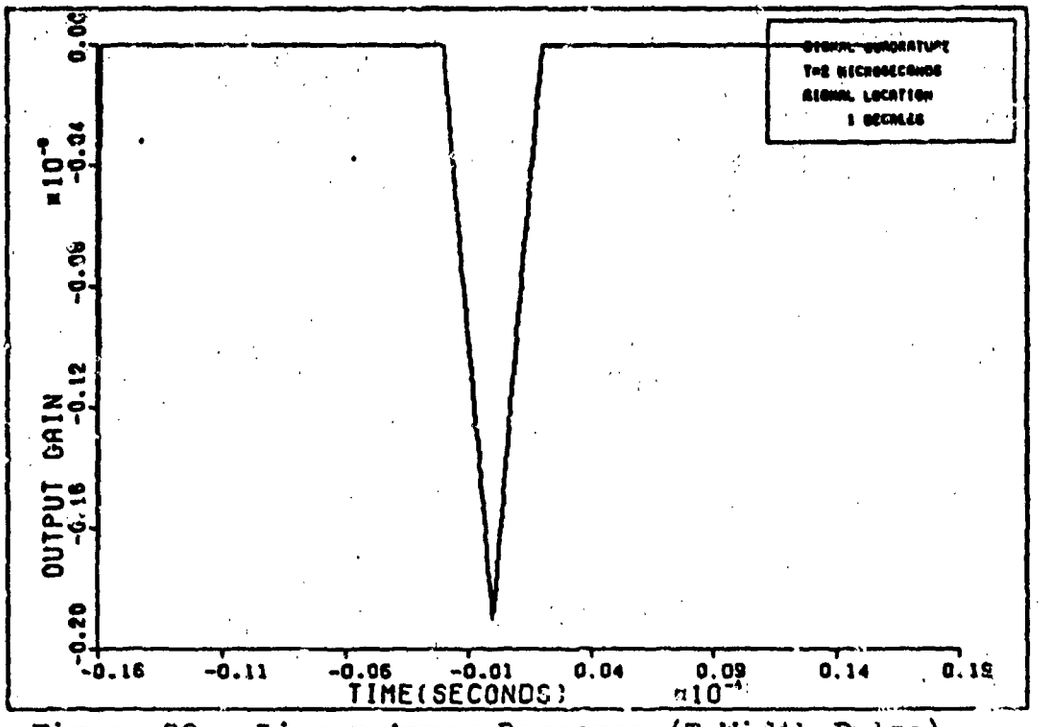

Figure 29. Linear Array Response (T Width Pulse).

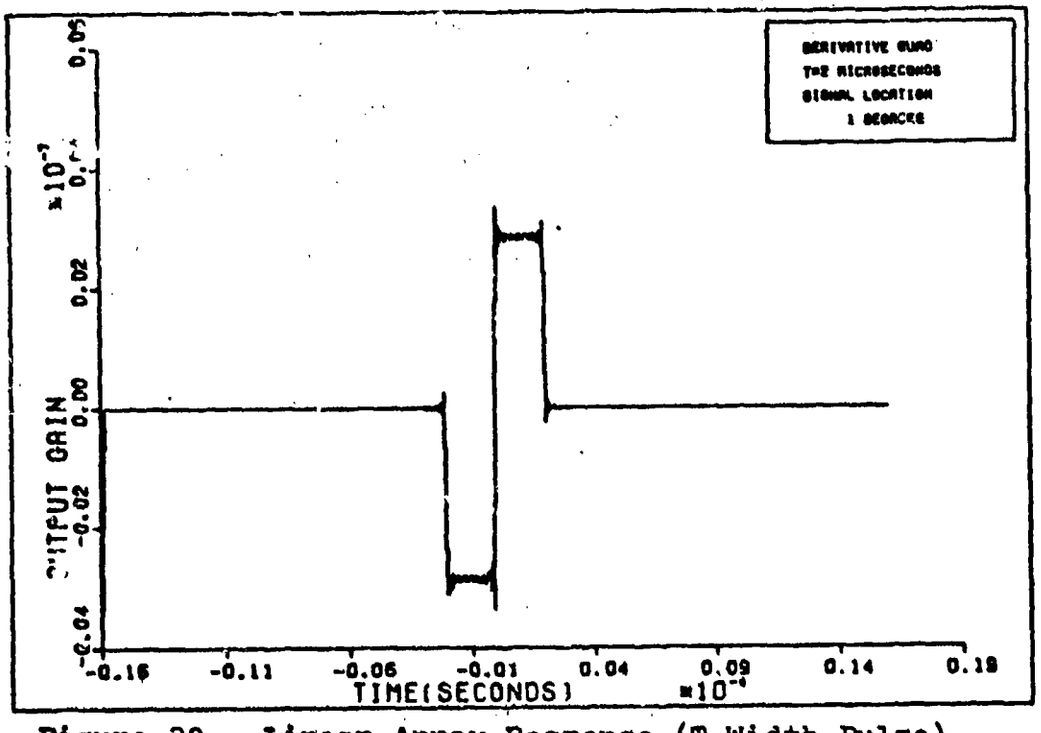

Figure 30. Linear Array Response (T Width Pulse).

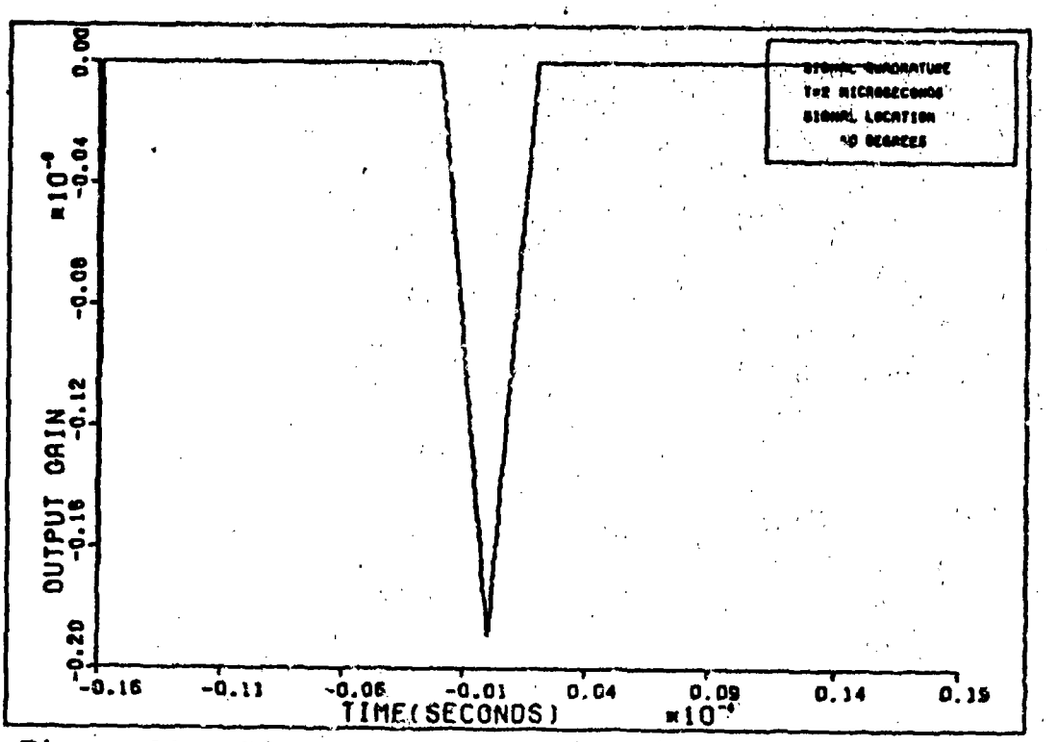

Figure 31. Linear Array Response (T Width Pulse).

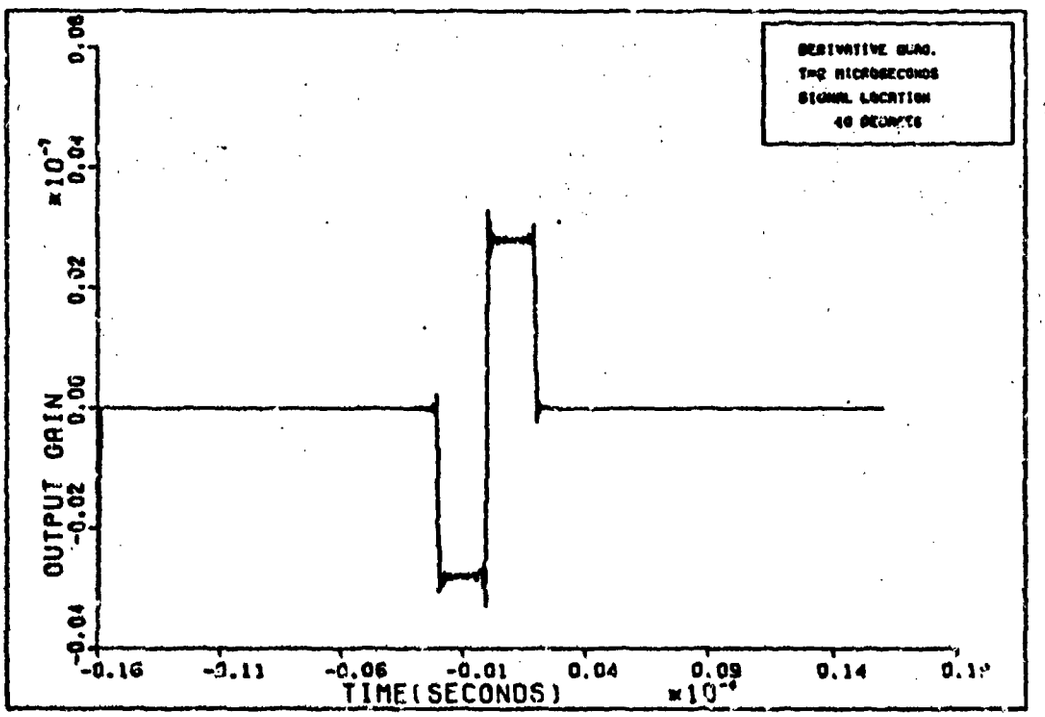

Figure 32. Linear Array Pulse (T Width Pulse).

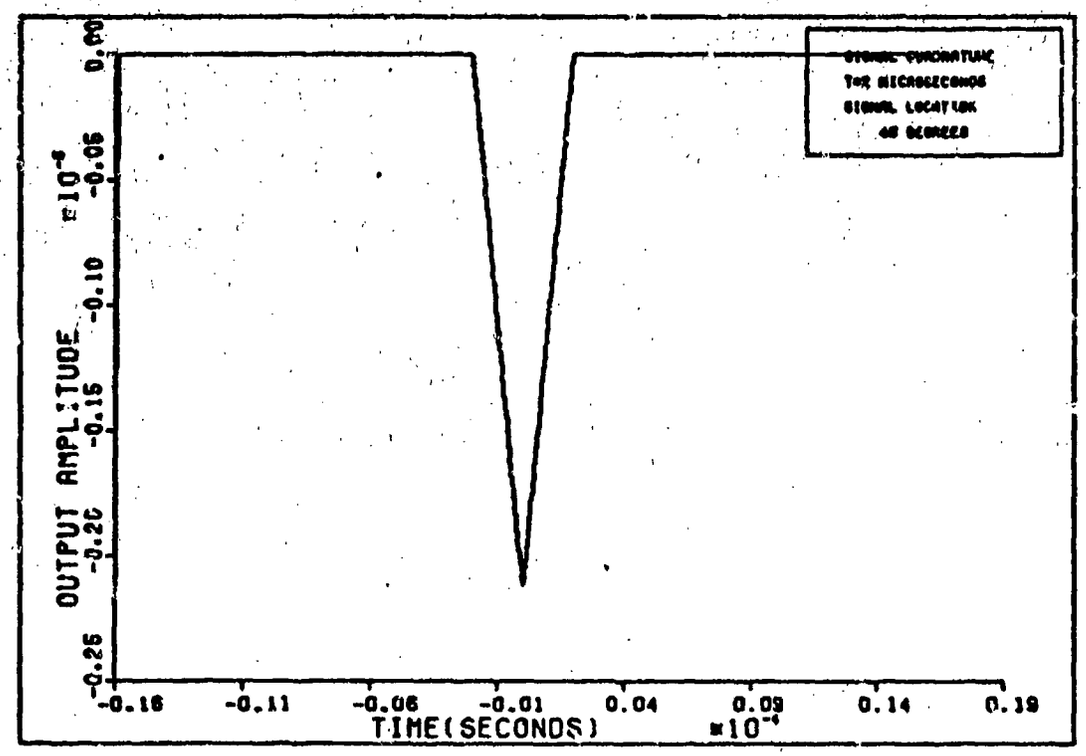

Figure 33. Linear Array Response (T Width Pulse).

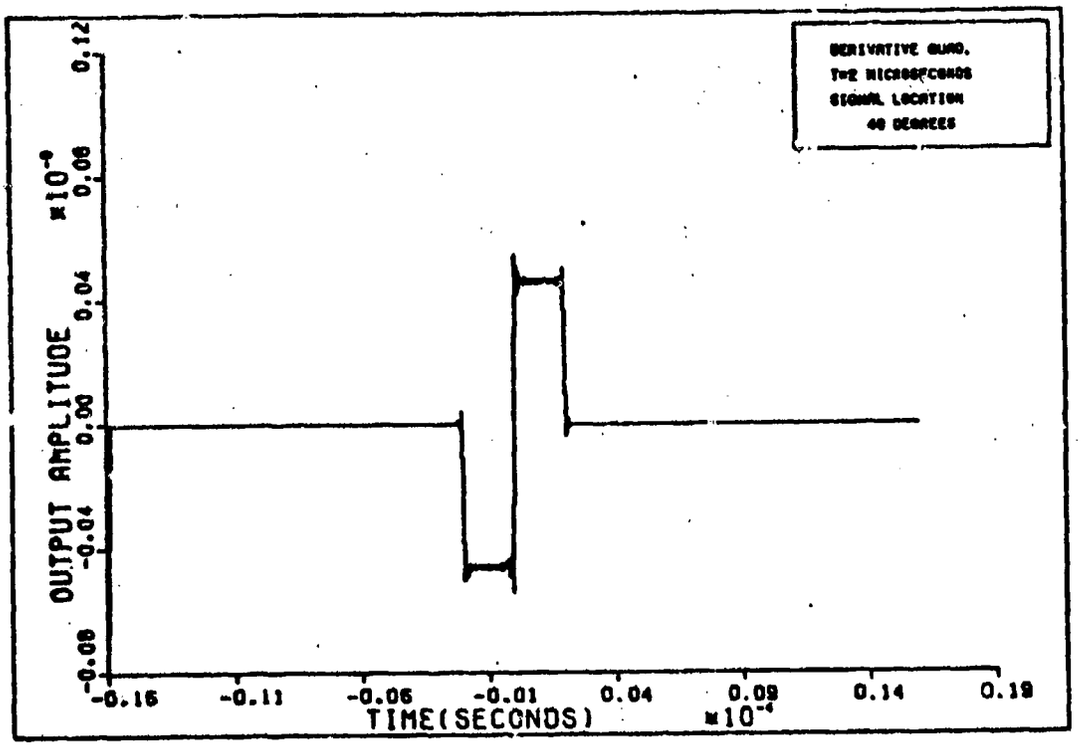

Figure 34. Linear Array Response (T Width Pulse).

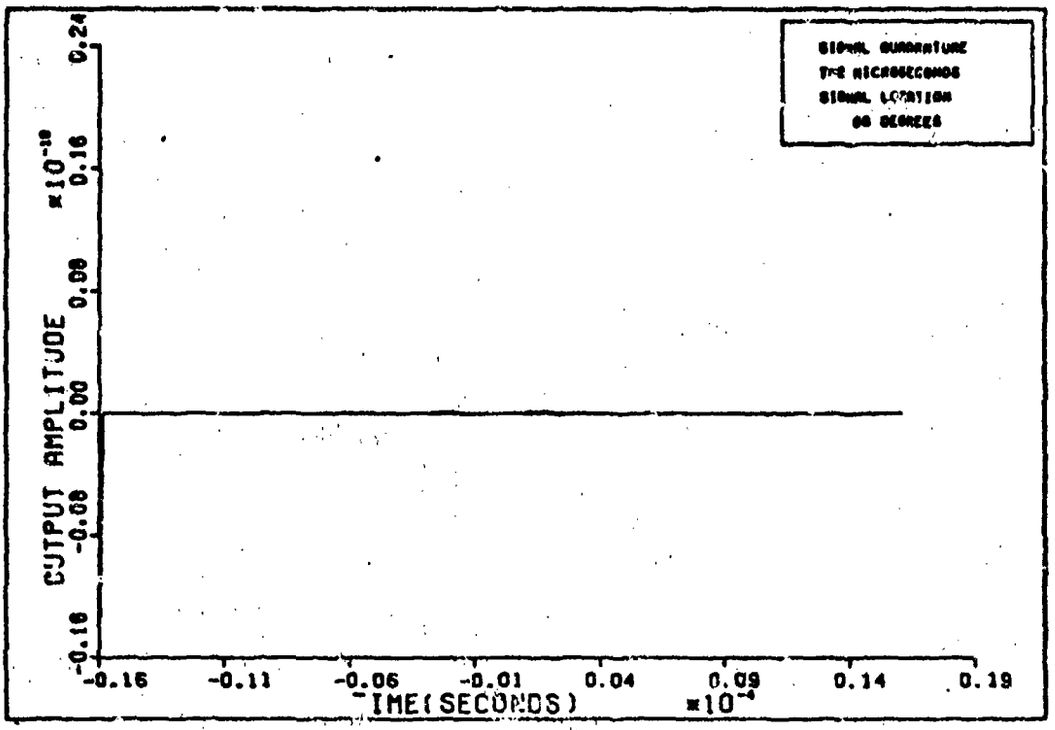

Figure 35. Linear Array Response (T Width Pulse).

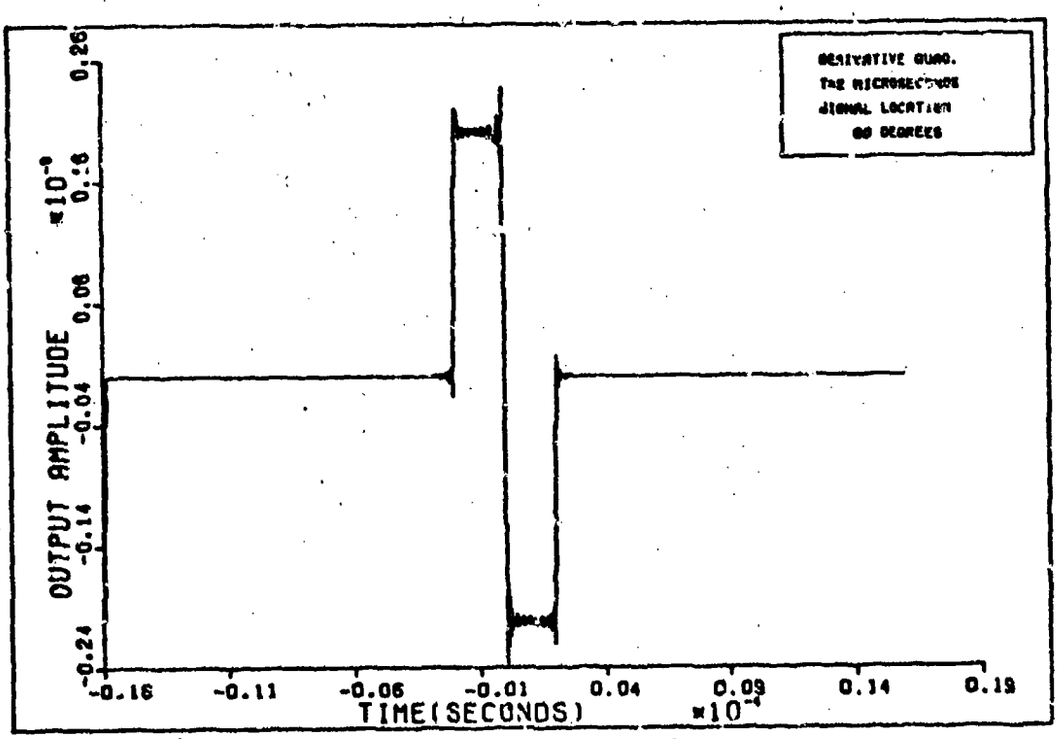

Figure 36. Linear Array Response (T Width Pulse).

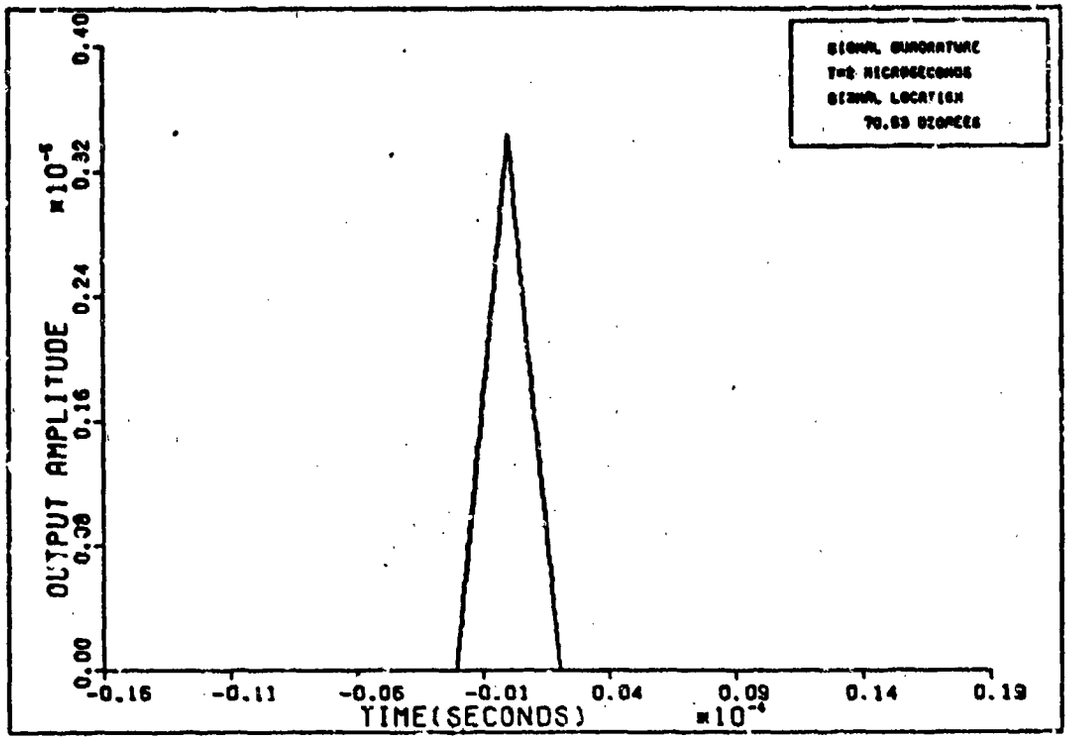

Figure 37. Linear Array Response (T Width Pulse).

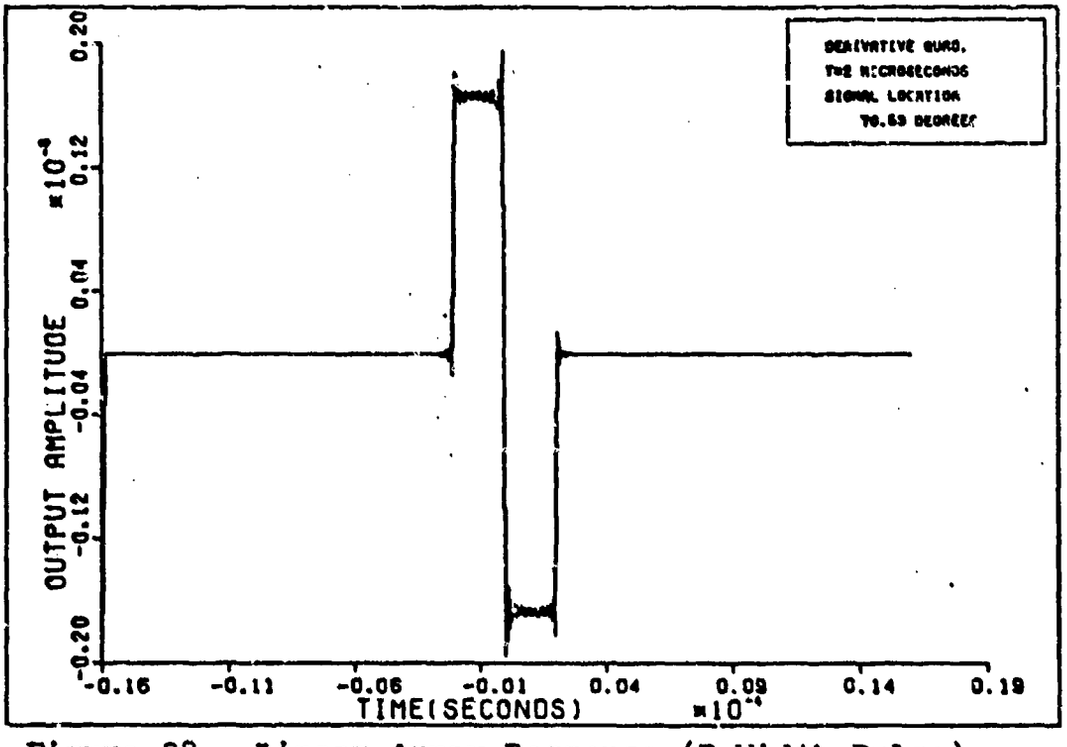

Figure 38. Linear Array Response (T Width Pulse).

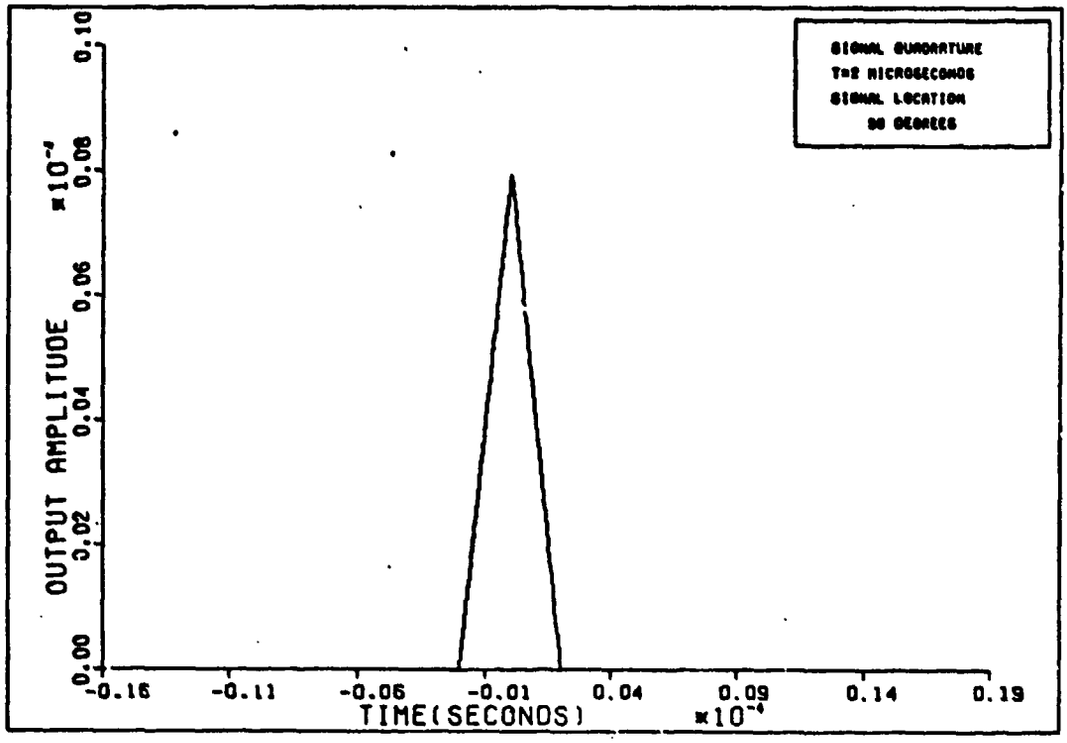

Figure 39. Linear Array Response (T Width Pulse).

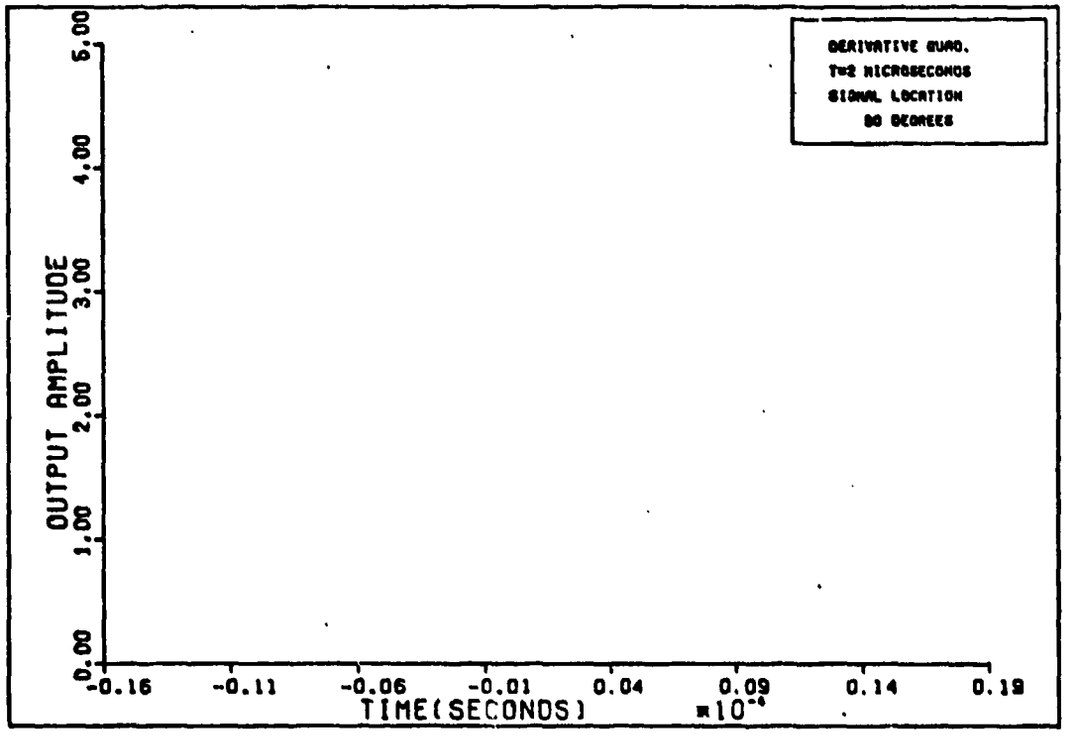

Figure 40. Linear Array Response (T Width Pulse).

this effect would occur with any antipodal signal set. Thus, a threshold detector of this type cannot operate properly with an array unless it has some additional mechanism to determine the expected sign of the signal.

The last operation performed by the program is to calculate the phase of the waveform and plot the results. Before looking at the plots it is helpful to obtain a feel for the type of result to expect. An example will bring out all the relevant ideas.

To simplify the discussion, assume that the term A and B from Table I are such that the output signal (the triangular waveform) and the output derivative (the square wave) have the same peak gain. Since these two outputs are in quadrature the output can be represented in a three dimensional representation of the form of Figure 41. The triangular waveform is in the 0° - t plane. The square wave is in the 90° - t plane. The system output is then the vector sum of these two signals.

From this drawing it can be seen that the system output phase will start at 90° at $t = -T$. As t goes from $t = -T$ toward $t = 0$, the phase will vary from 90° to 45°. As t passes through $t = 0$, the phase will instantaneously switch from 45° to -45°. Then as t proceeds toward $t = T$, the phase will transition from -45° to -90°.

Although a real system cannot instantaneously change phase, this figure indicates that the phase makes a

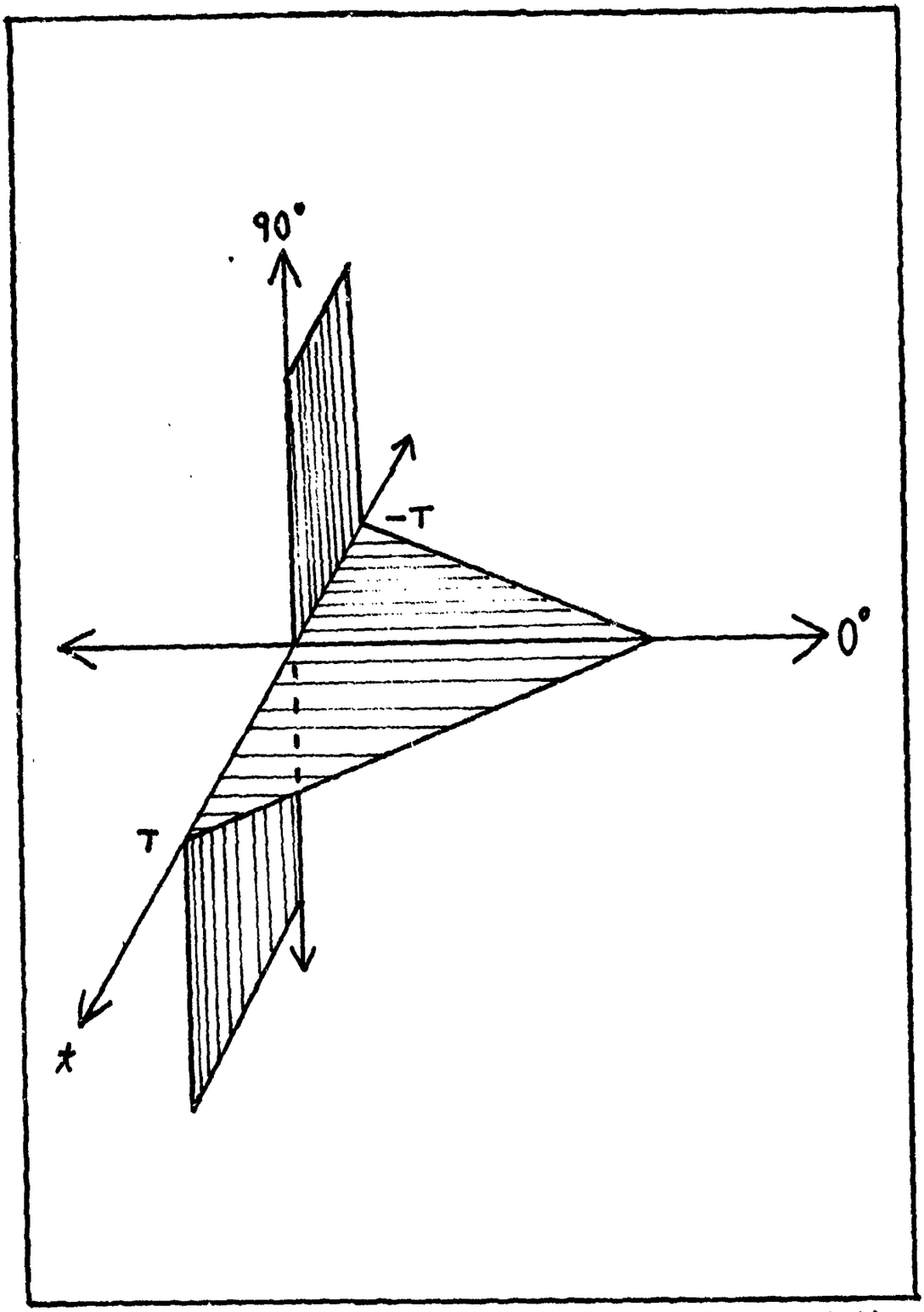

Figure 41. Signal-Derivative Time-Phase Space Representation.

significant and very rapid phase change over the duration of the signal when the signal and its derivative are both equally present. A phase tracking system would be hard pressed to track this degree of phase shifting.

Now the effect of changing the relative sizes of the signals in Figure 41 becomes more apparent. As the signal term is increased, the overall phase moves closer to the signal phase. Figures 42 through 48 show the results from the computer program.

The figures need some clarification before they become understandable. Figure 42 is the plot for 0°. At this point, the signal is zero and the phase plot should just be the phase of the derivative term which is either 90° or -90° depending on its sign. However, the calculations made by the computer do not yield exactly zero results for the signal quadrature. The calculations yield a signal term that oscillates above and below zero. The computer, using an algorithm for $\tan^{-1}(x)$ that ranges between 90° and -90°, calculates the phase to be -89.9° when in reality it would have been 90.1°. Thus, when the system phase oscillates about 90° or -90°, the computer calculates the phase oscillations to be wildly fluctuating between 90° and -90°. With additional programming, this effect could be eliminated. However, it only occurs when the phase is calculated at a null. Thus, it is left to the reader to understand the source of these graphic fluctuations at the two null points.

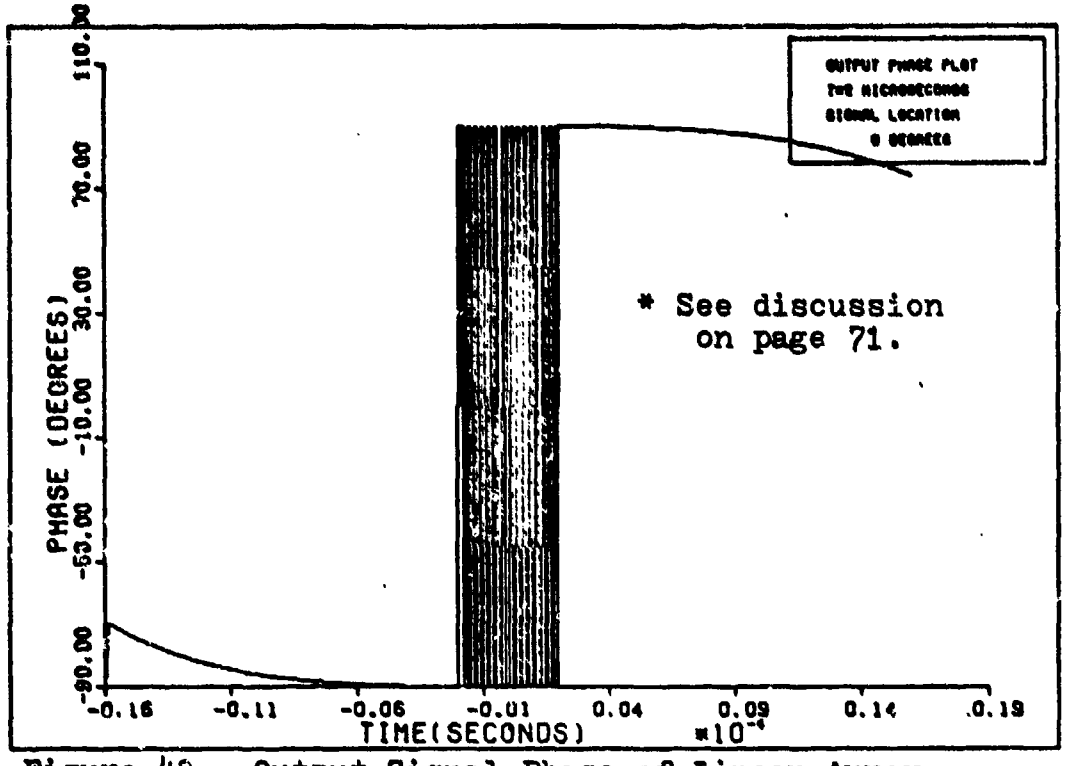

Figure 42. Output Signal Phase of Linear Array.

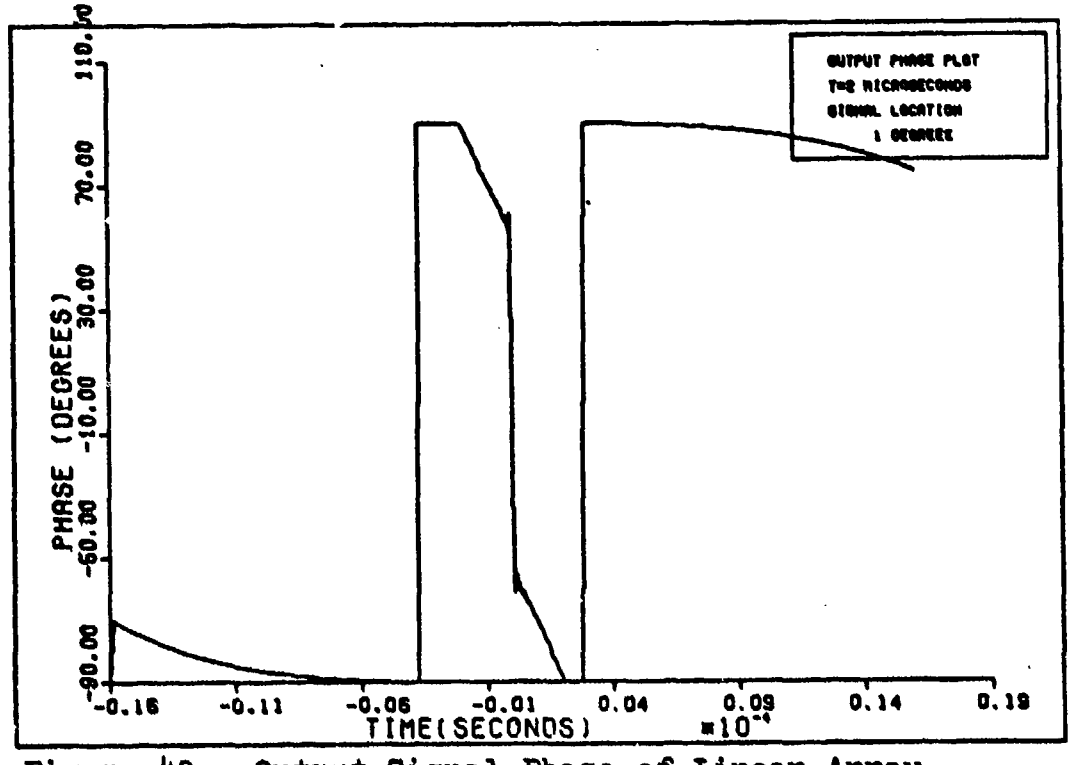

Figure 43. Output Signal Phase of Linear Array.

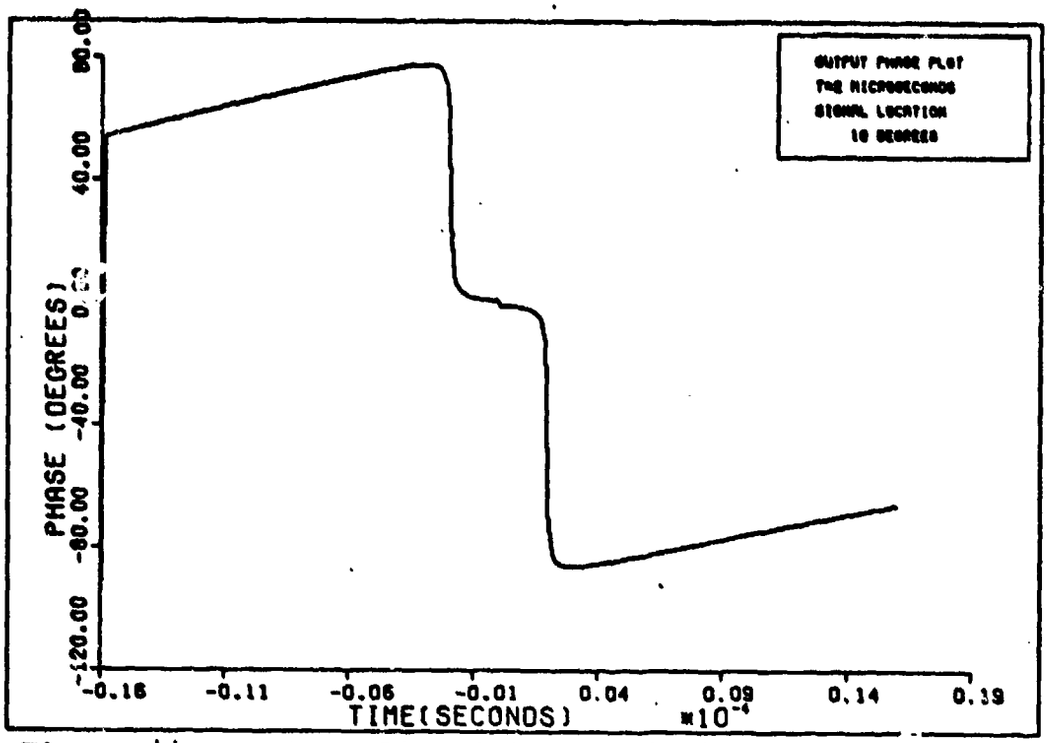

Figure 44. Output Signal Phase of Linear Array.

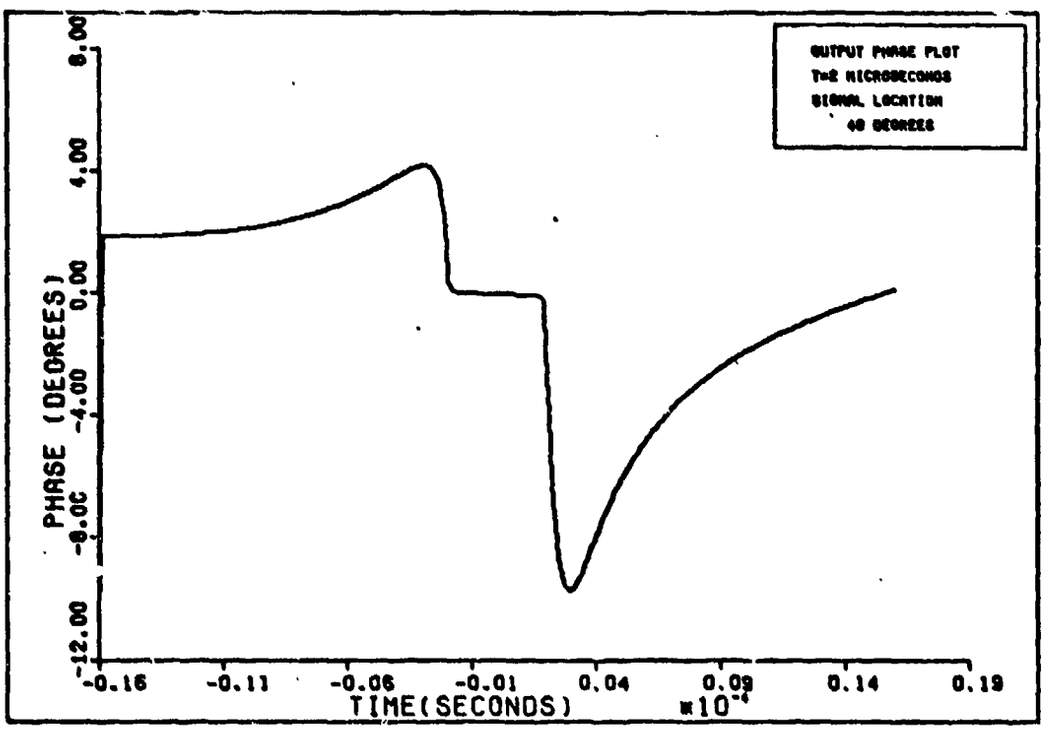

Figure 45. Output Signal Phase of Linear Array.

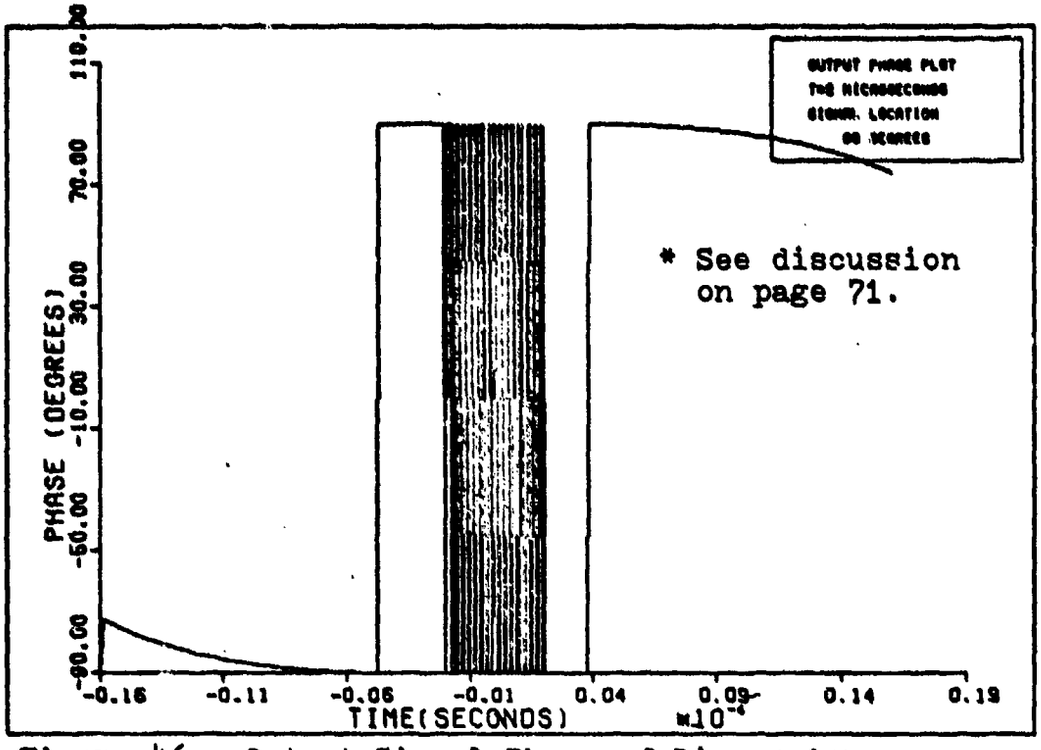

* See discussion on page 71.

Figure 46. Output Signal Phase of Linear Array.

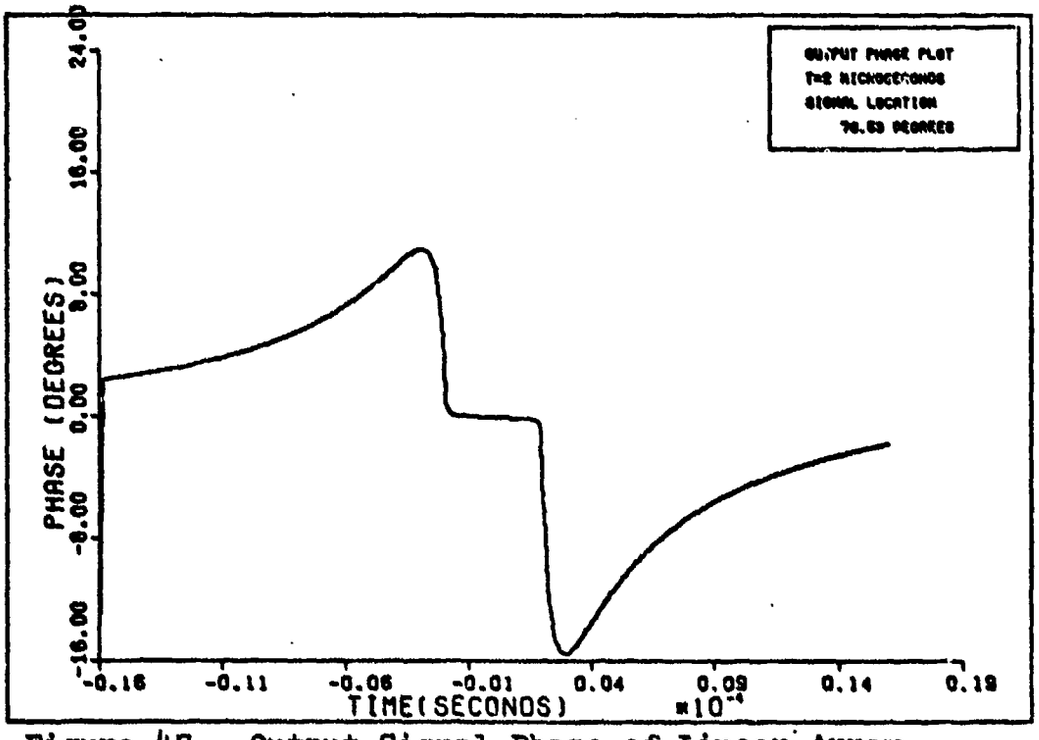

Figure 47. Output Signal Phase of Linear Array.

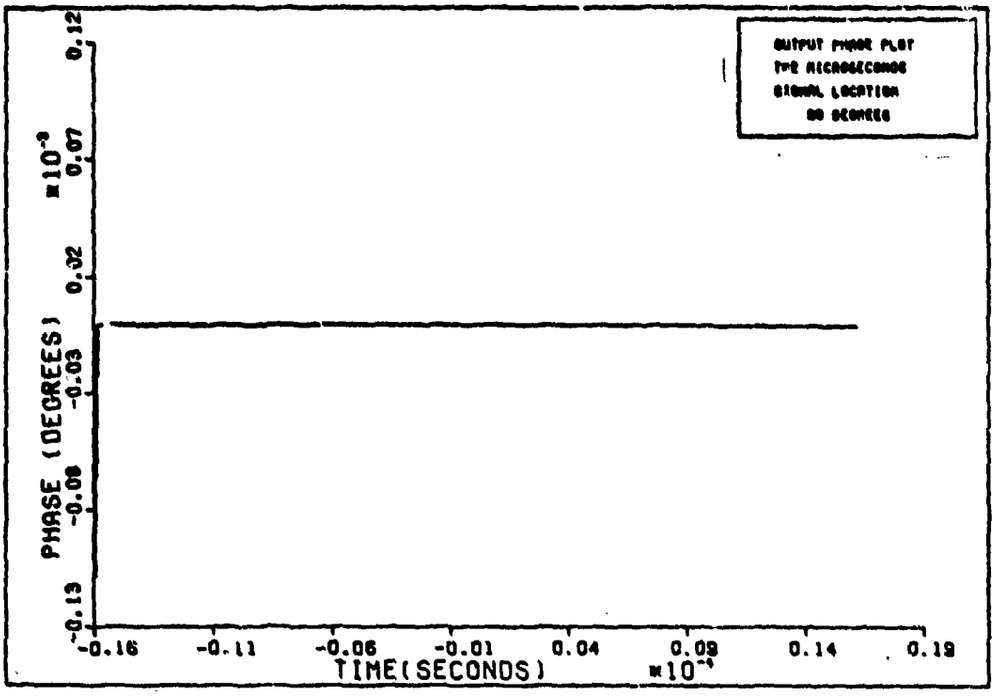

Figure 48. Output Signal Phase of Linear Array.

Figure 43 shows that the phase changes dramatically in the vicinity of nulls. Figures 44, 45, 47, and 48 show that the phase remains close to zero when the signal term is dominant. Thus, in most regions a phase tracking system can operate without difficulty. However, near the nulls typical phase tracking systems will probably lose track due to the fast changes in the output phase.

The computer program illustrated the effects of the array on incoming signals by using a triangular signal. This signal also yields insights into the signal/time derivative relationship.

As was mentioned earlier this waveform was initially selected because of a desire to study the array effects on the correlation properties of PN code pulses. What resulted

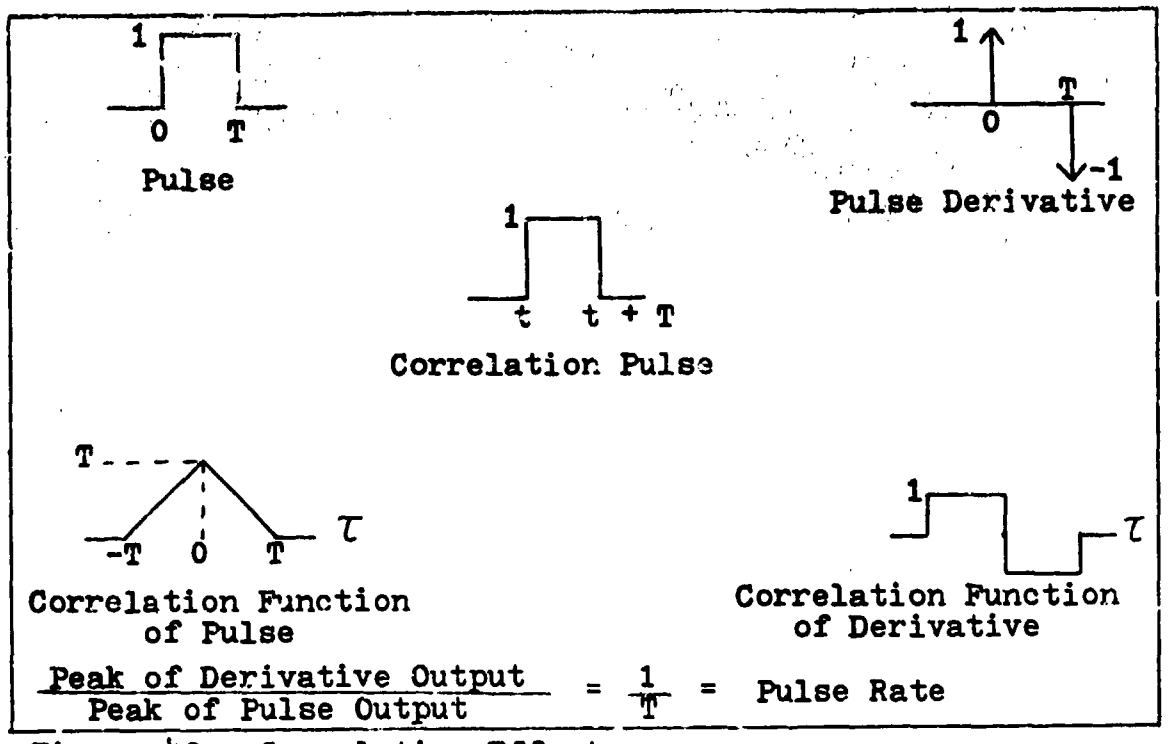

Figure 49. Correlation Effects.

is summarized in Figure 49. Simply stated, the figure illustrates that the derivative of a pulse has more effect on the output of the correlator than the pulse whenever the pulse width is less than one second. For a 5 MHz pulse rate, the effect of the derivative term is 5×10^6 times greater. This gain term will offset a lot of the insignificance of B in Table I.

The basic results obtained from studying this four element array can be summarized as follows: (1) the array equation does result in the output of both the signal and its time derivative; (2) for this example, the signal and its derivative are phase shifted by 90°; (3) in most areas the signal output is dominant; (4) in the neighborhood of nulls the phase of the output signal varies dramatically.

D. Sparse Arrays

In the previous section a computer program was used to illustrate the effects of a linear, equally spaced array on the incoming signal. The program just illustrated the results that had already been developed analytically. In this section we use the computer program to obtain results for two arrays that cannot be analyzed in closed form.

The first array to be analyzed is a four element, linear array. However, the spacing is unequal. The first three elements are spaced one half wavelength apart and the fourth element is located five wavelengths from the third element. This type of element arrangement is called a sparse or thinned array. The study of sparse arrays is useful for several reasons. First, they are still fairly easy to analyze because of the rotational symmetry of the antenna patterns: that is, the output waveform is still independent of ϕ (see Fig. 1). Second, in applications where the antenna elements are mounted on an aircraft surface, the aircraft configuration may force a sparse arrangement on the designer. Third, and probably the most important, is the fact that the elements are not really isotropic (due to their own design, due to the aircraft structure). This may force the designer to arrange the elements for a larger field of view. Finally, although it is not proven here, a properly designed sparse array can have some of the properties of larger arrays without the expense of the additional elements (Ref 7:121-126).

For the purpose of this analysis, the weighting

coefficients will be assumed to be real and of value one (i.e., $A_i = 1$, $\alpha_i = 0$). This has the effect of steering the main beam to broadside ($\theta = 90°$). The analysis focuses on the first two terms of Eq (25). This part of the equation can be written as

$$\tilde{e}(\theta, t) \approx A(\theta)\, m(t+t_c) + \frac{B(\theta)\, dm(t+t_c)}{dt} \qquad (48)$$

where

$$A(\theta) = \sum_{i=1}^{4} e^{j\left\{\frac{2\pi f_0 (d_i - d_c)\cos\theta}{c}\right\}} \qquad (49)$$

and

$$B(\theta) = \sum_{i=1}^{4} -\frac{(d_i - d_c)}{c}\cos\theta\; e^{j\left\{\frac{2\pi f_0 (d_i - d_c)\cos\theta}{c}\right\}} \qquad (50)$$

where $d_1 - d_c = -1\frac{7}{8}$, $d_2 - d_c = -1\frac{3}{8}$, $d_3 - d_c = -\frac{7}{8}$, and $d_4 - d_c = 4\frac{1}{8}$.

The analysis begins by evaluating A(θ) and B(θ) in terms of θ. Because of the symmetries involved, $A(\theta) = A(-\theta)$ and $B(\theta) = B(-\theta)$. Furthermore, $A(90° - \theta) = A(90° + \theta)$ with similar results holding for B(θ). Thus, all values of A(θ) and B(θ) can be easily obtained from values of A(θ) and B(θ) in the first quadrant. Table IV lists values for these two parameters in both rectangular and polar format for the first quadrant. The last column of the table also shows the ratio of $|A|/|B|$ for this array.

TABLE IV. VALUES OF A AND B FOR THE SPARSE ARRAY.

θ	A		B		|A|	∠A	|B|	∠B	|A/B|
DEG	REAL	IMAGINARY	REAL	IMAGINARY		DEGREES		DEGREES	
1	.223E+01	-.478E-03	.161E-08	-.431E-10	.209E+01	-.0	.163E-08	-1.7	.103E+10
2	.202E+01	-.191E-02	.161E-08	-.172E-09	.200E+01	-.1	.164E-08	-6.9	.124E+10
3	.229E+01	-.619E-02	.161E-08	-.137E-09	.200E+01	-.1	.168E-08	-15.2	.119E+10
4	.200E+01	-.758E-02	.142E-08	-.687E-09	.200E+01	-.2	.156E-08	-25.8	.128E+10
5	.200E+01	-.113E-01	.142E-08	-.107E-08	.200E+01	-.3	.174E-08	-37.1	.112E+10
6	.199E+01	-.177E-01	.141E-08	-.154E-08	.199E+01	-.5	.208E-08	-47.5	.957E+09
7	.199E+01	-.233E-01	.139E-08	-.209E-08	.199E+01	-.7	.251E-08	-56.2	.791E+09
8	.197E+01	-.307E-01	.137E-08	-.271E-08	.197E+01	-.9	.304E-08	-61.1	.649E+09
9	.195E+01	-.391E-01	.135E-08	-.341E-08	.195E+01	-1.1	.356E-08	-63.6	.537E+09
10	.191E+01	-.468E-01	.131E-08	-.417E-08	.191E+01	-1.4	.437E-08	-72.6	.441E+09
11	.193E+01	-.559E-01	.126E-08	-.530E-08	.193E+01	-1.7	.511E-08	-75.8	.376E+09
12	.185E+01	-.654E-01	.120E-08	-.518E-08	.185E+01	-2.0	.623E-08	-78.3	.297E+09
13	.185E+01	-.757E-01	.112E-08	-.479E-08	.185E+01	-2.6	.684E-08	-80.6	.262E+09
14	.173E+01	-.857E-01	.101E-08	-.774E-08	.173E+01	-2.8	.731E-08	-82.6	.237E+09
15	.165E+01	-.960E-01	.913E-09	-.159E-08	.165E+01	-3.3	.874E-08	-84.0	.189E+09
16	.155E+01	-.104E+00	.779E-09	-.964E-08	.156E+01	-3.3	.967E-08	-85.4	.161E+09
17	.144E+01	-.112E+00	.623E-09	-.105E-07	.144E+01	-4.4	.106E-07	-86.6	.137E+09
18	.131E+01	-.119E+00	.444E-09	-.114E-07	.131E+01	-5.2	.114E-07	-87.8	.115E+09
19	.115E+01	-.127E+00	.242E-09	-.122E-07	.116E+01	-6.1	.122E-07	-88.9	.952E+08
20	.994E+00	-.126E+00	.189E-10	-.129E-07	.931E+00	-7.2	.129E-07	-89.9	.721E+08
21	.795E+00	-.123E+00	-.225E-09	-.134E-07	.804E+00	-8.8	.134E-07	-91.0	.601E+08
22	.590E+00	-.119E+00	-.483E-09	-.139E-07	.601E+00	-11.3	.139E-07	-92.0	.432E+08
23	.369E+00	-.108E+00	-.765E-09	-.139E-07	.385E+00	-16.3	.139E-07	-93.1	.276E+08
24	.137E+00	-.972E-01	-.105E-08	-.119E-07	.168E+00	-35.4	.119E-07	-95.3	.119E+08
25	-.104E+00	-.717E-01	-.134E-08	-.116E-07	.126E+00	-145.4	.116E-07	-96.7	.109E+08
26	-.149E+00	-.467E-01	-.161E-08	-.113E-07	.156E+00	-172.6	.113E-07	-98.1	.138E+08
27	-.539E+00	-.107E-01	-.191E-08	-.112E-07	.539E+00	-179.0	.124E-07	-99.3	.477E+08
28	-.873E+00	.337E-01	-.217E-08	-.111E-07	.874E+00	177.9	.113E-07	-101.1	.727E+08
29	-.124E+01	.784E-01	-.249E-08	-.977E-08	.104E+01	175.7	.101E-07	-103.8	.104E+09
30	-.174E+01	.133E+00	-.253E-08	-.917E-08	.174E+01	173.9	.857E-08	-113.6	.145E+09
31	-.143E+01	.197E+00	-.271E-08	-.577E-08	.141E+01	172.2	.697E-08	-115.2	.204E+09
32	-.159E+01	.259E+00	-.260E-08	-.460E-08	.153E+01	170.6	.522E-08	-122.5	.292E+09
33	-.161E+01	.327E+00	-.261E-08	-.213E-08	.156E+01	168.5	.345E-08	-140.3	.451E+09
34	-.164E+01	.394E+00	-.273E-08	-.211E-09	.159E+01	166.4	.274E-08	-175.6	.617E+09
35	-.167E+01	.467E+00	-.257E-08	.137E-08	.159E+01	163.9	.317E-08	153.9	.531E+09
36	-.154E+01	.544E+00	-.241E-08	.151E-08	.153E+01	160.6	.447E-08	131.1	.355E+09
37	-.141E+01	.537E+00	-.197E-08	.559E-08	.151E+01	157.1	.592E-08	109.6	.256E+09
38	-.127E+01	.467E+00	-.153E-08	.706E-08	.135E+01	152.0	.723E-08	102.2	.183E+09
39	-.985E+00	.534E+00	-.103E-08	.318E-08	.120E+01	145.2	.824E-08	97.1	.145E+09
40	-.714E+00	.709E+00	-.493E-09	.898E-08	.101E+01	135.2	.843E-08	92.7	.119E+09
41	-.419E+00	.717E+00	.222E-09	.911E-08	.830E+00	120.4	.911E-08	88.6	.906E+08
42	-.112E+00	.697E+00	.902E-09	.856E-08	.702E+00	99.1	.891E-08	84.2	.798E+08
43	.189E+00	.649E+00	.159E-08	.814E-08	.675E+00	73.8	.823E-08	78.3	.819E+08
44	.465E+00	.578E+00	.227E-08	.697E-08	.742E+00	51.2	.733E-08	71.9	.101E+09
45	.702E+00	.483E+00	.291E-08	.543E-08	.849E+00	34.5	.615E-08	61.8	.138E+09
46	.876E+00	.357E+00	.346E-08	.359E-08	.946E+00	22.1	.499E-08	46.1	.189E+09
47	.981E+00	.207E+00	.392E-08	.159E-08	.100E+01	11.9	.423E-08	22.1	.237E+09
48	.101E+01	.745E-01	.424E-08	-.456E-09	.101E+01	2.0	.426E-08	-6.0	.236E+09
49	.945E+00	-.154E+00	.461E-08	-.233E-08	.963E+00	-9.3	.501E-08	-23.6	.191E+09
50	.797E+00	-.347E+00	.441E-08	-.407E-08	.871E+00	-23.9	.600E-08	-42.7	.145E+09
51	.575E+00	-.554E+00	.422E-08	-.539E-08	.798E+00	-44.0	.685E-08	-51.9	.117E+09
52	.292E+00	-.759E+00	.355E-08	-.623E-08	.804E+00	-68.7	.733E-08	-58.3	.110E+09
53	-.240E-01	-.929E+00	.331E-08	-.632E-08	.930E+00	-91.8	.732E-08	-63.1	.127E+09
54	-.365E+00	-.109E+01	.261E-08	-.674E-08	.114E+01	-103.5	.726E-08	-67.7	.159E+09
55	-.575E+00	-.120E+01	.178E-08	-.540E-08	.133E+01	-114.5	.554E-08	-71.9	.240E+09
56	-.965E+00	-.172E+01	.850E-09	-.605E-08	.154E+01	-120.5	.615E-08	-78.2	.363E+09
57	-.113E+01	-.179E+01	-.126E-09	-.213E-08	.177E+01	-131.1	.234E-08	-93.1	.756E+09
58	-.121E+01	-.125E+01	-.113E-08	-.169E-09	.173E+01	-133.7	.116E-08	-171.5	.150E+10
59	-.127E+01	-.115E+01	-.203E-08	.166E-08	.153E+01	-135.3	.262E-08	140.7	.625E+09
60	-.109E+01	-.190E+01	-.266E-08	.157E-08	.161E+01	-135.9	.457E-08	135.7	.352E+09
61	-.793E+00	-.797E+00	-.356E-08	.519E-08	.103E+01	-131.9	.628E-08	124.3	.167E+09
62	-.209E+00	-.911E+00	-.403E-08	.635E-08	.959E+00	-119.4	.752E-08	122.4	.793E+08
63	.205E+00	-.704E+00	-.417E-08	.695E-08	.733E+00	-46.5	.810E-08	121.7	.753E+08
64	.743E+00	.137E+00	-.437E-08	.692E-08	.755E+00	10.1	.818E-08	122.3	.922E+08
65	.120E+01	.475E+00	-.414E-08	.525E-08	.135E+01	20.5	.753E-08	123.8	.161E+09
66	.175E+01	.914E+00	-.379E-08	.502E-08	.194E+01	24.9	.629E-08	127.1	.309E+09
67	.213E+01	.111E+01	-.327E-08	.332E-08	.240E+01	27.9	.461E-08	133.9	.522E+09
68	.224E+01	.119E+01	-.246E-08	.137E-08	.272E+01	30.7	.279E-08	151.5	.975E+09
69	.237E+01	.154E+01	-.161E-09	-.756E-09	.285E+01	33.0	.170E-08	-154.5	.168E+10
70	.218E+01	.171E+01	-.211E-09	-.326E-08	.277E+01	38.0	.295E-08	-104.4	.971E+09
71	.179E+01	.177E+01	.174E-09	-.447E-08	.243E+01	44.1	.467E-08	-87.8	.547E+09
72	.122E+01	.167E+01	.990E-09	-.577E-08	.207E+01	54.3	.581E-08	-80.2	.357E+09
73	.652E+00	.160E+01	.169E-08	-.662E-08	.187E+01	73.2	.664E-08	-75.3	.276E+09
74	-.337E+00	.125E+01	.203E-08	-.651E-08	.130E+01	107.5	.689E-08	-71.1	.190E+09
75	-.127E+01	.903E+00	.258E-08	-.691E-08	.156E+01	144.7	.655E-08	-66.7	.239E+09
76	-.298E+01	.511E+00	.274E-08	-.509E-08	.215E+01	166.3	.572E-08	-61.3	.376E+09
77	-.273E+01	.756E-01	.271E-08	-.367E-08	.273E+01	178.4	.456E-08	-53.6	.611E+09
78	-.328E+01	-.381E+00	.250E-09	-.206E-08	.330E+01	-173.4	.325E-08	-39.8	.101E+10
79	-.352E+01	-.321E+00	.215E-08	-.503E-09	.367E+01	-169.9	.221E-08	-13.2	.164E+10
80	-.347E+01	-.127E+01	.171E-09	.921E-09	.365E+01	-160.6	.194E-08	24.1	.190E+10
81	-.312E+01	-.195E+01	.121E-08	.209E-08	.369E+01	-157.5	.230E-08	59.6	.167E+10
82	-.269E+01	-.199E+01	.715E-09	.278E-08	.307E+01	-144.1	.287E-08	75.6	.107E+10
83	-.163E+01	-.194E+01	.260E-09	.308E-08	.251E+01	-130.0	.304E-08	85.1	.827E+09
84	-.595E+00	-.197E+01	-.957E-10	.277E-08	.207E+01	-106.8	.297E-08	91.9	.653E+09
85	.514E+00	-.197E+01	-.351E-09	.284E-08	.193E+01	-74.5	.297E-08	97.9	.723E+09
86	.119E+01	-.155E+01	-.643E-09	.191E-08	.195E+01	-45.8	.197E-08	106.2	.117E+10
87	.285E+01	-.136E+01	-.431E-09	.121E-08	.316E+01	-27.6	.130E-08	112.2	.227E+10
88	.319E+01	-.965E+00	-.393E-09	.580E-09	.367E+01	-15.0	.701E-09	124.1	.495E+10
89	.381E+01	-.492E+00	-.217E-09	.132E-09	.395E+01	-7.3	.265E-09	145.0	.146E+11
90	.409E+01	.495E-13	.721E-22	.169E-15	.406E+01	.0	.221E-22	.0	.181E+24

We recall from earlier analyses that $A(\theta)$ is the usual array factor. It is graphed in Figure 50 in a polar plot. This would normally be called the antenna pattern for this array. Figure 51 is a polar plot of $B(\theta)$. We called this the time derivative radiation pattern in the last section. The first interesting thing to note about Figure 50 is that it is vastly different from the four element pattern of Figure 9; it has a quickly changing antenna pattern with a lot of sidelobes and dips in the gain. The second thing to note is that there are no deep nulls for this array.

Having no deep nulls results in two consequences. First, the signal term is never completely attenuated. This is confirmed by the $A(\theta)$ term in Table IV. Second, since $A(\theta)$ is never nulled, it and $B(\theta)$ are never comparable in magnitude. The ratio of their magnitudes is never less than 10^8. Thus, the derivative term will have to be 10^8 times larger than the signal term in order for the derivative term of the output to be equal to the signal term. If we use the signal of Section III. C. on this array and an envelope detector, the signal will always be the dominant part of the output.

Comparing Figures 50 and 51 illustrates that $A(\theta)$ and $B(\theta)$ are still reciprocally related as was noted with the equally spaced array of the last section. As was stated earlier, though, this relationship is simply stated as an observation here and no attempt has been made to analyze this apparent inverse relationship.

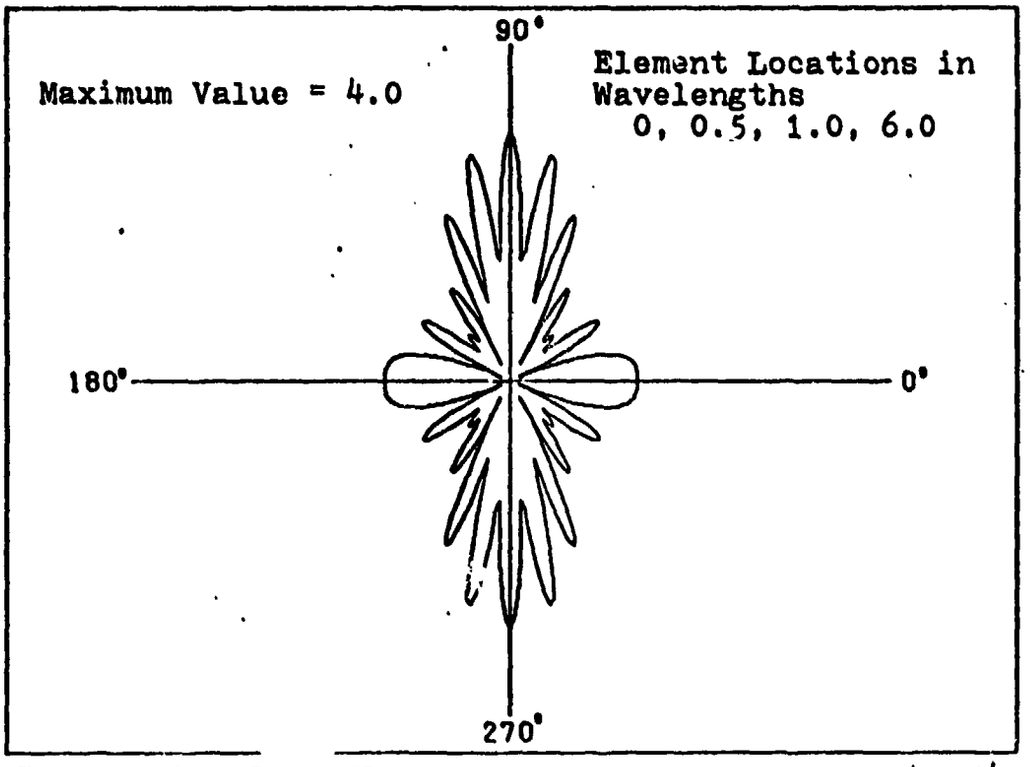

Figure 50. Four Element Sparse Array, Plot of $|A(\theta)|$.

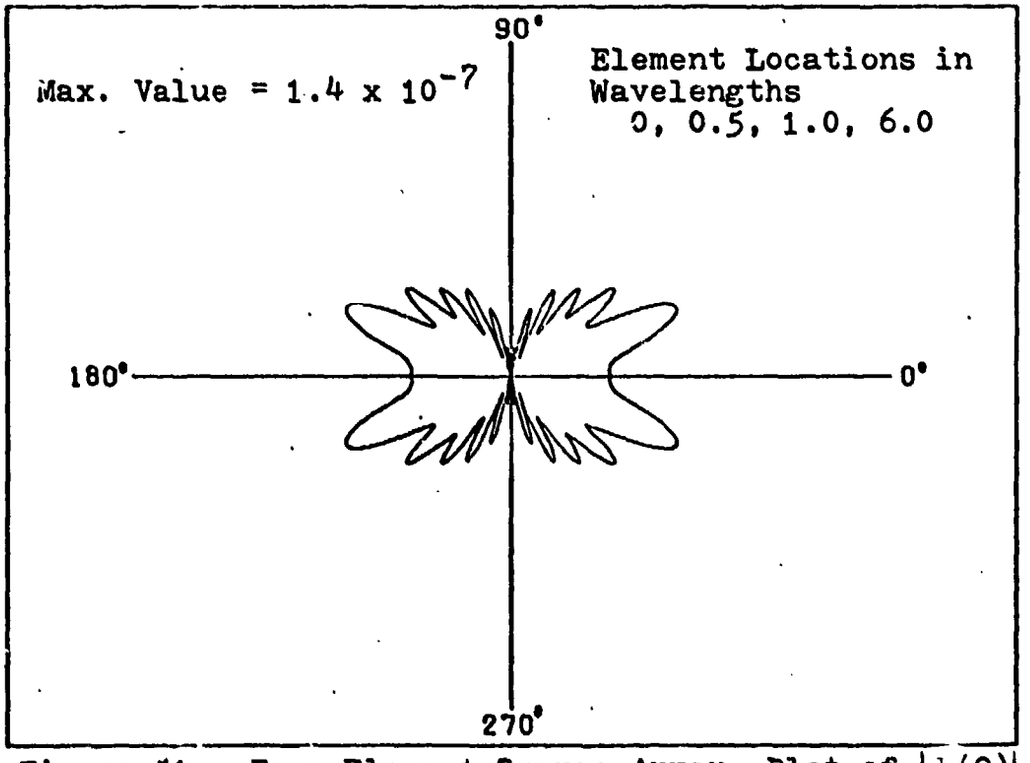

Figure 51. Four Element Sparse Array, Plot of $|B(\theta)|$.

In the last section, the signal and its first derivative were always 90° out of phase. By looking at the phase terms in Table IV, we see that A(θ) and B(θ) are not separated by 90°. In fact, they are not even separated by a constant phase. There is only one way to isolate only one signal term with this array. To see the derivative term, the system would have to track the phase of A(θ) and then coherently detect the output at a phase that is 90° removed from the phase of A(θ). The output would then contain only that portion of the derivative term that projects onto this phase.

If one is interested in being able to detect the signal regardless of its location, this sparse array is a good array in that it never nulls the signal term. However, the usual purpose for using an array is to be able to place nulls on interference sources. Since this array has no nulls, the interference source cannot be nulled.

At this point we drop discussion of this particular sparse array and focus attention on the second sparse array. This array is identical to the first array except that the fourth element is located 4.5 wavelengths from the third element instead of 5. Table V shows values for A(θ) and B(θ) for this array. Figure 52 is the polar plot of A(θ) for this array and Figure 53 is the plot of B(θ). They are somewhat different from the plots obtained for the first sparse array. A(θ) still has a large number of sidelobes and dips, but in this case there are nulls associated with

THIS PAGE IS BEST QUALITY PRACTICABLE
FROM COPY FURNISHED TO DDC

TABLE V. VALUES OF A AND B FOR THE SPARSE ARRAY.

θ	A		B		|A|	∠A	|B|	∠B	|A/B|
DEG	REAL	IMAGINARY	REAL	IMAGINARY		DEGREES		DEGREES	
1	-.229E-06	.470E-02	-.143E-07	-.137E-11	.470E-02	90.0	.143E-07	-180.0	.339E+06
2	-.365E-05	.191E-01	-.143E-07	-.548E-11	.191E-01	90.0	.143E-07	-180.0	.134E+07
3	-.103E-04	.431E-01	-.143E-07	-.173E-10	.431E-01	90.0	.143E-07	-180.0	.302E+07
4	-.585E-04	.763E-01	-.142E-07	-.219E-10	.763E-01	90.0	.142E-07	-179.9	.537E+07
5	-.149E-03	.117E+00	-.142E-07	-.370E-10	.119E+00	90.1	.142E-07	-179.9	.841E+07
6	-.295E-03	.172E+00	-.141E-07	-.435E-10	.172E+00	90.1	.141E-07	-179.8	.121E+08
7	-.545E-03	.236E+00	-.141E-07	-.635E-10	.236E+00	90.1	.141E-07	-179.7	.166E+08
8	-.924E-03	.304E+00	-.140E-07	-.945E-10	.304E+00	90.2	.140E-07	-179.7	.218E+08
9	-.147E-02	.381E+00	-.138E-07	-.137E-09	.384E+00	90.2	.138E-07	-179.6	.278E+08
10	-.221E-02	.472E+00	-.135E-07	-.127E-09	.472E+00	90.3	.136E-07	-179.5	.347E+08
11	-.317E-02	.563E+00	-.134E-07	-.148E-09	.563E+00	90.3	.134E-07	-179.4	.420E+08
12	-.444E-02	.672E+00	-.131E-07	-.165E-09	.672E+00	90.4	.131E-07	-179.3	.514E+08
13	-.596E-02	.781E+00	-.127E-07	-.148E-09	.781E+00	90.4	.127E-07	-179.1	.616E+08
14	-.777E-02	.895E+00	-.122E-07	-.234E-09	.895E+00	90.5	.122E-07	-179.0	.734E+08
15	-.985E-02	.101E+01	-.117E-07	-.211E-09	.101E+01	90.6	.117E-07	-179.0	.870E+08
16	-.121E-01	.113E+01	-.110E-07	-.216E-09	.113E+01	90.6	.110E-07	-178.9	.103E+09
17	-.146E-01	.125E+01	-.107E-07	-.206E-09	.125E+01	90.7	.102E-07	-178.8	.123E+09
18	-.172E-01	.137E+01	-.936E-08	-.188E-09	.137E+01	90.7	.936E-08	-178.9	.147E+09
19	-.192E-01	.149E+01	-.838E-08	-.153E-09	.149E+01	90.7	.838E-08	-179.0	.179E+09
20	-.203E-01	.153E+01	-.729E-08	-.110E-09	.153E+01	90.8	.729E-08	-179.2	.219E+09
21	-.215E-01	.165E+01	-.605E-08	-.707E-10	.165E+01	90.7	.609E-08	-179.7	.272E+09
22	-.216E-01	.177E+01	-.440E-08	.483E-10	.177E+01	90.7	.440E-08	179.2	.370E+09
23	-.196E-01	.184E+01	-.342E-08	.101E-09	.184E+01	90.6	.342E-08	177.0	.537E+09
24	-.155E-01	.185E+01	-.197E-08	.320E-09	.185E+01	90.5	.223E-08	170.8	.943E+09
25	-.451E-02	.191E+01	-.479E-09	.480E-09	.190E+01	90.1	.677E-09	134.9	.281E+10
26	.195E-02	.190E+01	.103E-08	.659E-09	.190E+01	89.9	.123E-08	32.5	.155E+10
27	.163E-01	.187E+01	.253E-08	.852E-09	.187E+01	89.5	.267E-08	18.6	.698E+09
28	.354E-01	.180E+01	.399E-08	.105E-08	.180E+01	88.9	.413E-08	14.8	.436E+09
29	.595E-01	.170E+01	.536E-08	.125E-08	.170E+01	88.0	.551E-08	13.2	.308E+09
30	.883E-01	.157E+01	.661E-08	.144E-08	.157E+01	86.8	.677E-08	12.3	.232E+09
31	.121E+00	.141E+01	.771E-08	.161E-08	.141E+01	85.0	.787E-08	11.8	.180E+09
32	.153E+00	.122E+01	.869E-08	.174E-08	.123E+01	82.4	.878E-08	11.4	.140E+09
33	.206E+00	.994E+00	.926E-08	.181E-08	.102E+01	78.3	.944E-08	11.1	.108E+09
34	.253E+00	.757E+00	.967E-08	.182E-08	.799E+00	71.5	.984E-08	10.7	.811E+08
35	.300E+00	.500E+00	.979E-08	.175E-08	.583E+00	59.0	.995E-08	10.1	.586E+08
36	.346E+00	.233E+00	.963E-08	.158E-08	.417E+00	34.0	.975E-08	9.3	.427E+08
37	.337E+00	-.364E-01	.917E-08	.130E-08	.393E+00	-5.1	.926E-08	8.1	.419E+08
38	.420E+00	-.294E+00	.843E-08	.916E-09	.513E+00	-35.0	.848E-08	6.2	.604E+08
39	.440E+00	-.537E+00	.745E-08	.422E-09	.693E+00	-50.7	.746E-08	3.2	.932E+08
40	.445E+00	-.759E+00	.624E-08	-.173E-09	.875E+00	-59.9	.625E-08	-1.6	.140E+09
41	.428E+00	-.937E+00	.488E-08	-.321E-09	.103E+01	-65.4	.499E-08	-9.9	.208E+09
42	.387E+00	-.109E+01	.341E-08	-.159E-08	.116E+01	-70.3	.376E-08	-25.0	.308E+09
43	.317E+00	-.117E+01	.191E-08	-.235E-08	.121E+01	-74.8	.303E-08	-50.9	.401E+09
44	.218E+00	-.121E+01	.441E-09	-.319E-08	.123E+01	-79.8	.313E-08	-81.8	.394E+09
45	.979E-01	-.120E+01	-.916E-09	-.378E-08	.121E+01	-85.4	.389E-08	-103.6	.310E+09
46	-.714E-01	-.114E+01	-.210E-08	-.435E-08	.115E+01	-93.6	.483E-08	-115.7	.238E+09
47	-.255E+00	-.104E+01	-.304E-08	-.479E-08	.107E+01	-103.8	.564E-08	-122.7	.190E+09
48	-.460E+00	-.897E+00	-.372E-08	-.494E-08	.101E+01	-117.2	.618E-08	-126.9	.163E+09
49	-.674E+00	-.725E+00	-.408E-08	-.438E-08	.931E+00	-132.9	.636E-08	-130.0	.146E+09
50	-.866E+00	-.549E+00	-.415E-08	-.432E-08	.104E+01	-146.6	.614E-08	-132.5	.169E+09
51	-.103E+01	-.361E+00	-.392E-08	-.330E-08	.110E+01	-162.8	.552E-08	-139.2	.206E+09
52	-.125E+01	-.177E+00	-.343E-08	-.294E-08	.125E+01	-172.1	.454E-08	-139.1	.275E+09
53	-.137E+01	-.178E-01	-.275E-08	-.130E-08	.137E+01	-179.3	.304E-08	-146.9	.417E+09
54	-.143E+01	.101E+00	-.194E-08	-.421E-09	.143E+01	175.8	.198E-08	-167.7	.723E+09
55	-.141E+01	.185E+00	-.137E-08	.109E-09	.142E+01	172.5	.153E-08	174.7	.911E+09
56	-.131E+01	.221E+00	-.245E-09	.264E-08	.133E+01	170.4	.265E-08	95.1	.501E+09
57	-.111E+01	.215E+00	.475E-09	.417E-08	.113E+01	169.1	.415E-08	83.4	.272E+09
58	-.821E+00	.167E+00	.107E-08	.543E-08	.835E+00	168.5	.553E-08	79.3	.152E+09
59	-.446E+00	.915E-01	.135E-08	.547E-08	.455E+00	168.4	.551E-08	75.2	.827E+08
60	.140E-13	-.272E-14	.143E-08	.714E-08	.143E-13	-11.3	.728E-08	78.7	.196E-05
61	.495E+00	-.927E-01	.127E-08	.736E-08	.504E+00	-10.6	.749E-08	80.3	.673E+08
62	.101E+01	-.170E+00	.883E-09	.714E-08	.103E+01	-9.5	.719E-08	82.9	.143E+09
63	.151E+01	-.215E+00	.455E-09	.641E-08	.153E+01	-8.1	.642E-08	85.9	.238E+09
64	.195E+01	-.218E+00	-.796E-09	.525E-08	.196E+01	-6.3	.525E-08	93.2	.376E+09
65	.233E+01	-.167E+00	-.955E-09	.370E-08	.233E+01	-4.1	.383E-08	104.5	.619E+09
66	.256E+01	-.610E-01	-.115E-08	.190E-08	.256E+01	-1.4	.245E-08	129.3	.105E+10
67	.256E+01	.977E-01	-.201E-08	-.435E-10	.256E+01	2.1	.201E-08	-179.9	.127E+10
68	.255E+01	.298E+00	-.228E-08	-.137E-08	.257E+01	6.7	.301E-08	-139.2	.854E+09
69	.227E+01	.524E+00	-.231E-08	-.372E-08	.233E+01	13.0	.438E-08	-121.9	.532E+09
70	.181E+01	.757E+00	-.211E-08	-.517E-08	.196E+01	22.6	.558E-08	-112.2	.351E+09
71	.119E+01	.953E+00	-.168E-08	-.620E-08	.153E+01	38.9	.642E-08	-105.1	.238E+09
72	.442E+00	.112E+01	-.107E-08	-.674E-08	.120E+01	68.4	.682E-08	-99.1	.176E+09
73	-.384E+00	.121E+01	-.355E-09	-.674E-08	.127E+01	107.7	.675E-08	-93.0	.188E+09
74	-.123E+01	.120E+01	.390E-09	-.624E-08	.172E+01	135.7	.626E-08	-86.4	.275E+09
75	-.203E+01	.110E+01	.119E-08	-.530E-08	.231E+01	151.7	.542E-08	-78.2	.427E+09
76	-.273E+01	.887E+00	.169E-08	-.402E-08	.287E+01	162.0	.436E-08	-67.2	.657E+09
77	-.325E+01	.591E+00	.210E-08	-.255E-08	.331E+01	169.9	.330E-08	-50.5	.100E+10
78	-.356E+01	.197E+00	.230E-08	-.102E-08	.357E+01	176.8	.251E-08	-23.9	.142E+10
79	-.361E+01	-.237E+00	.227E-08	.412E-09	.362E+01	-176.2	.231E-08	10.3	.157E+10
80	-.340E+01	-.639E+00	.205E-08	.167E-08	.347E+01	-169.6	.251E-08	38.3	.138E+10
81	-.292E+01	-.111E+01	.165E-08	.249E-08	.312E+01	-159.1	.300E-08	56.4	.104E+10
82	-.220E+01	-.149E+01	.118E-08	.301E-08	.265E+01	-146.1	.322E-08	68.6	.823E+09
83	-.130E+01	-.177E+01	.665E-09	.312E-08	.219E+01	-126.6	.319E-08	77.9	.643E+09
84	-.277E+00	-.188E+01	.197E-09	.289E-08	.191E+01	-98.3	.290E-08	86.1	.658E+09
85	.787E+00	-.189E+01	-.174E-09	.241E-08	.204E+01	-67.4	.241E-08	94.1	.847E+09
86	.181E+01	-.174E+01	-.406E-09	.177E-08	.251E+01	-43.8	.182E-08	102.9	.138E+10
87	.273E+01	-.143E+01	-.484E-09	.110E-08	.307E+01	-28.1	.121E-08	113.7	.254E+10
88	.349E+01	-.105E+01	-.417E-09	.527E-09	.365E+01	-16.9	.673E-09	128.3	.542E+10
89	.395E+01	-.561E+00	-.234E-09	.138E-09	.399E+01	-8.0	.276E-09	150.1	.145E+11
90	.402E+01	.333E-13	.245E-22	.135E-35	.400E+01	.0	.246E-22	.0	.163E+24

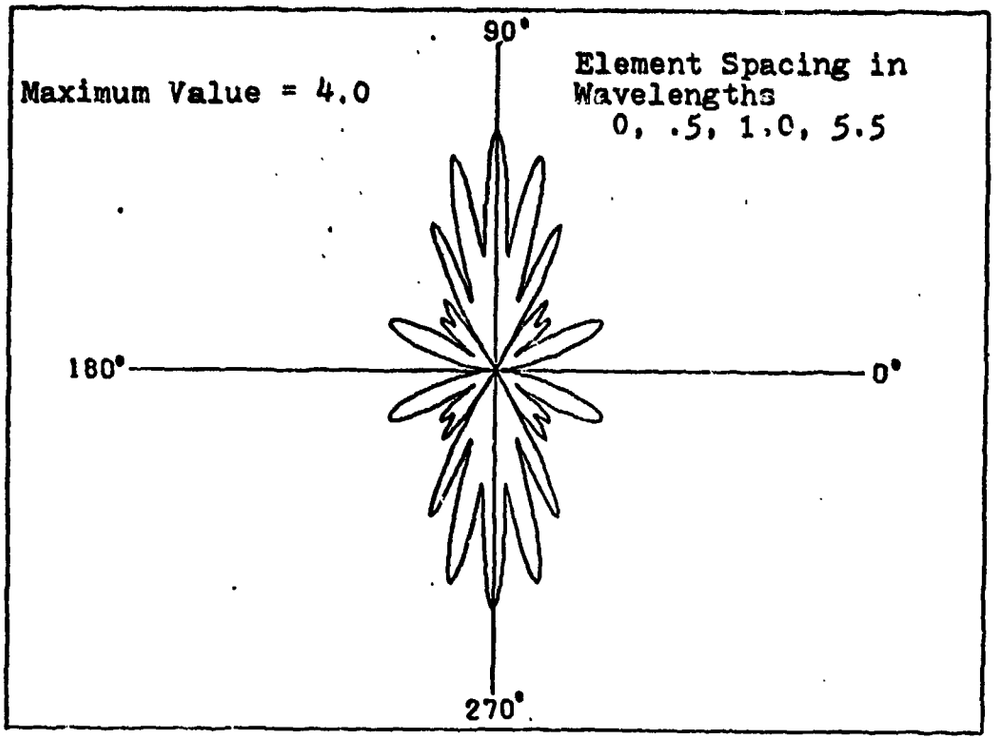

Figure 52. Four Element Sparse Array, Plot of $|A(\theta)|$.

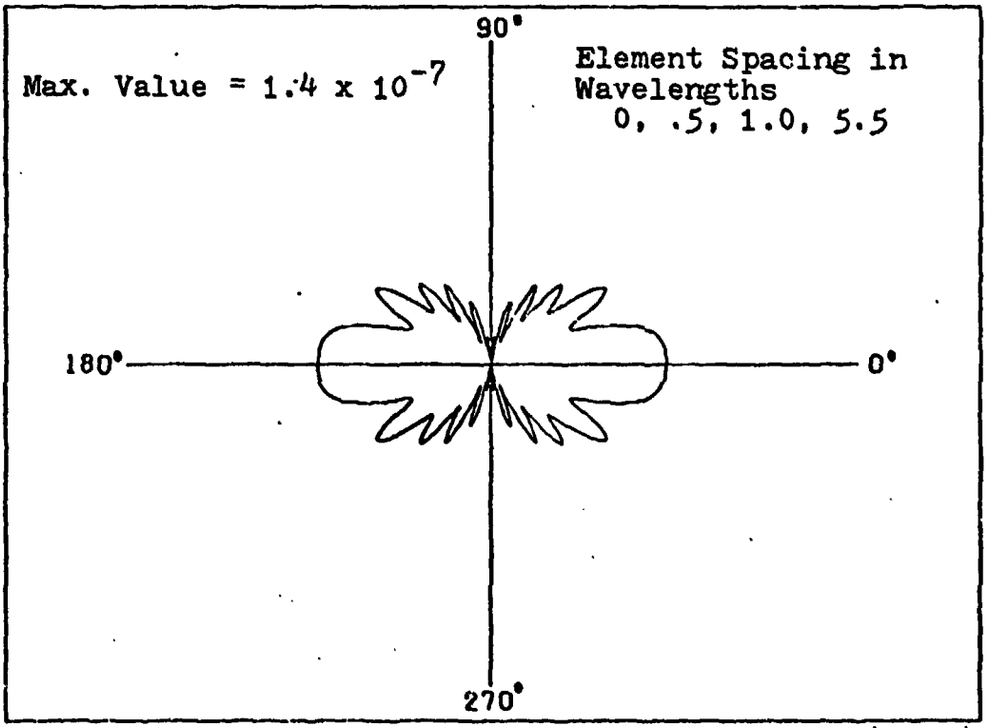

Figure 53. Four Element Sparse Array, Plot of $|B(\theta)|$.

it. Thus, in the neighborhood of the nulls at 0° and 60° the derivative term should become the dominant output of the array. The computer program was set up for this array and the output at 0° is shown in Figure 54. As is evident, the derivative term comes through.

In the last section we used the ratio $|A(\theta)/B(\theta)|$ to obtain a measure of the relative importance of the signal to the derivative. The plot of this term was used in conjunction with the ratio $m'(t)/m(t)$ to determine when the output would have a significant time derivative component. Plots of the ratio $|A(\theta)/B(\theta)|$ for these two sparse arrays are included as Figures 55 and 56. Figure 55 shows that $m'(t)/m(t)$ would have to be about 10^8 in order for the derivative to be significant. Figure 56 shows that this array has two null regions that would make the derivative significant. The ratio $m'(t)/m(t)$ would determine how far from these two nulls that the derivative remains significant.

By comparing the three plots of $B(\theta)$ (Figures 10, 51, and 53) we can observe that $B(\theta)$ is actually a fairly constant function. Except for the region near the main beam ($\theta = 90°$) its values do not fluctuate that much. $A(\theta)$, on the other hand, is observed to change amplitude quite a bit depending on the value of θ. It is a possibility that this constancy of $B(\theta)$ can be of value in the design of systems that rely on the derivative term. For example, a jammer that is designed to jam using the signal derivative can be assured of passage at a constant level except along the

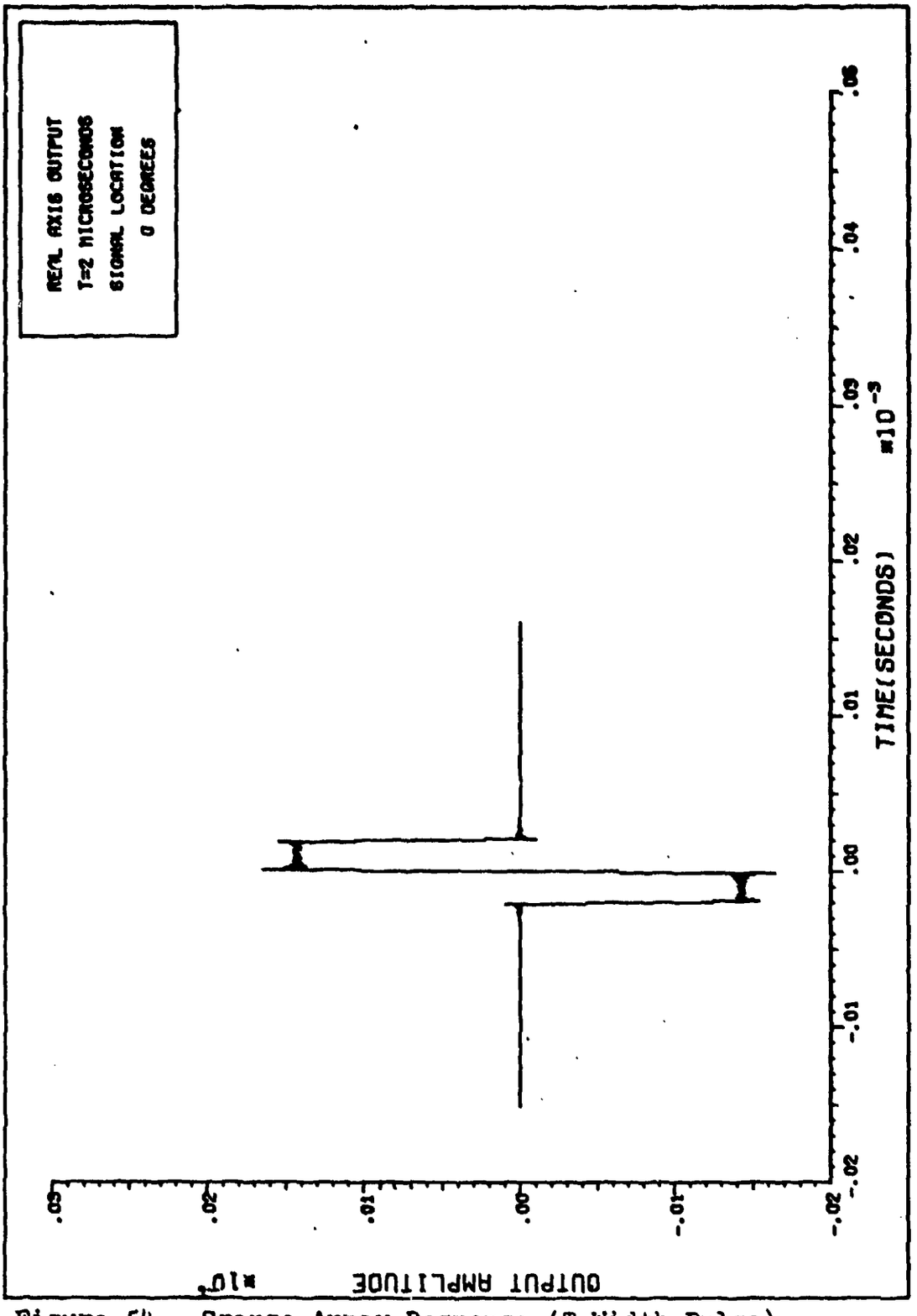

Figure 54. Sparse Array Response (T Width Pulse).

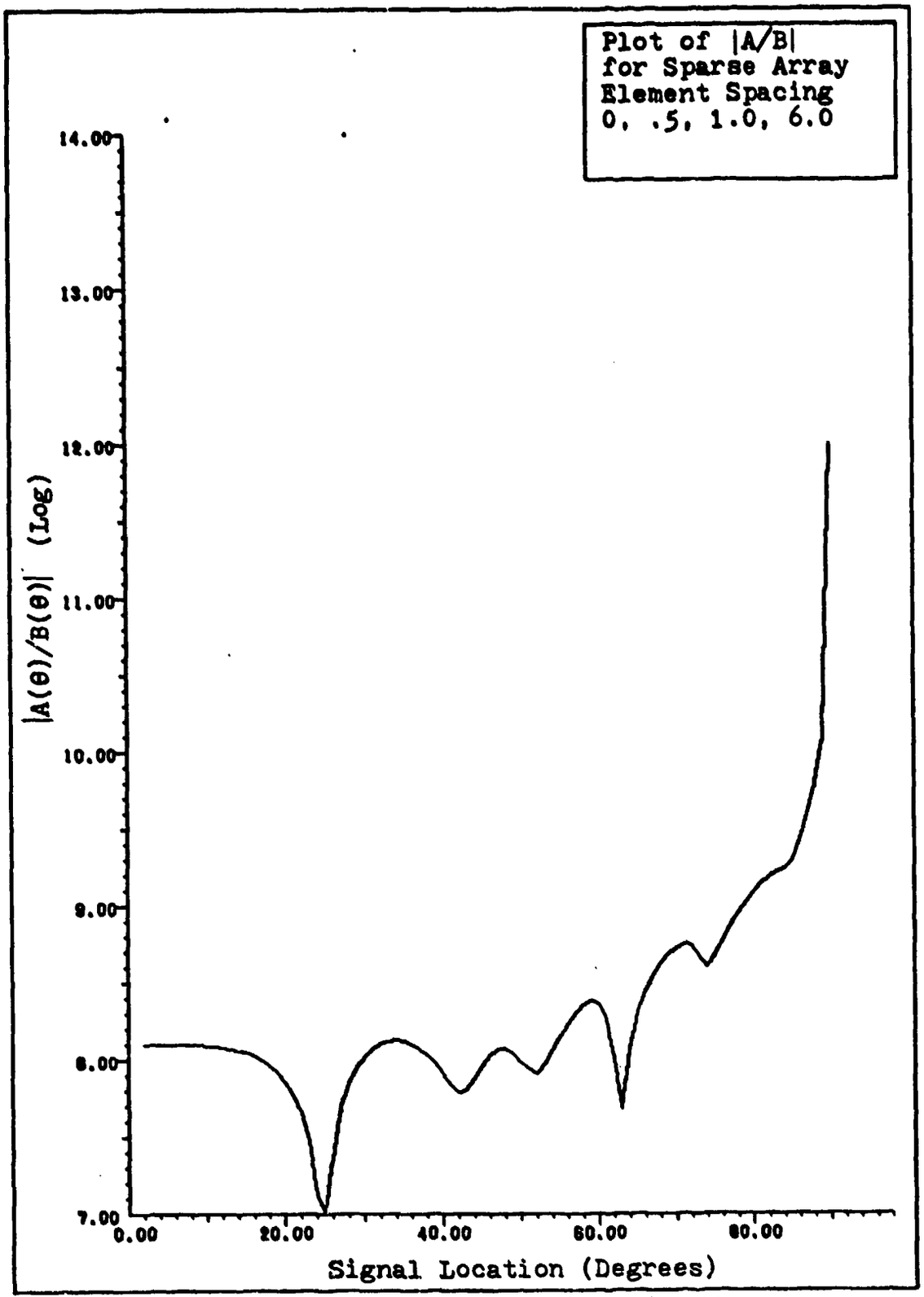

Figure 55. Sparse Array, Plot of $|A(\theta)/B(\theta)|$.

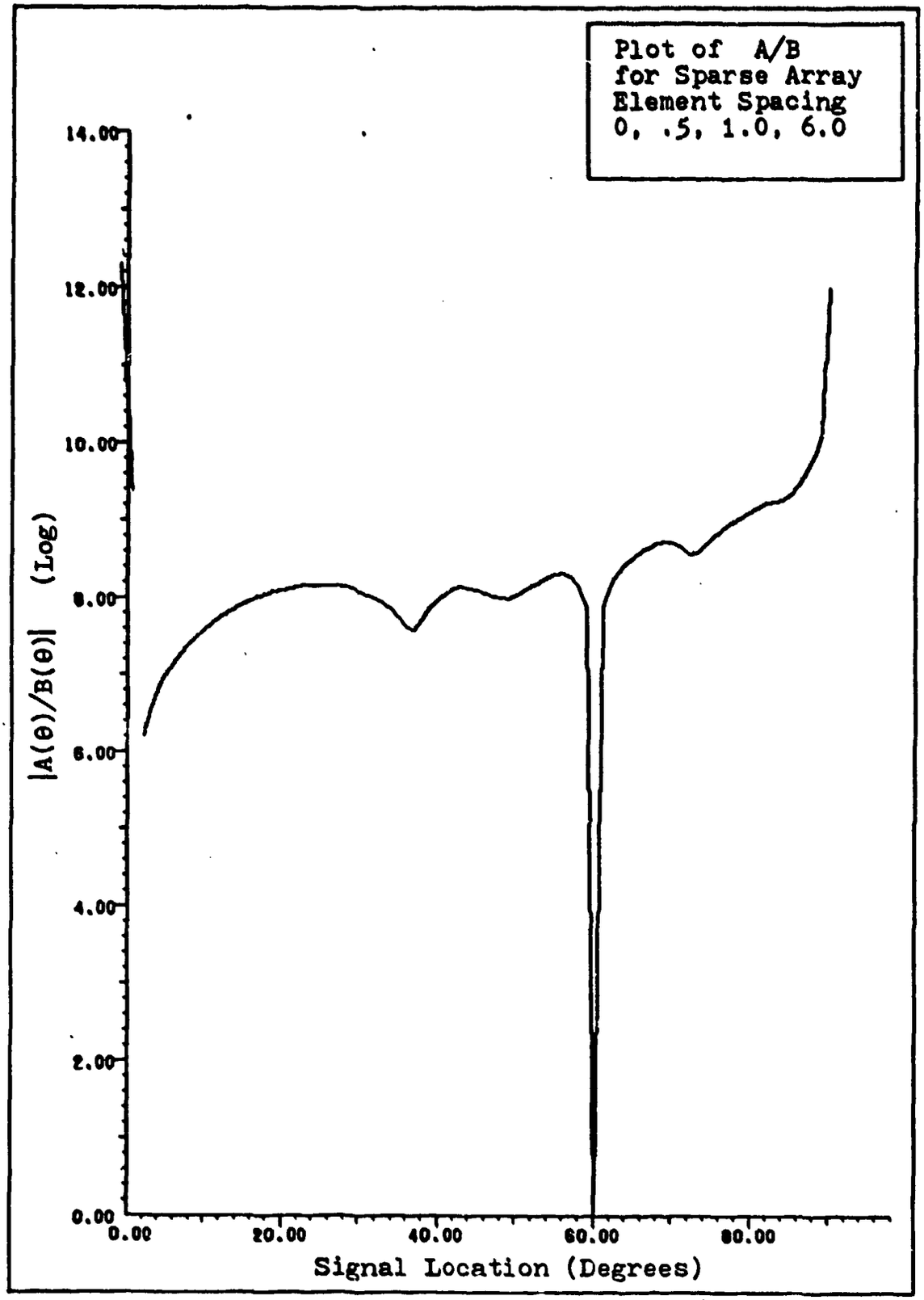

Figure 56. Sparse Array, Plot of $|A(\theta)/B(\theta)|$.

main beam axis.

By observing the nulls in Figures 9 and 52 and then comparing the values in Tables I and V, it becomes obvious that the nulls in the sparse array are narrower than in the equally spaced array. This has the advantage of cutting down on the region where the derivative is an effective output signal.

These two examples plus the linear array of the last section indicate how much the basic array pattern can be changed by element spacing. There is another aspect of arrays that these examples can illustrate. Phase steering of arrays (as discussed in the next section) can have the same effect as moving the elements. By electronically delaying the signal on one of the elements, it can effectively be moved away from the other elements. However, the more practical use for phase steered arrays will be discussed in the next section.

The basic results to be obtained from this section are summarized as follows: sparse arrays have nulls and the output in the neighborhood of the nulls will be dominated by the derivative term. The signal and derivative terms are at different phases. Unlike the linear arrays studied earlier, this phase difference varies depending on the signal location.

E. Phase-Steered Array

There is one last example to be investigated before leaving this chapter on static arrays. The main beam of

arrays can be moved electronically through a technique called phase steering. This is done by effectively delaying the signal coming out of each element of the array by a specific predetermined amount. The array model of Chapter II does not explicitly illustrate this particular technique. However, phase steering can be viewed as a linear phase shift in the frequency domain. This means that a phase steered antenna can be modeled by replacing α_i in Eq (14) by the expression $-2\pi(f+f_o)t_{oi}$ where $t_{oi} = \frac{r_i \cos\psi_{oi}}{c}$ and ψ_{oi} is the desired location of the main beam axis. This expression allows for both a linear phase shift and a constant phase shift. With this change, Eq (14) becomes

$$\tilde{s}(\theta, \phi, f) = M(f) \sum_{i=1}^{N} e^{j2\pi(f+f_o)(t_i - t_{oi})} \tag{51}$$

By factoring out the phase center terms and then expanding the summation using the Taylor series we obtain

$$\tilde{s}(\theta, \phi, f) = M(f) e^{j2\pi(f+f_o)t_c} \sum_{i=1}^{N} A_i e^{j2\pi f_o(t_i - t_{oi} - t_c)} \left\{ 1 + (j2\pi)(t_i - t_{oi} - t_c) f \right.$$

$$\left. + \cdots + \frac{[j2\pi(t_i - t_{oi} - t_c)f]^m}{(m-1)!} + \cdots + \cdots \right\} \tag{52}$$

Inverse transforming yields

$$\tilde{s}(\theta,\varphi,t) = m(t+t_c)e^{j2\pi f_o t_c}\sum_{i=1}^{N} A_i e^{j2\pi f_o(t_i - t_{oi} - t_c)}$$

$$+ \frac{dm(t+t_c)}{dt}\sum_{i=1}^{N}(t_i - t_{oi} - t_c)A_i e^{j2\pi f_o(t_i - t_{oi} - t_c)} + \ldots$$

$$+ \frac{d^m m(t+t_c)}{dt^m}\sum_{i=1}^{N}\frac{(t_i - t_{oi} - t_c)^m}{(m-1)!} A_i e^{j2\pi f_o(t_i - t_{oi} - t_c)} + \ldots \qquad (53)$$

As can be seen this is precisely Eq (25) with t_i replaced by $t_i - t_{oi}$. Thus, all the results obtained from Eq (25) are still valid in this case. The signal and its derivatives are still present. The derivatives will still tend to be insignificant compared to the signal due to the presence of the factors $(t_i - t_{oi} - t_c)^m$ in the summations. The summations are still just complex numbers that tend to phase shift the signal and its derivatives by different amounts. However, this phase shift has become a function of t_{oi} and can now introduce a phase-shift that varies with the steering term.

In the linear array the signal and its derivative were separated by 90°. To observe the effects of the phase steering term on linear arrays substitute the simple four element array parameters of Section III. C. into Eq (51). It becomes

$$s(\theta,f) = M(f)\sum_{i=1}^{4} e^{j2\pi(f+f_o)(t_i - t_{oi})} \qquad (54)$$

where

$$x_i = \frac{i-1}{2c}\lambda_0 \cos\theta$$

$$x_{0i} = \frac{i-1}{2c}\lambda_0 \cos\theta$$

θ_0 = desired steering angle

Upon performing the summation

$$\tilde{o}(\theta, f) = M(f) \exp\left[j \tfrac{3\pi}{2}(\cos\theta - \cos\theta_0)\right] \exp\left[j \tfrac{3\pi}{2}(\cos\theta - \cos\theta_0)\right]$$

$$\times \frac{\sin\left[2\pi\left(1+\frac{f}{f_0}\right)(\cos\theta - \cos\theta_0)\right]}{\sin\left[\frac{\pi}{2}\left(1+\frac{f}{f_0}\right)(\cos\theta - \cos\theta_0)\right]} \qquad (56)$$

where the two exponentials are the phase-center terms. By following the example of Eq (41) the trigonometric term is expanded as

$$\frac{\sin\left[2\pi\left(1+\frac{f}{f_0}\right)(\cos\theta - \cos\theta_0)\right]}{\sin\left[\frac{\pi}{2}\left(1+\frac{f}{f_0}\right)(\cos\theta - \cos\theta_0)\right]} = \frac{\sin[2\zeta_0]}{\sin\left[\frac{1}{2}\zeta_0\right]}$$

$$+ \frac{\zeta_0}{f_0}\left[\frac{2\sin\left(\frac{1}{2}\zeta_0\right)\cos(2\zeta_0) - \frac{1}{2}\cos\left(\frac{1}{2}\zeta_0\right)\sin(2\zeta_0)}{\sin^2\left(\frac{1}{2}\zeta_0\right)}\right] f$$

$$+ \cdots \qquad (56)$$

where

$$\zeta_o = \pi(\cos\theta - \cos\theta_o) \tag{57}$$

Thus,

$$A(\theta,\theta_o) = \frac{\sin[2\zeta_o]}{\sin[\frac{1}{2}\zeta_o]} \tag{58}$$

and

$$B(\theta,\theta_o) = \frac{-1}{\pi f_o}\left[\frac{2\sin(\frac{1}{2}\zeta_o)\cos(2\zeta_o) - \frac{1}{2}\cos(\frac{1}{2}\zeta_o)\sin(2\zeta_o)}{\sin^2(\frac{1}{2}\zeta_o)}\right] \tag{59}$$

At this point it should be obvious that phase steering is not going to cause any new effects. The signal and its derivative will still be 90° out of phase. The signal is still dominant except in the neighborhood of the nulls. The steering will just change the location of the main beam, the nulls, and the sidelobes. In fact it will change all the quantitative results somewhat but not any of the qualitative results. Thus, it appears that phase steering will not cause any new effects to the incoming signal.

The one area of quantitative interest in this example would be to investigate how much the width of the nulls are affected by phase steering. In the previous sections we showed how the derivative term is dominant for some small angular distance around the null points. It would be of interest to determine if this angular distance varies much

due to the steering. The author feels that the effect is small but did not have the opportunity to investigate this point thoroughly.

F. Summary of Static Array Results

This chapter has focused attention on the effects of antenna arrays on incoming signals. Although we focused our examples on the effects to the autocorrelation function of a spread spectrum signal, the main analysis is valid for any signal.

The truly unique result obtained from the foregoing analysis was the fact that the output of antenna arrays is, in fact, a combination of the incoming signal and all its time derivatives. The development that led to this result also indicated that the signal will be the only significant output except in the neighborhood of nulls. In the neighborhood of the nulls the first derivative will also become significant due to the attenuation of the signal. The analysis also showed that the system output phase changes rapidly near nulls. Finally, it was shown that the use of pulses as signals and correlators as detectors will accentuate the effects of the derivative and expand the neighborhood around the nulls where the effects are observable.

IV Dynamic Effects

The majority of the effort in this thesis has concerned itself with the effects of fixed arrays on signals. However, most large arrays in use today are adaptive in nature. Thus, we felt that it was necessary to look at aspects of adaptive arrays and analyze their effect on the incoming signal.

Adaptive arrays use a variety of algorithms to control the weighting coefficients of the antenna elements. These algorithms process the incoming signals, noise, and interference to determine the values of the coefficients. If these external conditions are unknown, then the adaptive effects can be viewed as a form of noise. This approach will be taken in this chapter.

The array model of Eq (10) incorporated the adaptive nature of the arrays by making the weighting coefficients functions of time. However, Chapter III assumed that these coefficients were constants. The resulting fixed array calculations yielded very important properties about arrays and their effect on wideband signals. In this chapter, we will assume that the adaptive array is trying to seek a desired static (steady-state) condition and the environment is causing perturbations around this desired state.

Eq (10) is used to develop some results that illustrate the effect that time varying, weighting coefficients have on the signal. Two models for the weighting coefficients are

introduced and the analysis performed. It is hoped that these simple models will yield insight into more complex situations.

To start the analysis, Eq (10) is repeated here.

$$s(\theta, \phi, t) = \sum_{i=1}^{N} A_i(t)\, v(t - t_i)\, e^{j[\phi_p(t - t_i) + 2\pi f_0 t_i + \alpha_i(t)]} \tag{10}$$

Recall that this is the complex baseband model of the array and its output becomes the input to the receiver processor. Next, recall that in Section III. E., an equation for phase steering was developed. By combining those results with Eq (10) we obtain a generalized adaptive array equation that includes phase steering.

$$s(\theta, \phi, t) = \sum_{i=1}^{N} A_i(t)\, v(t - t_i - t_{oi})\, e^{j[\phi_p(t - t_i - t_{oi}) + 2\pi f_0 (t_i - t_{oi}) + \alpha_i(t)]} \tag{60}$$

A. Sinusoidal Perturbations

Assume,

$$A_i(t) e^{j\alpha_i(t)} \equiv A_i e^{j(\beta_i \sin 2\pi f_m t + \alpha_i)} \tag{61}$$

where $\beta_i \sin 2\pi f_m t$ is a perturbation of the steady state phase steering coefficients. This model can be used for several purposes. (1) $\beta_i \sin 2\pi f_m t$ can be considered a noise jitter and the effect of this noise on the signal can be calculated for a variety of noise levels, β_i, and noise jitter rates, f_m. (2) Another approach would be to assume

that the $\beta_i \sin 2\pi f_m t$ are a modulation resulting from a jamming attempt. In either case we are interested in the effect this sinusoidal perturbation has on the incoming signal. By substituting these assumptions into Eq (60), the output becomes

$$\tilde{s}(\theta, \phi, t) = \sum_{i=1}^{N} A_i v(t + \tau_i - \tau_{oi})$$

$$\times e^{j[\phi_p(t+\tau_i-\tau_{oi}) + 2\pi f_c(t-\tau_{oi})]} e^{j(\beta_i \sin 2\pi f_m t + \alpha_i)} \tag{62}$$

The $e^{j\beta_i \sin 2\pi f_m t}$ terms can be expanded in a Fourier series (Ref 21:116) yielding

$$e^{j\beta_i \sin 2\pi f_m t} = \sum_{l=-\infty}^{\infty} J_l(\beta_i) e^{jl2\pi f_m t} \tag{63}$$

where the $J_l(\beta_i)$ are Bessel functions of the first kind and order l. Substituting these results into Eq (62) yields

$$\tilde{s}(\theta, \phi, t) = \sum_{i=1}^{N} v(t + \tau_i - \tau_{oi}) e^{j[\phi_p(t+\tau_i-\tau_{oi}) + 2\pi f_c(\tau_i - \tau_{oi})]}$$

$$\times A_i e^{j\alpha_i} \sum_{l=-\infty}^{\infty} J_l(\beta_i) e^{jl2\pi f_m t}$$

$$= \sum_{l=-\infty}^{\infty} \sum_{i=1}^{N} v(t + \tau_i - \tau_{oi}) e^{j[\phi_p(t+\tau_i-\tau_{oi}) + 2\pi f_c(\tau_i - \tau_{oi})]}$$

$$\times A_i J_l(\beta_i) e^{j(\alpha_i + l2\pi f_m t)} \tag{64}$$

Notice that the $l = 0$ term is the static phase steered

array of Section III. E., except for the $J_0(\beta_i)$ amplitude weight. The $\ell \cdot g$ term is

$$\sum_{i=1}^{N} v(t - t_1 - t_m) e^{j[\phi_p(t - t_1 - t_m) - 2\pi f_c(t_i - t_m)]}$$

$$\times A_i e^{j\theta_i} J_g(\beta_i) e^{jg 2\pi f_m t} \tag{65}$$

As can be seen this is the phase steered equation modified by the $J_g(\beta_i)$ terms and then modulated by a carrier frequency of $g f_m$ Hz .

Thus, the noise jitter has caused two effects. The β_i have changed the phase steered equation by multiplying each output by $J_m(\beta_i)$. If the β_i are quite different, this could affect the basic array pattern immensely. This effect cannot be determined without more information about the β_i and the array structure. If the β_i are all about the same, then they act basically as an attenuation of the array output. The f_m term causes an infinite series of modulated versions of the signal to appear at the output. Depending on the modulation frequency, f_m , and the signal bandwidth these terms can cause signal aliasing effects.

The extent that these modulation terms interfere depends on both f_m and on $J_g(\beta_i)$. f_m determines how many of the Bessel series terms are located in the bandwidth region of the signal. The $J_g(\beta_i)$ determine if the terms that are in the aliasing region are significant enough in amplitude

(compared to the $\ell = 0$ term) to cause distortion. A study of the Bessel function will yield some information on this point.

The Bessel functions can be written as power series (Ref 5:143).

$$J_\ell(x) = \sum_{k=0}^{\infty} \frac{(-1)^k \left(\frac{x}{2}\right)^{2k+\ell}}{k!(k+\ell)!} \tag{66}$$

From this it is easy to see that

$$J_0(0) = 1$$

$$J_\ell(0) = 0, \text{ for } \ell \neq 0 \tag{67}$$

Thus, for $\beta_1 = 0$, Eq (64) reduces precisely to the static phase-steered array of Section III. E. For small β_1 (less than .2), $J_0(\beta_1) \geq .99$ and $J_1(\beta_1) \leq .1$. The higher order Bessel terms are also small. Thus, for small β_1 the output is mostly the phase-steered output with a small amount of the modulated terms being passed. This indicates that the aliasing effects should be small and not cause much signal interference. However, if the β_1 become larger than ~2, the $J_1(\beta_1)$ increase rapidly. At this point, the effect of the first modulation term will become significant and the value of f_m will become important.

Eq (64) is the time domain output of the array. If we perform a Fourier transform of this equation, the result is

$$\tilde{o}(\theta,\phi,f) = \sum_{\ell=-\infty}^{\infty} \left\{ \sum_{n=1}^{M} A_n J_\ell(\beta_n) e^{j\phi_n} e^{j2\pi(f-f_0-\ell f_m)(t_n-t_0)} \right\} M(f-\ell f_m) \qquad (68)$$

where

$$M(f) = \mathcal{F}\left\{ v(t)\, e^{j\phi_p(t)} \right\} \qquad (69)$$

In this form the discussion above is easily confirmed. First, it is simple to see that the inner sum is the static phase-steered array of Chapter III except for the $J_\ell(\beta_n)$ and ℓf_m terms. It is obvious from this form that the $J_\ell(\beta_n)$ effects are equivalent to changing the weighting coefficients, A_n and the ℓf_m are equivalent to changing the α_n. Thus, if the $J_\ell(\beta_n)$ and ℓf_m take on a wide range of values, the array pattern will change considerably.

Next, the effect of the perturbation frequency, f_m, is to shift the inner sum up and down in the frequency spectrum. Figure 57 portrays this frequency viewpoint graphically. It shows that the spectrum at each harmonic is different than the actual signal spectrum due to the $J_\ell(\beta_n)$ and ℓf_m modifications to the static array equation.

The above analysis has crudely shown the effect of a sinusoidal oscillation of the array's weighting coefficients on a desired signal. Roughly, it illustrated that the array

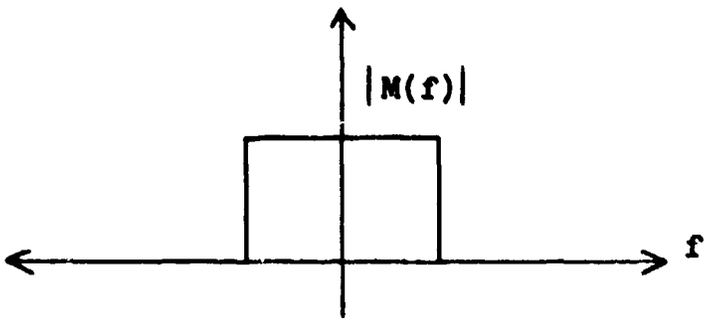

a. Signal Spectrum

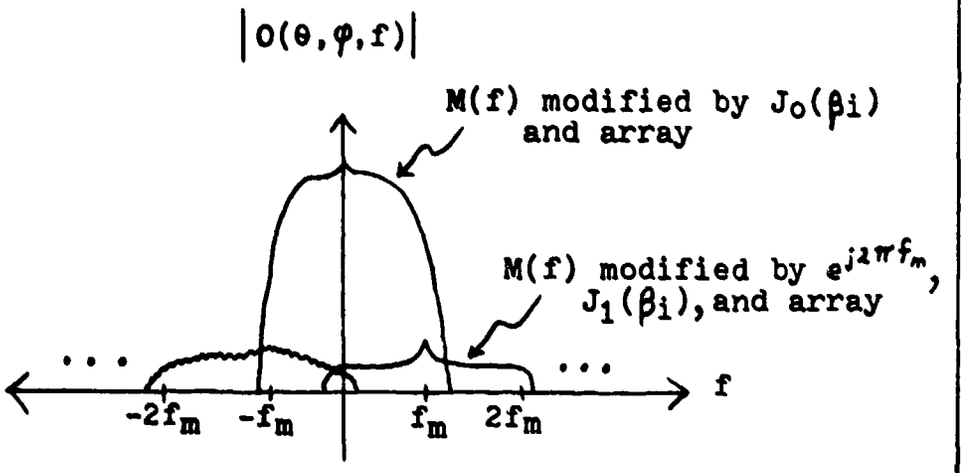

b. Array Output with Aliasing Assumed

Figure 57. Frequency Domain Output of Array.

function output is first modified by the $J_l(\beta_i)$ and lf_m and then modulated by the harmonics of the sinusoidal frequency, f_m . It appears that these effect are minor for small perturbation levels. It was not shown what effects the Bessel functions $J_l(\beta_i)$ and lf_m have on the overall array pattern. If the β_i are quite different, then the array pattern can be changed extensively. This could cause the same kind of effects as phase steering (e.g., change the pattern so that the signal is in a null).

B. Gaussian Noise

In this section we assume a different model for the coefficients. Assume

$$A_i(t)e^{j\alpha_i(t)} = A_i e^{j[\alpha_i + m_i(t)]} \tag{70}$$

where $m_i(t)$ are gaussian random processes, with means $m_i(t)$ and covariances $C_i(t_1, t_2)$ and cross covariances $C_{ij}(t_1, t_2)$. Eq (60) becomes

$$\tilde{o}(\theta, \phi, t) = \sum_{i=1}^{N} \underbrace{A_i v(t + t_i - t_{oi})\, e^{j\phi_p(t + t_i - t_{oi}) + 2\pi f_o(t_i - t_{oi}) + \alpha_i}}_{\gamma_i(\theta, \phi, t)} e^{jm_i(t)} \tag{71}$$

where $\gamma_i(\theta, \phi, t)$ is defined as shown. Now we determine the statistics of the output.

We use the accepted notation for expected values, $E[x]$, to stand for

$$E[x] = \int_{-\infty}^{\infty} x f(x)\, dx \tag{72}$$

where $f(x)$ is the probability density function of x (Ref 3:229). First, the expected value of the output of Eq (71) becomes

$$E[\delta(\theta,\varphi,t)] = \sum_{i=1}^{N} \gamma_i(t)\, E[e^{j m_i(t)}] \tag{73}$$

The characteristic function of a random variable is defined as (Ref 3:419)

$$\phi_x(v) = E[e^{jvx}] \tag{74}$$

Furthermore, the characteristic function of a gaussian random variable is (Ref 3:420)

$$\phi_x(v) = \exp[jvm - v^2 \frac{\sigma^2}{2}] \tag{75}$$

where m is the mean of x and σ^2 is the variance of x. If $v = 1$, then Eq (74) reduces to

$$\phi_x(1) = E[e^{jx}] \tag{76}$$

This is precisely the form of the expectation in Eq (73) except for the time dependence. Therefore, it can be evaluated by determining its characteristic function and then letting $v = 1$. This can be accomplished in the following fashion. Let $t = t_k$ in Eq (73). Then $n(t_k)$ becomes a gaussian random variable. As such, the

expectation can be evaluated using the results of Eqs (74) and (75). Finally, by letting $v = 1$, Eq (73) becomes

$$E[s(\theta, \varphi, t_k)] = \sum_{i=1}^{N} g_i(\theta, \varphi, t_k) \exp\left[j m_i(t_k) - \frac{\sigma_i^2(t_k)}{2}\right] \tag{77}$$

where $\sigma_i^2(t_k) = C_i(t_k, t_k)$. This operation is valid for any value of t_k. Therefore, the result can be generalized to

$$E[s(\theta, \varphi, t)] = \sum_{i=1}^{N} g_i(\theta, \varphi, t) \exp\left[j m_i(t) - \frac{\sigma_i^2(t)}{2}\right] \tag{78}$$

This shows that the effect of gaussian noise on the expected output is to introduce a phase shift and an attenuation of the output of each element. This will change the antenna pattern. The new pattern will then determine the effect on the signal. If the m_i are all approximately equal, the phase shift introduced will have no new effects on the signal. Notice that the expected output decreases in amplitude as the variance, σ^2, increases. In essence, this says that as the noise variance increases, the output looks less like the signal and more like zero mean noise. This should agree with intuitive notions about system operations (i.e., the noisier the system, the poorer the performance).

A final point needs to be made about Eq (78). If the noise is zero mean and has small variance, the expected output of the array is expected to be the phase-steered

output. This is also intuitive in that it simply says that if there is little noise, then the system is basically fixed and the fixed array analysis is valid.

The expected value of the output is important but we also need to have a feel for how close to the expected output the actual output sample functions will be. This leads to a determination of the variance of the output. The variance can be calculated from

$$\sigma_{\tilde{o}}^2(\theta,\phi,t) = E\left[\tilde{o}(\theta,\phi,t)\,\tilde{o}^*(\theta,\phi,t)\right] - E\left[\tilde{o}(\theta,\phi,t)\right] E^*\left[\tilde{o}(\theta,\phi,t)\right] \tag{79}$$

where * denotes the complex conjugate. The first term on the right side of the equality is evaluated as follows

$$E\left[\tilde{o}(\theta,\phi,t)\,\tilde{o}^*(\theta,\phi,t)\right]$$

$$= E\left[\sum_{i=1}^{N} \gamma_i(\theta,\phi,t)\, e^{j m_i(t)} \sum_{j=1}^{N} \gamma_j^*(\theta,\phi,t)\, e^{-j m_j(t)}\right]$$

$$= E\left[\sum_{i=1}^{N}\sum_{j=1}^{N} \gamma_i(\theta,\phi,t)\,\gamma_j^*(\theta,\phi,t)\, e^{j\{m_i(t) - m_j(t)\}}\right]$$

$$= \sum_{i=1}^{N}\sum_{j=1}^{N} \gamma_i(\theta,\phi,t)\,\gamma_j^*(\theta,\phi,t)\, E\left[e^{j\{m_i(t) - m_j(t)\}}\right] \tag{80}$$

If the $m_i(t), m_j(t)$ are considered to be jointly normal processes, then the random variables obtained by sampling them at $t = t_k$ are jointly normal. The characteristic function

of these random variables becomes (Ref 3:503)

$$E\left[e^{j(v_i m_i(t_k) + v_j m_j(t_k))}\right]$$

$$= \exp\left[j\{m_i(t_k)v_i + m_j(t_k)v_j\}\right.$$

$$\left. - \tfrac{1}{2}\{\sigma_i^2(t_k)v_i^2 + 2C_{ij}(t_k, t_k)v_{ij} + \sigma_j^2(t_k)v_j^2\}\right] \qquad (81)$$

By observing that this result holds for any t_k and by setting $v_i = 1$ and $v_j = -1$, the value of the expectation in Eq (80) can be determined. By doing this, Eq (80) becomes

$$E[\tilde{\sigma}(\theta, \phi, t)]\, E[\tilde{\sigma}^*(\theta, \phi, t)]$$

$$= \sum_{i=1}^{N}\sum_{j=1}^{N} \gamma_i(\theta, \phi, t)\, \gamma_j^*(\theta, \phi, t) \exp\left[j\{m_i(t) - m_j(t)\}\right.$$

$$\left. - \tfrac{1}{2}\{\sigma_i^2(t) - 2C_{ij}(t, t) + \sigma_j^2(t)\}\right] \qquad (82)$$

Next, we realize that the last term of Eq (79) is just the magnitude of Eq (78). Thus,

$$E[\tilde{\sigma}(\theta, \phi, t)]\, E[\tilde{\sigma}^*(\theta, \phi, t)]$$

$$= \sum_{i=1}^{N}\sum_{j=1}^{N} \gamma_i(\theta, \phi, t)\, \gamma_j^*(\theta, \phi, t) \exp\left[j\{m_i(t) - m_j(t)\}\right.$$

$$\left. - \frac{\sigma_i^2(t) + \sigma_j^2(t)}{2}\right] \qquad (83)$$

Combining Eqs (82) and (83), we finally obtain the variance

$$\sigma_s^2(\theta,\phi,t) = \sum_{i=1}^{N}\sum_{j=1}^{N} \gamma_i(\theta,\phi,t)\,\gamma_j^*(\theta,\phi,t)\exp\left[\frac{1}{2}\left\{m_i(t) - m_j(t)\right\} - \left(\frac{\sigma_i^2(t)+\sigma_j^2(t)}{2}\right)\right]$$

$$\times\left[\exp\left\{C_{ij}(t,t)\right\} - 1\right] \tag{84}$$

The variance is a complicated function of the signal, array, and noise parameters.

There are several things that can be noted. First, if there is no noise, then the $C_{ij}(t,t) \rightarrow 0$ and Eq (84) reduces to zero as expected. Second, the means, $m_i(t)$, of the noise cause a relative phase shift between the cross component signals; i.e., the mean is a steering term that changes the variance. Third, the individual variances cause an attenuation of the cross-term products. This seems to say that the system variance decreases as the individual variances increase. In fact, it appears that the system variance decreases to zero as the individual term variances approach infinity. However, look at the $i = j$ terms. They are of the form

$$|\gamma_i(\theta,\phi,t)|^2 \exp\left[\sigma_i^2(t)\right]\left\{\exp\left[\sigma_i^2(t)\right] - 1\right\}$$

$$= |\gamma_i(\theta,\phi,t)|^2\left\{1 - \exp\left[-\sigma_i^2(t)\right]\right\} \tag{85}$$

In this form it is obvious that these terms become larger as the $\sigma_i^2(t)$ become larger. Thus, due to these terms the system variance does not go to zero as it first appeared.

As a final look at the variance, assume the noise processes have equal means and are uncorrelated. Thus, $C_{ij}(t,t) = 0$ for $i \neq j$. Under these conditions Eq (84) becomes

$$\sigma_s^2(\theta,\phi,t) = \sum_{i=1}^{N} |\gamma_i(\theta,\phi,t)|^2 \left\{1 - \exp\left(-\sigma_i^2(t)\right)\right\}$$

$$\leq \sum_{i=1}^{N} |\gamma_i(\theta,\phi,t)|^2 \qquad (86)$$

Thus, under these conditions we have a bound on the system variance; a bound that is independent of the noise levels. This tells us that the system variance level can be completely controlled by the designer. However, it is controlled by the same parameters that determine the signal level. Thus, as the variance is decreased so is the signal.

A measure of performance in this case would be to look at a version of the signal-to-noise (SNR) ratio. Thus, for this example of equal mean, independent gaussian processes the SNR ratio becomes

$$SNR = \frac{E[\tilde{o}(\theta,\phi,t)]\,E[\tilde{o}^*(\theta,\phi,t)]}{\sigma_s^2(\theta,\phi,t)}$$

$$= \frac{\sum_{i=1}^{N}\sum_{j=1}^{N} \gamma_i(\theta,\phi,t)\,\gamma_j^*(\theta,\phi,t)\exp\left[-\frac{\sigma_i^2(t)+\sigma_j^2(t)}{2}\right]}{\sum_{i=1}^{N}|\gamma_i(\theta,\phi,t)|^2\left\{1-\exp\left(-\sigma_i^2(t)\right)\right\}} \qquad (87)$$

If, in addition, we assume equal variance terms, then

$$SNR = \frac{1}{exp[\sigma^2(t)]-1} \cdot \frac{\sum_{i=1}^{N}\sum_{j=1}^{N} \gamma_i(\theta,\phi,t)\,\gamma_j^*(\theta,\phi,t)}{\sum_{i=1}^{N} |\gamma_i(\theta,\phi,t)|^2} \tag{88}$$

The double sum can be rewritten as the product of the sums

$$SNR = \frac{1}{exp[\sigma^2(t)]-1} \cdot \frac{\sum_{i=1}^{N} \gamma_i(\theta,\phi,t) \sum_{j=1}^{N} \gamma_j^*(\theta,\phi,t)}{\sum_{i=1}^{N} |\gamma_i(\theta,\phi,t)|^2}$$

$$= \frac{1}{exp[\sigma^2(t)]-1} \cdot \frac{\left|\sum_{i=1}^{N} \gamma_i(\theta,\phi,t)\right|^2}{\sum_{i=1}^{N} |\gamma_i(\theta,\phi,t)|^2} \tag{89}$$

In this form we notice that the SNR is a product of a noise controlled gain and an array controlled gain. The noise factor shows that the SNR becomes very large as the noise variance approaches zero.

Eq (89) has shown that the noise variance affects the signal-to-noise ratio. Eq (86) showed that the noise variance is bounded. These two equations allow the system designer to pick the parameters to minimize the effects of a jammer that somehow has managed to inject a noise signal into the weighting coefficient control loops. From the jammer's viewpoint, he can use these equations to determine how much jamming effect he can have if he can inject noise into the coefficient loops.

The analysis using sinusoidal weighting coefficient noise and gaussian noise has revealed a method for degrading the output of the array. This method involves developing some technique for affecting the control loops of the array so that they are not allowed to stabilize. This implies some very sophisticated knowledge of the array operation.

The more traditional approach to jamming is to simply overload the system with a high power interference source. The standard measure of effectiveness of this method is to determine the signal-to-jammer power ratio. Recall that $\gamma_i(\theta,\varphi,t)$ is the incoming signal. However, it can be viewed as the sum of the desired signal and the jamming signal. Thus,

$$\gamma_i(\theta,\varphi,t) = \gamma_{si}(\theta,\varphi,t) + \gamma_{ji}(\theta_j,\varphi_j,t) \tag{90}$$

where $\gamma_{si}(\theta,\varphi,t)$ is the signal component and $\gamma_{ji}(\theta_j,\varphi_j,t)$ is the jammer component. With these definitions we can form the usual signal-to-jammer (SJR) ratio.

$$SJR = \frac{\left|\sum_{i=1}^{N}\gamma_{si}(\theta,\varphi,t)\right|^2}{\left|\sum_{i=1}^{N}\gamma_{ji}(\theta_j,\varphi_j,t)\right|^2} \tag{91}$$

This ratio affects the overall system SNR. It shows very clearly that one effective jamming technique is to increase the jamming output of the array. It is not, however, as simple as increasing the jammer power (though increased

jamming power works). Arrays are designed to counter the effect of the jammer by making this part of the output small. The array accomplishes this by placing a null at the location (θ_j, ϕ_j). In Chapter III we showed that one technique for transmitting through a null is to transmit a signal with high derivative content. Thus, rather than increase the jammer power, pick a jammer signal with most of the power in the derivative.

The next point to make about this SJR is that with the use of spread spectrum, the jammer will also have to counter those anti-jamming techniques in addition to getting through the array.

In this chapter we derived the effects of two noise models on the output of the array. The basic result was that noise in the array weighting coefficients results in degraded signal output. It was also stated that a possible jamming technique is to induce noise in the array control loops. No method was illustrated to show how a jammer might manage to get control of the array's control loops.

V Conclusions and Recommendations

This thesis has investigated the effects of antenna arrays on wideband signals. The effort began by developing a complex baseband model for the array's output that includes the antenna's frequency effects (Eq (10)). Chapter III converted this to the equation for a static array (Eq (12) and Eq (14)). At this point the array was viewed as a filter and its transfer function was obtained from Eq (14).

The transfer function was expanded in a Taylor series. This expansion was then used to determine the properties of the resulting output waveform. The basic conclusions drawn from this investigation follow.

(1) The output of an array consists of an infinite sum of components. The components consist of the signal and all the n'th order time derivatives of the signal.

(2) Each of the components is weighted by a complex number that adjusts its phase and amplitude before the components are added together.

(3) In general, the coefficient of the signal term is many orders of magnitude larger than the first derivative term coefficient, the first derivative coefficient is many orders of magnitude larger than the second derivative coefficient, etc. Because of this, the signal term is usually dominant. The only exception is in the neighborhood of nulls, where the signal coefficient vanishes. Then the first derivative

term becomes the main output of the array.

(4) For wideband signals the derivative term tends to be orders of magnitude larger than the signal term. This tends to offset the small coefficient of the derivative term. This means that the derivative term becomes observable farther from the null points than would otherwise be expected.

(5) The signal and the derivative terms have different phases. In the case of linear arrays the signal and its first derivative are separated in phase by 90°. This can be used by coherent receivers to isolate either the signal or the derivative. For other arrays, the phase difference is not fixed and in general is not 90°.

(6) The cases studied indicated that an envelope detector tends to yield the signal as the system output more often than coherent receivers. However, we did not investigate the effect an envelope detector would have on the PSK version of a spread spectrum code.

Chapter IV looked at two representations of the array where the weighting coefficients were modeled as static components plus an added noise signal. The first representation modeled the noise term as a precise sinusoidal. The conclusions drawn from this model follow.

(7) The array output is carrier modulated by all of the sinusoid harmonics. Thus, the frequency spectrum of the array output is moved up and down the frequency axis by integer amounts of the sinusoidal frequency. If this

frequency is not high enough aliasing will occur.

(8) Each of the modulated array outputs is modified by Bessel function coefficients. These coefficients alter the array output. Thus, the signal at one harmonic is not the same as the signal at other harmonics.

The second approach to the study of noise effects assumed that the noise terms were gaussian random processes. This analysis resulted in the following conclusions.

(9) The noise tends to drive the expected output of the array away from the static array output toward zero output.

(10) The variance of the system output increases as the noise level increases.

A crude look at using noise to jam adaptive arrays was investigated. One conclusion was drawn.

(11) The jammer has two ways available to change the expected output of the array. First, the jammer can simply increase the power of its jamming signal. This will increase the variance of the noise output of the array. Second, the jammer can transmit a signal that controls the variance of the steering coefficients.

The analysis performed in this thesis brought to light a variety of information about arrays. This information indicates areas where further research might be able to take advantage of the results obtained in this thesis. We recommend the following.

(1) The first derivative term exists at the output of the array. Research should be performed to see if receivers can

be designed to take advantage of the presence of this signal.

(2) Some systems may want to minimize the effects of the derivative terms. Research should be directed toward finding signal sets that have small derivatives. More specifically, research should be directed toward finding signal sets whose correlation functions have small derivatives.

(3) For the purposes of jamming, signals with high power in the derivative terms would be difficult to null. Studies in this area could result in valuable information about jamming of arrays.

(4) One of the original purposes of this thesis was to investigate the effects of the array on spread spectrum signals. The details of this analysis were never carried out for the specific spread spectrum model. This analysis should be completed.

(5) The effects of specific models of adaptive arrays need to be investigated. Specifically, transient effects should be investigated when the array adapts from one steady state to another.

(6) It was observed that there appears to be an inverse relationship between A, the multiplier of the signal, and B, the multiplier of the derivative. This might imply that the deeper the null, the higher the derivative. This relationship should be studied in detail. It might reveal insights into more optimum nulling techniques.

Bibliography

1. Cheng, D. K. "Optimization Techniques for Antenna Arrays," Proceedings of the IEEE, Vol 59:1664-1673 (December 1971)

2. Courant, R. Methods of Mathematical Physics. New York: Interscience Publishers, Inc., 1953.

3. Davenport, W. B. Probability and Random Processes. New York: McGraw-Hill Book Company, 1970.

4. Dixon, R. C. Spread Spectrum Systems. New York: John Wiley and Sons, Inc., 1976.

5. Hildebrand, F. B. Advanced Calculus for Applications. Englewood Cliffs, New Jersey: Prentice-Hall, Inc., 1962.

6. Kinsey, R. R. and A. L. Horvath. "Transient Response on Center-Series Fed Array," Phased Array Antennas, edited by A. A. Oliner and George H. Knittel. Dedham, Mass.: Artech House, Inc., 1972.

7. Knuckey, R. L. "On the Effects of Eliminating the Passive Elements from a Thinned Array," Phased Array Antennas, edited by A. A. Oliner and G. H. Knittel. Dedham, Mass.: Artech House, Inc., 1972.

8. Kraus, J. D. Antennas. New York: McGraw-Hill Book Company, 1950.

9. Lindsey, W. C. Telecommunications Systems Engineering. Englewood Cliffs, New Jersey: Prentice-Hall, Inc., 1973.

10. Ma, M. T. Theory and Application of Antenna Arrays. New York: John Wiley and Sons, Inc., 1974.

11. Mayhan, J. T. "Adaptive Nulling with Multiple-Beam Antennas," Technical Note 1976-18. Lexington, Mass.: Lincoln Laboratory, 30 Sept. 1976.

12. Mayhan, J. T. "Physical Limitations on Interference Reduction by Antenna Pattern Shaping," IEEE Transactions on Antennas and Propagation," Vol AP-23, No. 5: 639-646 (September 1975).

13. Oppenheim, A. V. Digital Signal Processing. Englewood Cliffs, New Jersey: Prentice-Hall, Inc., 1975.

14. Papoulis, A. Probability, Random Variables, and Stochastic Processes. New York: McGraw-Hill Book Company, 1965.

15. Papoulis, A. Systems and Transforms with Applications in Optics. New York: McGraw-Hill Book Company, 1968.

16. Ricardi, L. J. "A Summary of Methods for Producing Nulls in an Antenna Radiation Pattern," Technical Note 1976-38. Lexington, Mass.: Lincoln Laboratory, 2 September 1976.

17. Schell, A. C. "Survey of Ground Based Phased Array Antennas," Phased Array Antennas, edited by A. A. Oliner and G. H. Knittel. Dedham, Mass.: Artech House, Inc., 1972.

18. Tables of the Bessel Functions of the First Kind. Cambridge: Harvard University Press, 1947.

19. Thourel, L. The Antenna. New York: John Wiley and Sons Inc., 1960.

20. Walter, C. H. Traveling Wave Antennas. New York: Dover Publications, Inc., 1965.

21. Ziemer, R. E. and W. H. Tranter. Principles of Communications Systems, Modulation, and Noise. Boston: Houghton Mifflin Company, 1976.

Appendix: Analysis of Computer Program

Introduction

The purpose of this Appendix is to present the details of the computer program used in this thesis. It is divided into four parts: theoretical analysis, computer program description, discussion of data, and summary.

Theoretical Analysis

Eq (14) is the starting point with $A_i = 1$ and $\alpha_i = 0$. Next, the array is assumed to be linear. The ℓ_i become $\ell_i = \frac{r_i}{c} \cos\theta$. With these substitutions Eq (14) becomes

$$\tilde{\sigma}(\theta, f) = M(f) \sum_{i=1}^{N} e^{j2\pi(f+f_0)\frac{r_i}{c}\cos\theta} \tag{92}$$

The signal is assumed to be a pulse of unit height and duration, T.

This waveform is passed through the array and the resultant signal is correlated with another pulse of the same duration. The resultant operation is

$$c(\tau) = \int_{-\infty}^{\infty} m(t) * \{\text{array function}\}\, m(\tau + t)\, dt \tag{93}$$

which in the frequency domain is

$$c(f) = M(f) \sum_{i=1}^{N} e^{j2\pi(f+f_0)\frac{r_i}{c}\cos\theta} \; M^*(f)$$

$$= |M(f)|^2 \sum_{i=1}^{N} e^{j2\pi(f+f_0)\frac{r_i}{c}\cos\theta} \tag{94}$$

$|M(f)|^2$ is simply the transform of the autocorrelation function of the pulse. Thus,

$$|M(f)|^2 = T^2 \text{sinc}^2(fT) \equiv T^2 \frac{\sin^2 \pi f t}{(\pi f t)^2} \tag{95}$$

When inverse transformed this function is a triangle of height T and width 2T (Fig. A-1). This then is considered the ideal undistorted signal waveform to be passed through the array for detection. Eqs (94) and (95) were used as the basis for the computer program that was written to investigate and demonstrate the properties of the array.

Computer Program Analysis

The program was written to be quite versatile in its applications for this study. A series of specialized subroutines were written to perform most of the work. The main program, THESIS, was basically a series of calls to these subroutines to obtain a variety of results for visual analysis. The major subroutines used were SIGNALS, ARRAY, and FFT. The supporting subroutines were FREQ, GRAPH, ROTATE, DFT, and IDFT. The Fast Fourier Transform (FFT) algorithm used relies on the data list being some positive integer power of two, 2^M. Thus, all the subroutines were written to conform to this specification for vector sizes.

Subroutine SIGNALS fills a vector, Sigspec, with equally spaced frequency samples of the right side of Eq (95). Since the frequency spectrum of Eq (95) is infinitely wide, the frequency spacing must be chosen so that an adequate

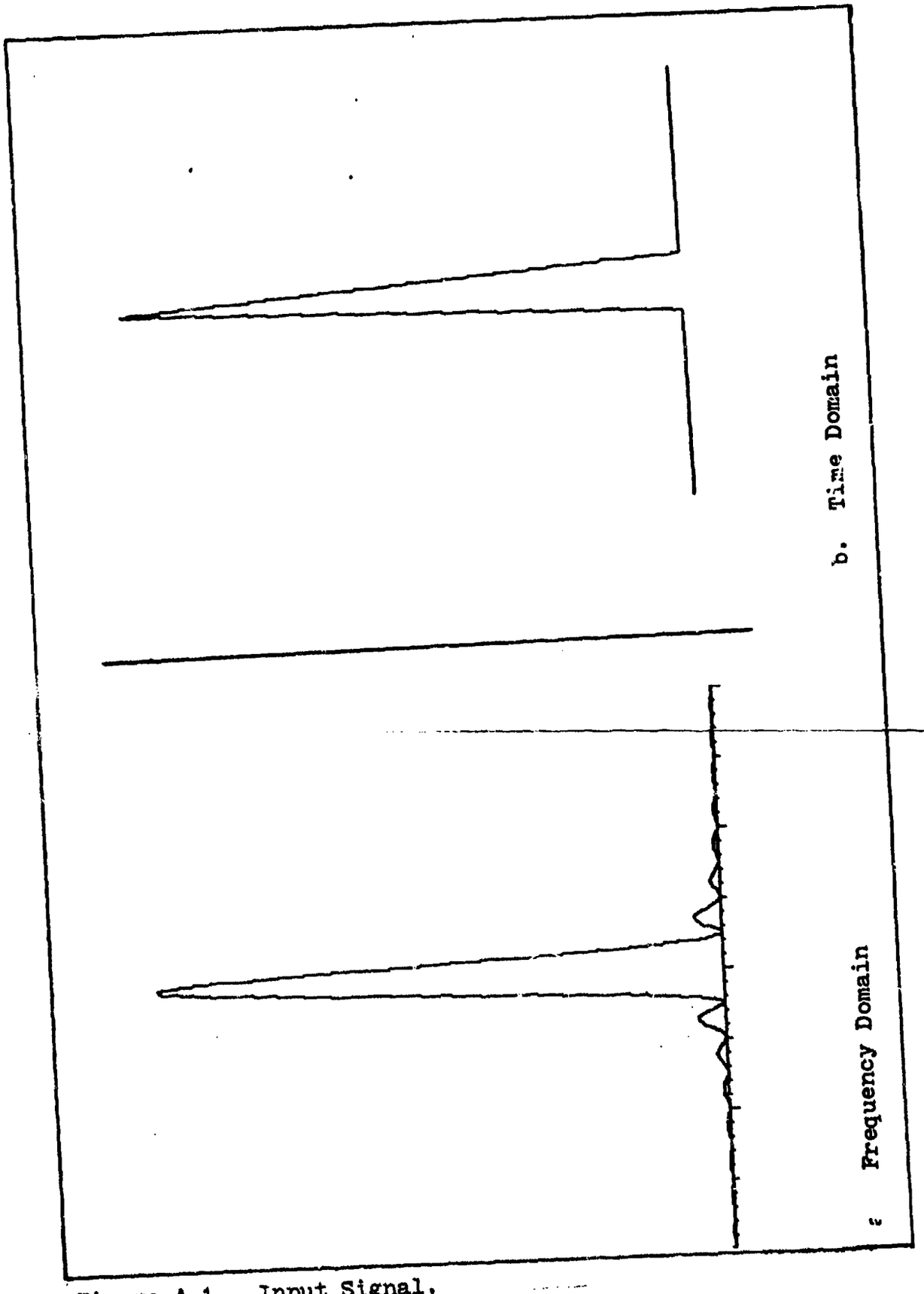

Figure A-1. Input Signal.

amount of the spectrum content is sampled to yield acceptable signal waveshapes in the time domain after inverse transforming. This particular waveshape ($\text{sinc}^2 x$) has been studied extensively and it is well known that sampling algorithms that include samples from one or two of the sidelobes yield adequate results for most operations. For this program, the frequency spectrum is sampled so that samples from at least the seventh sidelobe on either side of the main lobe are included in Sigspec.

Subroutine ARRAY implements the complex summation in Eq (94). However, the form of the summation was altered slightly before implementation. An f_o was factored from $(f + f_o)$ leaving $f_o(1 + f/f_o)$. Next r_i was redefined as $r_i = d_i \lambda_o$ where λ_o is the wavelength of f_o. Thus, d_i is the distance r_i measured in units of λ_o . Substituting these changes into Eq (94) yields

$$\sum_{i=1}^{N} e^{j2\pi(f+f_o)\frac{r_i}{c}\cos\theta} = \sum_{i=1}^{N} e^{j2\pi\frac{f_o\lambda_o}{c}(1+\frac{f}{f_o})d_i\cos\theta}$$

$$= \sum_{i=1}^{N} e^{j2\pi(1+\frac{f}{f_o})d_i\cos\theta} \qquad (96)$$

because $f_o \lambda_o = c$. Finally, f_o was chosen arbitrarily to be 350 MHz, a UHF frequency. Subroutine ARRAY then fills a vector, ANTENNA, with equally spaced frequency samples of Eq (96). These are the same frequency samples used in subroutine SIGNALS.

The third major subroutine is FFT. It is a Discrete

Fourier Transform (DFT) that uses the decimation-in-time principle (Ref 13:290-302) for computing the DFT of vectors that are a power of two in element length. The routine was written so that either a discrete transform or a discrete inverse transform could be obtained by calling FFT.

These three subroutines then became the workhorses for the computer analysis. SIGNALS was called to create the signal spectrum, ARRAY was called to create the antenna spectrum, and a simple term by term product of the two resulted in the array output vector (Fig. A-2). This output vector was then passed to the FFT for inverse transforming. The resultant signal was then graphed so that it could be visually compared with the ideal output signal of Figure A-1.

The five supporting subroutines were written to support the details of graphing the output of the three main subroutines. FREQ has the simple function of placing the appropriate values in the horizontal axis vectors. It creates the appropriate time and frequency vectors that match the sampling values used by SIGNALS and ARRAY. GRAPH has the function of graphing the output in an acceptable format by using basic CALCOMP plotting routines. This routine is only useful with the facilities available at FIT's computer center.

ROTATE is a subroutine that was used in the analysis of the linear, equally spaced array. Section III. C. proved that the signal and its first time derivative were 90° out of phase. ROTATE determines the phase of the signal and then

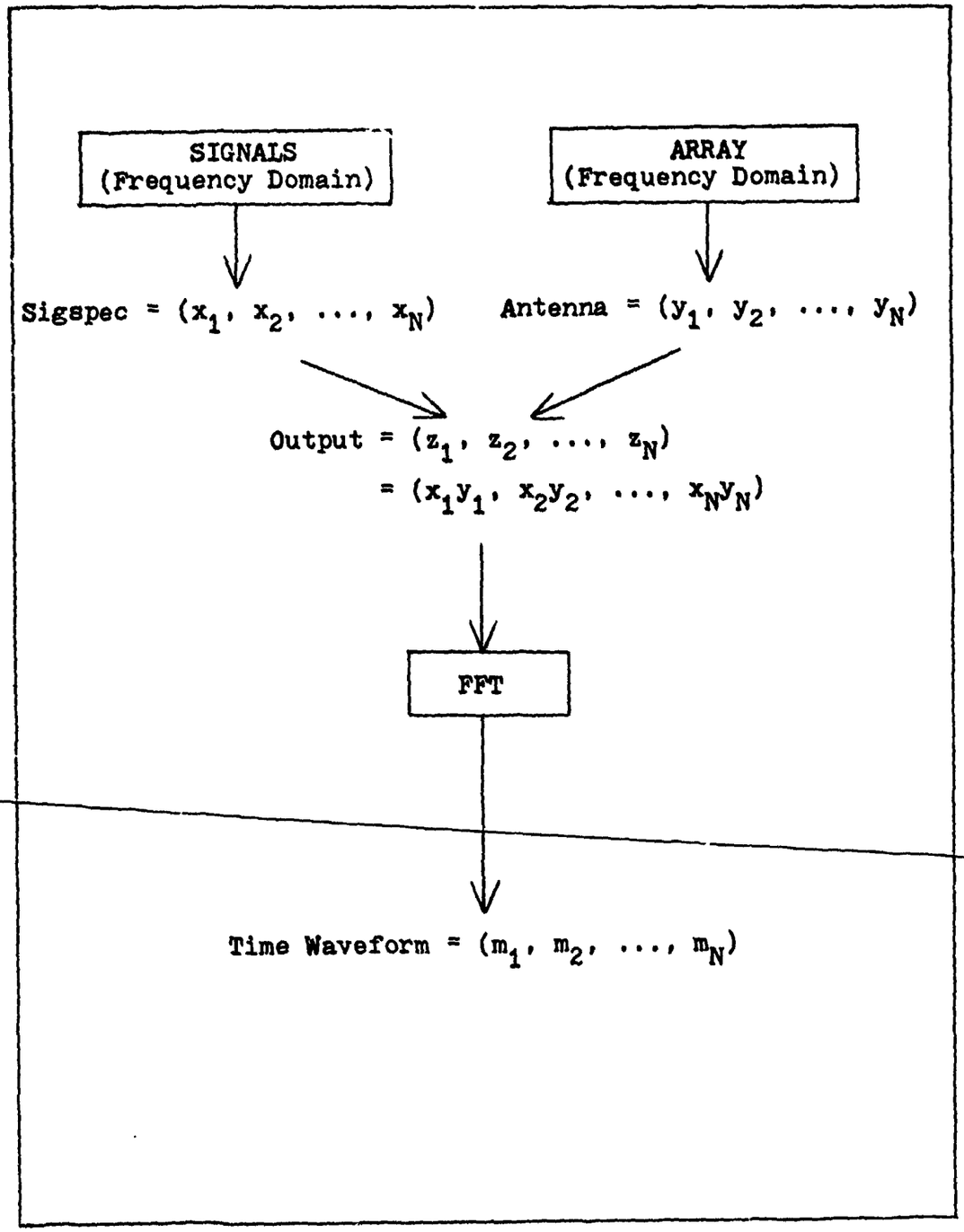

Figure A-2. Implementation of Equation (94).

shifts the phase of the output so that the signal can be found on the real axis. The first time derivative is then located on the imaginary axis. In this format these two quadrature signals can easily be graphed separately.

DFT and IDFT were written to support FFT. DFT and IDFT set the parameters of FFT to cause FFT to calculate either the discrete transform or the discrete inverse transform, respectively.

All the above subroutines were designed so that they need no changes for any run. Obviously, subroutine SIGNALS would have to be rewritten if a different input signal is desired.

The main program, THESIS, is written with all the parameters for various situations included. The program was written for batch processing and little consideration was given to optimizing this routine. The various parameter cards were simply replaced with new cards that contained the new parameters. A listing of the most often used program is included as Figure A-3.

Discussion of Data

Any time a digital computer is used to simulate a continuous system errors are introduced. These errors must be identified and accounted for. This computer program introduces errors into the output from three major sources. All three are discussed here.

The first effect is roundoff error. The computer performs calculations to a certain degree of accuracy. Rarely

```
      PROGRAM TWFSIG(INPUT,OUTPUT,PLOT)
      REAL B,IBUF,S,FR,TI,MANY
      COMPLEX SIGSPEC,ANTENNA,SIGNAL,MAN2
      COMMON  B(10), IBUF(1024),SIGSPEC(1024),FR(1024),TI(1024),S(1024),
     1ANTENNA(1024),SIGNAL(1024),MANY(1024),MAN2(1024)
      IOUT=6LOUTPUT
      CALL PLOTS(IBUF,1024,6HPLOT)
      CALL PLOT(0.,-4.,-3)
      CALL PLOT(0.,8.0,-3)
      PI=3.1415926535898
C
C*************************************
C   THE FOLLOWING CARDS MUST BE UPDATED PROPERLY BEFORE EACH RUN.
      M=10
      FMAX=16000000
      T=.000002
      B(1)=0.
      B(2)=.5
      B(3)=1.
      B(4)=3.5
      NSPEC=0
      NTIME=0
      NREAL=1
      NMAG=1
      NSIG=0
C*************************************
      NUMBER=2**M
C
C   SCALE THE TIME AND FREQUENCY AXES.
      CALL FREQ(FR,TI,FMAX,NUMBER)
C   CREATE THE SPECTRUM OF THE SIGNAL.
      CALL SIGNALS(T,FMAX,NUMBER)
C
C   IF DESIRED, PLOT THE SIGNAL SPECTRUM AND/OR ITS TIME WAVEFORM.
C   IF NSPEC IS 1, THE SPECTRUM WILL BE PLOTTED.
      IF(NSPEC.NE.1) GO TO 20
      DO 10 I=1,NUMBER
10    S(I)=REAL(SIGSPEC(I))
C   PLOT THE SIGNAL SPECTRUM.
      CALL GRAPH(1.,1,'F',NUMBER)
C   IF NTIME IS 1, THE TIME SIGNAL WILL BE PLOTTED.
20    IF(NTIME.NE.1) GO TO 25
      DO 21 I=1,NUMBER
21    SIGNAL(I)=SIGSPEC(I)
      CALL IDFT(SIGNAL,M)
      DO 22 I=1,NUMBER
22    S(I)=REAL(SIGNAL(I))*FMAX
C   PLOT THE SIGNAL TIME REPRESENTATION.
      CALL GRAPH(0.,1,'T',NUMBER)
C
25    CONTINUE
C*************************************
C   'THE' IS THE PARAMETER USED AS THE ANGLE WHERE THE SIGNAL IS LOCATED.
      THE=0.
      CALL ARRAY(FMAX,THE,4,NUMBER)
C   DETERMINE ARRAY OUTPUT
      DO 30 I=1,NUMBER
30    ANTENNA(I)=SIGSPEC(I)*ANTENNA(I)
      CALL IDFT(ANTENNA,M)
C SCALE ARRAY OUTPUT
      DO 33 I=1,NUMBER
33    ANTENNA(I)=FMAX*ANTENNA(I)
C   IF NREAL IS 1, THE REAL PART OF THE OUTPUT IS PLOTTED.
      IF(NREAL.NE.1) GO TO 40
      DO 39 I=1,NUMBER
38     S(I)=REAL(ANTENNA(I))
      CALL GRAPH(2.,1,'F',NUMBER)
C    IF NMAG IS 1, THE ENVELOPE IS PLOTTED.
40    IF(NMAG.NE.1) GO TO 50
      DO 45 I=1,NUMBER
45    S(I)=CABS(ANTENNA(I))
      CALL GRAPH(2.,1,'F',NUMBER)
C   IF NSIG IS 1, THE SIGNAL AXIS, THE DERIVATIVE AXIS, AND
C   THE PHASE ARE PLOTTED.
50    IF(NSIG.NE.1) GO TO 100
      CALL ROTATE(ANTENNA, THE, NUMBER)
      DO 106 I=1,NUMBER
      S(I)=REAL(ANTENNA(I))
      IF(ABS(S(I)).LE.0.000000000001) S(I)=0.0
106   CONTINUE
      CALL GRAPH(2.,1,'F',NUMBER)
      DO 107 I=1,NUMBER
      S(I)=AIMAG(ANTENNA(I))
      IF(ABS(S(I)).LE.0.000000000001) S(I)=0.0
107   CONTINUE
      CALL GRAPH(2.,1,'F',NUMBER)
      DO 108 I=1,NUMBER
      S(I)=ATAN( AIMAG(ANTENNA(I))/REAL(ANTENNA(I)))
108   S(I)=S(I)*180./PI
      CALL GRAPH(2.,1,'F',NUMBER)
105    CONTINUE
      CALL PLOTE(0)
      END
```


Figure A-3. Fortran Program. Page 1 of 4

```
      SUBROUTINE SIGNAL.SIT,FMAX,NUM)
C-----------------------------------------------------------------------
C   THIS SUBROUTINE CREATES THE SAMPLED SIGNAL SPECTRUM.                *
C                                                                       *
C   IT USES THE PARAMETER, FMAX, TO DETERMINE WHICH FREQUENCIES TO SAMPLE.*
C   THE PARTICULAR SIGNAL USED IN THIS SUBROUTINE IS A TRIANGULAR SIGNAL.*
C   THUS, THE FREQUENCY SPECTRUM THAT IS SAMPLED IS THE SQUARE OF THE SINC*
C   FUNCTION,  (SIN(PI*T*F)/(PI*F))**2                                  *
C   WHERE T IS THE WIDTH AND 2*T IS THE DURATION OF THE TRIANGLE.       *
C                                                                       *
C   THE PARAMETERS THAT MUST BE FED TO THIS ROUTINE ARE THE PULSE DURATION, T,*
C   THE FREQUENCY RANGE TO BE SAMPLED, FMAX, AND THE NUMBER OF FREQUENCIES TO*
C   BE SAMPLED, NUM.                                                    *
C   THE FREQUENCIES SAMPLED RANGE FROM -FMAX/2 TO +FMAX/2.              *
C-----------------------------------------------------------------------*
      COMPLEX SIGSPEC,ANTENNA,SIGNAL,SIGS
      COMMON  D(10), IFUF(1024),SIGSPEC(1024),FR(1026),TI(1026),S(1026),
     1ANTENNA(1024),SIGNAL(1024),MANY(1026),SIGS(1024)
      PI=3.14159265358797
      FDEL=FMAX/(NUM-1.)
      ILAST=NUM/2-1
      DO 10 K=1,ILAST
      F=(K-NUM/2)*FDEL
10    SIGS(K)=(SIN(PI*T*F)/PI /F)**2.
      IFIRST=NUM/2+1
      DO 12 K=IFIRST,NUM
      F=(K-NUM/2)*FDEL
12    SIGS(K)=(SIN(PI*T*F)/PI /F,**2.
      SIGS(NUM/2)=T*T
      DO 20 K=1,IFIRST
20    SIGSPEC(K)=SIGS(K+NUM/2-1)
      IFIRST=NUM/2+2
      DO 30 K=IFIRST,NUM
30    SIGSPEC(K)=SIGS(K-NUM/2-1)
      RETURN
      END
      SUBROUTINE ARRAY(FMAX,THE,N,NUM)
C-----------------------------------------------------------------------
C   THIS SUBROUTINE CREATES THE SAMPLED ANTENNA ARRAY SPECTRUM.         *
C                                                                       *
C   IT EVALUATES THE ARRAY EQUATION AT THE SAME FREQUENCY POINTS THAT THE*
C   SIGNAL WAS SAMPLED.                                                 *
C   THE ANTENNA EQUATION IS  THE SUMMATION FROM 1 TO N OF THE PARAMETER, K,*
C   WITH THE TERM IN THE SUMMATION BEING                                *
C   EXP(J*2*PI*(1+F/350,000,000)*D(K)*COS(THETA))                       *
C                                                                       *
C   THE PARAMETERS THAT MUST BE FED TO THIS ROUTINE ARE THE FREQUENCY RANGE*
C   TO BE SAMPLED, FMAX, THE NUMBER OF ELEMENTS IN THE ANTENNA ARRAY, N, THE*
C   LOCATION OF THE SIGNAL FROM THE MAIN AXIS IN DEGREES, THE, AND THE  *
C   NUMBER OF POINTS TO BE SAMPLED, NUM.                                *
C   AS WITH SUBROUTINE SIGNALS THE FREQUENCY RANGE SAMPLED IS           *
C   -FMAX/2 TO +FMAX/2.                                                 *
C-----------------------------------------------------------------------*
      COMPLEX SIGSPEC,ANTENNA,SIGNAL,ANT
      COMMON  D(11), IFUF(1024),SIGSPEC(1024),FR(1026),TI(1026),S(1026),
     1ANTENNA(1024),SIGNAL(1024),MANY(1026), ANT(1024)
      PI=3.14159265358
      THETA=THE*PI/180.
      ANGLE=COS(THETA)
      FDEL=FMAX/(NUM-1.)
      DO 100 I=1,NUM
      F=FDEL*(I-NUM/2)
      ANTENNA(I)=(0.,0.)
      DO 80 K=1,N
      DIP=PI*(1+F/350000000)*D(K)*ANGLE*2
      ANTENNA(I)=ANTENNA(I)+COS(DIP)*(1.,0.)+SIN(DIP)*(0.,1.)
80    CONTINUE
100   CONTINUE
      ILAST=NUM/2+1
      DO 120 I=1,ILAST
120   ANT(I)=ANTENNA(I+NUM/2-1)
      IFIRST=NUM/2+2
      DO 130 I=IFIRST,NUM
130   ANT(I)=ANTENNA(I-NUM/2-1)
      DO 140 I=1,NUM
140   ANTENNA(I)=ANT(I)
      RETURN
      END
```

Figure A-3. Fortran Program. Page 2 of 4

```
      SUBROUTINE DFT(X,N)
C-----------------------------------------------------------------------
C   THIS SUBROUTINE AND THE NEXT TWO CONSTRUCT TO CALCULATE THE DISCRETE
C   FOURIER TRANSFORM OR ITS INVERSE OF A VECTOR OF VALUES.
C
C   DFT TELLS THE FFT TO CALCULATE THE TRANSFORM.
C   IDFT TELLS THE FFT TO CALCULATE THE INVERSE TRANSFORM.
C   BOTH DFT AND IDFT REQUIRE TWO PARAMETERS:
C   1.  THE VECTOR OF COMPLEX VALUES TO BE TRANSFORMED
C   2.  THE EXPONENT, N, OF THE NUMBER OF VALUES TO BE TRANSFORMED, 2**N
C
C   FFT IS A DECIMATION-IN-TIME DISCRETE FOURIER TRANSFORM.
C   IT REQUIRES THE NUMBER OF DATA POINTS TO BE AN INTEGER POWER OF TWO IN
C   ORDER TO OPERATE PROPERLY.
C   IT IS CALLED AUTOMATICALLY BY DFT AND IDFT.
C-----------------------------------------------------------------------
      COMPLEX X(1024)
      CALL FFT(X,N,1)
      RETURN
      END
      SUBROUTINE IDFT(X,N)
      COMPLEX X(1024)
      CALL FFT(X,N,0)
      RETURN
      END
      SUBROUTINE FFT(X,N,ITRANS)
      COMPLEX X(1024),U,W,T
      N=2**N
      NV2=N/2
      NM1=N-1
      J=1
      DO 7 I=1,NM1
      IF(I.GE.J) GO TO 5
      T=X(J)
      X(J)=X(I)
      X(I)=T
5     K=NV2
6     IF(K.GE.J) GO TO 7
      J=J-K
      K=K/2
      GO TO 6
7     J=J+K
      PI=3.14159265358979
      DO 20 L=1,N
      LE=2**L
      LE1=LE/2
      U=(1.0,0.0)
      IF(ITRANS.EQ.0) W=CMPLX(COS(PI/FLOAT(LE1)),-SIN(PI/FLOAT(LE1)))
      IF(ITRANS.NE.0) W=CMPLX(COS(PI/FLOAT(LE1)),SIN(PI/FLOAT(LE1)))
      DO 20 J=1,LE1
      DO 10 I=J,N,LE
      IP=I+LE1
      T=X(IP)*U
      X(IP)=X(I)-T
10    X(I)=X(I)+T
20    U=U*W
      IF(ITRANS.EQ.0) GO TO 30
      DO 25 I=1,N
25    X(I)=X(I)/N
30    RETURN
      END
      SUBROUTINE FREQ(FR,TI,FMAX,NUMBER)
C-----------------------------------------------------------------------
C   THIS SUBROUTINE ENSURES THAT THE TIME AND FREQUENCY AXES WILL BE SCALED
C   PROPERLY WHEN PLOTS ARE REQUESTED.  IT FILLS THE VECTOR, TI, WITH THE TIME
C   SAMPLES AND THE VECTOR, FR, WITH THE FREQUENCY SAMPLE VALUES.
C
C   IT REQUIRES TWO PIECES OF INFORMATION:
C     1.  THE FREQUENCY RANGE TO BE SAMPLED, FMAX
C     2.  THE NUMBER OF SAMPLE POINTS, NUMBER
C-----------------------------------------------------------------------
      DIMENSION FR(NUMBER),TI(NUMBER)
      FDEL=FMAX/(NUMBER-1.)
      DO 1 I=1,NUMBER
      TI(I)=(I-NUMBER/2.)/FMAX
1     FR(I)=(I-NUMBER/2.)*FDEL
      RETURN
      END
```

Figure A-3. Fortran Program. Page 3 of 4

```
      SUBROUTINE ROTATE(ANTENNA,THE,NUM)
C-----------------------------------------------------------------------
C   THIS SUBROUTINE IS ONLY USEFUL WITH THE LINEAR, EQUALLY SPACED ARRAYS.
C   IT HAS THE FUNCTION OF SHIFTING THE PHASE OF THE OUTPUT, SO THAT THE REAL
C   AXIS CONTAINS THE SIGNAL AND THE IMAGINARY AXIS CONTAINS THE SIGNAL
C   DERIVATIVE.
C
C   THE PARAMETERS NECESSARY FOR THIS SUBROUTINE TO FUNCTION PROPERLY ARE THE
C   VECTORS OF COMPLEX VALUES, ANTENNA, THE ANGLE OF PHASE SHIFT, THE, AND THE
C   NUMBER OF VALUES TO BE SHIFTED, NUM.
C-----------------------------------------------------------------------
      COMPLEX ANTENNA(NUM)
      PI=3.1415926535898
      THE=THE*PI/180.
      BIG=1.5*PI*COS(THE)
      DO 10 I=1,NUM
10    ANTENNA(I)=(COS(BIG)*(1.,0.)+SIN(BIG)*(0.,1.))*ANTENNA(I)
      RETURN
      END
      SUBROUTINE GRAPH(XAXIS,IGIN,J,NUM)
C-----------------------------------------------------------------------
C   THIS SUBROUTINE HAS THE SOLE FUNCTION OF GRAPHING THE DATA IN AN
C   ACCEPTABLE FORMAT.  IT PERFORMS SEVERAL FUNCTIONS.
C     1.  IT READS IN 4 CARDS THAT CONTAIN THE LABELLING INFORMATION FOR THE
C         GRAPH.
C     2.  IT SHIFTS THE OUTPUT SO THAT THE DESIRED SIGNAL IS IN THE CENTER OF
C         THE GRAPH.
C     3.  IT ELIMINATES THE FIRST 25% OF THE POINTS AND THE LAST 25% OF THE
C         POINTS.
C-----------------------------------------------------------------------
      DIMENSION ID(17)
      DIMENSION X(514),Y(514)
      COMPLEX SIGSPEC,ANTENNA,SIGNAL,MAN2
      COMMON  D(10), IOUT(1024),SIGSPEC(1024),FR(1024),TI(1024),S(1024),
     1ANTENNA(1024),SIGNAL(1024),   T(1024),MAN2(1024)
      IN=5,IOUTPUT
C
C   THESE STEPS READ IN THE DATA NECESSARY TO LABEL THE BOX, THE TWO AXES,
C   AND THE FIGURE LABEL.
      READ(IN,1) (ID(K),K=1,8)
      READ(IN,1) (ID(K),K=9,16)
      READ(IN,2) ID(17)
1     FORMAT(8A10)
2     FORMAT(A10)
C
C   THESE STEPS REARRANGE THE DATA INTO A MORE VISUALLY ACCEPTABLE
C   FORMAT.   THIS IS NECESSARY BECAUSE OF THE FACT THAT THE NEGATIVE
C   FREQUENCY AND NEGATIVE TIME TERMS ARE STORED TO THE RIGHT OF THE
C   POSITIVE TIME TERMS.  THUS, A STRAIGHT PLOT OF THE DATA WOULD RESULT IN A
C   SPLIT GRAPH.
      ILAST=NUM/2+1
      DO 3 K=1,ILAST
3     T(K+NUM/2-1)=S(K)
      IFIRST=NUM/2+2
      DO 4 K=IFIRST,NUM
4     T(K-NUM/2-1)=S(K)
      DO 5 K=1,NUM
5     S(K)=T(K)
C
C   THESE STEPS ELIMINATE THE LOWER AND UPPER QUARTER OF THE POINTS FROM THE
C   GRAPH.  THIS WAS DONE BECAUSE THE DATA USED IN THIS THESIS WAS NEARLY
C   ALWAYS ZERO AT THESE EXTREMES AND WAS OF NO VALUE IN THE GRAPHICS.
      NUMB=NUM/2
      IFIRST=NUM/4
      DO 6 I=1,NUMB
      Y(I)=S(I+IFIRST)
      IF(XAXIS.EQ.1.) X(I)=FR(I+IFIRST)
      IF(XAXIS.EQ.2.) X(I)=TI(I+IFIRST)
6     CONTINUE
      CALL HGRAPH(X,Y,NUMB,ID,IGIN,25,J)
      RETURN
      END
```

Figure A-3. Fortran Program. Page 4 of 4

is this precisely the right number. Under most circumstances this causes no real problems. However, if the correct answer is in itself a very small number, then the error can be large compared to the actual answer. This effect was observed in the Tables of Chapter III where A and B were tabulated. The computer never calculated their values to be precisely zero at locations where it was shown that they are zero.

Roundoff errors caused other problems; problems that affected the output of the graphics routine. To illustrate the biggest effects of roundoff we will use Figure 28 and Figure 43. Figure 28 shows that the output is zero. The program did not calculate all the output samples to be precisely zero. They had values that ranged from 10^{-28} to -10^{-28}. When the graphics routine went to graph these points it scaled the axes so that the details of the "noise" were visual. We had three possible ways to deal with this situation. (1) Let the system graph the "noise". After a few runs we decided this method was visually unacceptable. (2) Artificially set the range of the scaling so that the "noise" is graphed as zero. This was a possible route. (3) Pick a value that is considered the noise threshold. Any values below this will be replaced by zero. We took this option because it was so simple to implement. However, it must be emphasized that we only performed this replacement at the time of graphing. The calculated values were used as is for all operations. Figure 43 shows the other

effect that the roundoff errors caused. The roundoff noise causes the phase to be calculated as slightly less than 90° or slightly greater than 90°. This combined with the second source of computer error to produce the results of Figure 43. The arctangent function interprets results only in the range from 90° to -90°. Thus, a value slightly greater than 90° is viewed as a value slightly less than -90°. Thus, the noise around 90° or -90° of phase shift causes wild fluctuations in the graph of Figure 43. There were several methods thought up to artificially eliminate this graphics problem, but they were not implemented.

The third error deals with the discrete nature of the FFT. The FFT is a truncated Fourier Series representation of the data. In order to include enough frequency harmonics to make the square wave look exactly square would require a large value of FMAX and the number of frequency samples 2^n. This is due to Gibbs phenomenon which states that signals with discontinuities cannot be represented by finite length Fourier Series. The result of a finite Fourier Series representation is the oscillation near the discontinuity that appear in Figures A-4, A-5, and A-6 (Ref 2:105-107). Figures A-4, A-5, and A-6 illustrate how the oscillations on the square wave decrease as the frequency range and the number of samples is increased. Figure A-4 used a 256 point FFT and only sampled frequency components up to 2 MHz. Figure A-5 used a 512 point FFT and sampled to 4 MHz. Finally, a 1024 point FFT and a maximum frequency of 8 MHz

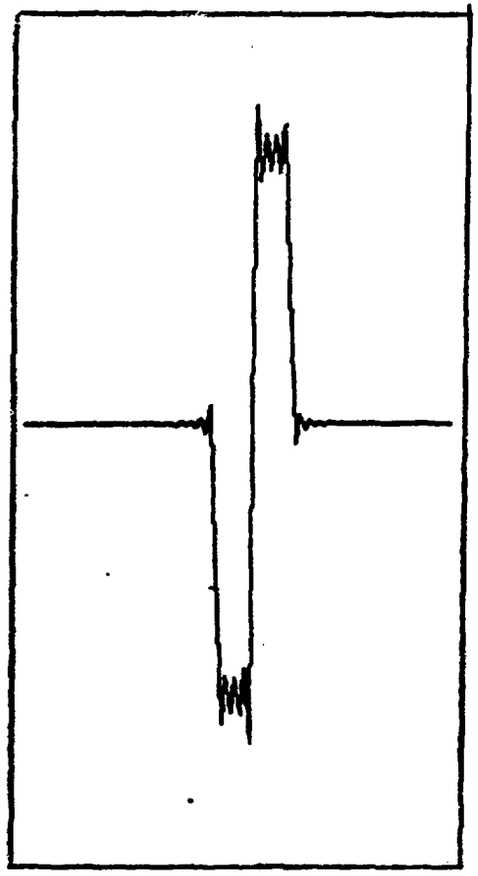

Figure A-4. 256 point DFT.

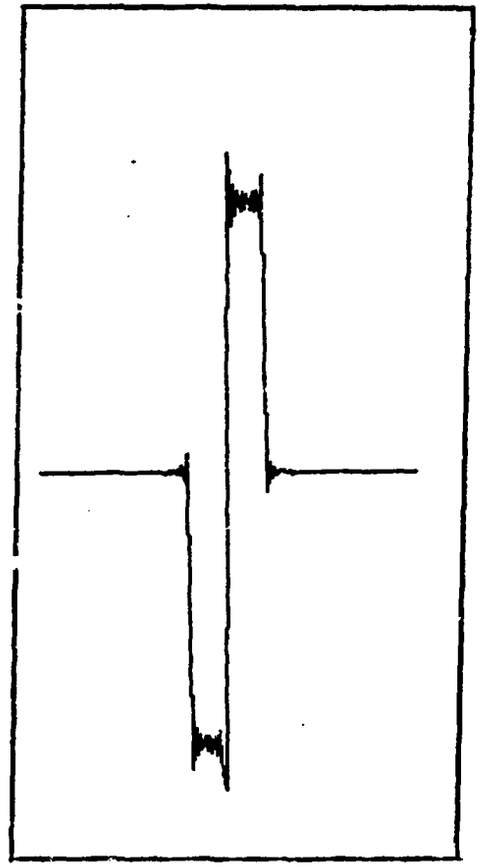

Figure A-5. 512 point DFT.

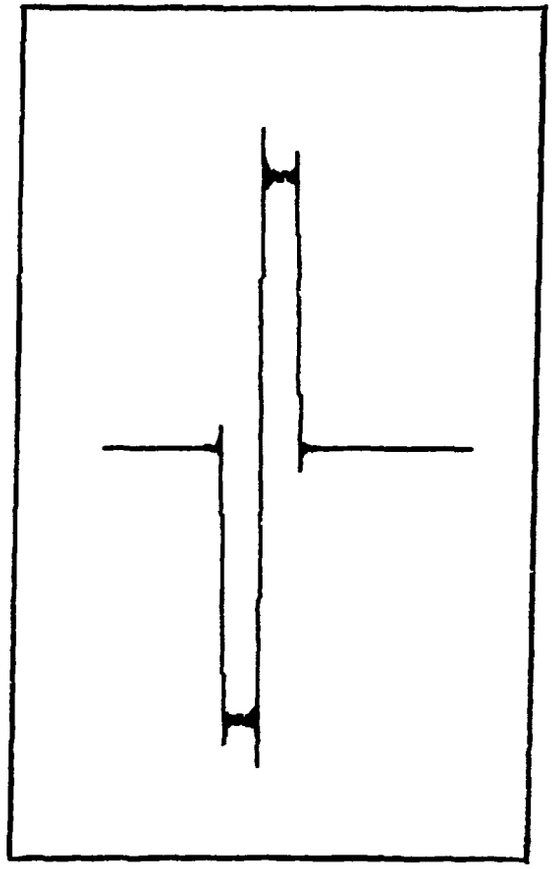

Figure A-6. 1024 point DFT.

were used to obtain Figure A-6. These figures clearly illustrate that the higher harmonics aid in making the square wave more square. The plots in the main text all used the 1024 point FFT.

Summary

This appendix has presented the details of the computer program that was used to obtain most of the plots presented in the text of this thesis. It has described the equations that were programmed and the actual Fortran program has been included. As a final step a discussion was given of the effects that the digital program had on the form of the output. This included the observed effects of roundoff errors, the limitations of the arctangent routine used, and the observable effects of using a finite length Fourier Series representation of waveforms.

VITA

Edward Raska, Jr. was born on 30 December 1948 in Sinton, Texas. He graduated from East High School in Pueblo, Colorado in June 1967. He entered the Massachusetts Institute of Technology in September of that year and graduated in June 1971 with a Bachelor of Science degree in Aeronautics and Astronautics. He married the former Elsie T. Atencio in August 1969 and now has three children; Lois, 8; Karen, 6; and Christine, 3. In July 1971 he enlisted in the United States Air Force and became a missile systems analyst for the Strategic Air Command. In August 1973 he attended Officer Training School and was commissioned in November. From then until August 1977 he worked in the 4950th Test Wing at Wright-Patterson Air Force Base, Ohio as a flight test engineer. He then entered the School of Engineering, Air Force Institute of Technology, in August 1977.

Permanent Address: 1915 E. 12th Street
Pueblo, Colorado 81001

UNCLASSIFIED

SECURITY CLASSIFICATION OF THIS PAGE (When Data Entered)

REPORT DOCUMENTATION PAGE		READ INSTRUCTIONS BEFORE COMPLETING FORM
1. REPORT NUMBER AFIT/GE/EE/78-14	2. GOVT ACCESSION NO.	3. RECIPIENT'S CATALOG NUMBER
4. TITLE (and Subtitle) EFFECTS OF ANTENNA ARRAYS ON BROADBAND SIGNALS		5. TYPE OF REPORT & PERIOD COVERED
		6. PERFORMING ORG. REPORT NUMBER
7. AUTHOR(s) Edward Raska, Jr.		8. CONTRACT OR GRANT NUMBER(s)
9. PERFORMING ORGANIZATION NAME AND ADDRESS Air Force Institute of Technology (AFIT/EN) Wright-Patterson AFB, Ohio 45433		10. PROGRAM ELEMENT, PROJECT, TASK AREA & WORK UNIT NUMBERS
11. CONTROLLING OFFICE NAME AND ADDRESS Communications & Control Div. (RADC/DCID) Rome Air Development Center Griffiss AFB, New York 13441		12. REPORT DATE Sept. 1978 13. NUMBER OF PAGES 133
14. MONITORING AGENCY NAME & ADDRESS(if different from Controlling Office)		15. SECURITY CLASS. (of this report) Unclassified 15a. DECLASSIFICATION/DOWNGRADING SCHEDULE

16. DISTRIBUTION STATEMENT (of this Report)

Approved for public release; distribution unlimited

17. DISTRIBUTION STATEMENT (of the abstract entered in Block 20, if different from Report)

18. SUPPLEMENTARY NOTES

Approved for public release: IAW AFR 190-17

JOSEPH P. HIPPS, Major, USAF
Director of Information 1-23-79

19. KEY WORDS (Continue on reverse side if necessary and identify by block number)

Antenna Arrays
Wideband Signals
Broadband Signals
Spread Spectrum
Adaptive Arrays

20. ABSTRACT (Continue on reverse side if necessary and identify by block number)

This paper develops a complex, baseband model for an adaptive array. The array is assumed to have N isotropic elements. Only two aspects of arrays are modeled: spatial propagation delays and the weighting coefficients. The array model is used to determine the effects of arrays on wideband signals. The most important finding is that the output of the array consists of the input signal and its time derivatives. Each of these signal components is multiplied by a complex number that is a function

DD FORM 1 JAN 73 1473 EDITION OF 1 NOV 65 IS OBSOLETE

UNCLASSIFIED

SECURITY CLASSIFICATION OF THIS PAGE (When Data Entered)

of the array and signal parameters. Properties of these complex numbers are investigated. A four element linear array is used as a specific example to illustrate these properties. Two models of the weighting coefficients are analyzed to develop information about "adaptive" effects. These models are used to show how the array output is degraded by changing coefficients.